DOE Low Temperature Plasma Centers and User Facilities Annual Meeting

Center for Low Temperature Plasma Interactions with Complex Surfaces (PICI)

Sandia Plasma Research Facility (SPRF)

Princeton Collaborative Low Temperature Research Facility (PCRF)

Center for Studies of Plasma-Assisted Combustion and Plasma Catalysis (PACC)

September 23-24, 2021
Bethesda North Marriott Hotel and Conference Center
Bethesda, MD

Schedule (Hybrid Mode)

	Time (Eastern)	Speaker	Title	Mode
Thursday, September 23, 2021				
8:00 – 10:00 am		**Oral Session I: PICI** (White Oak room)		**In person**
1	8:00 – 8:20	Mark Kushner	Introduction to the LTP Centers and Facilities Annual Meeting 2021	In person
2	8:20 – 8:40	Bryan Goldsmith	Atomistic Modeling of Plasma-Assisted Catalysis: Opportunities and Challenges	In person
3	8:40 – 9:00	Aditya Bhan	Interactions of Atmospheric Plasmas with Catalytic Surfaces	In person
4	9:00 – 9:20	Gottlieb Oehrlein	DRIFTS and Gas Phase FTIR Characterization of Plasma-enhanced Catalysis	In person
5	9:20 – 9:40	Selma Mededovic-Thagard	Treatment of Aqueous Pollutants in Gas-liquid Plasma Reactors: Identification of the Key Parameters Controlling the Removal	In person
6	9:40 – 10:00	Igor Adamovich	N_2 Vibrational Excitation in Atmospheric Pressure Ns Pulse and RF Plasma Jets	In person
10:00 – 10:20 am		**Break**		
10:20 am – 12:20 pm		**Oral Session II: PCRF** (White Oak room)		**Hybrid**
1	10:20 – 10:40	Yevgeny Raitses	ExB Plasmas for Processing of Nanomaterials	Remote
2	10:40 – 11:00	Arthur Dogariu	Advanced Optical Diagnostics for Low Temperature Plasmas; Neutral Density Mapping and Dynamics in RF-Heated PFRC Plasma	In person
3	11:00 – 11:20	Sophia Gershman	Plasma Diagnostics of Mesoporous Silica Packed Bed Reactors for Ammonia Syn-thesis	Remote
4	11:20 – 11:40	Igor Kaganovich	PPPL Modeling Tools for Low Temperature Plasmas Available through the Princeton Collaborative Research Facility	Remote
5	11:40 – 12:00	Mikhail Shneider	Coherent Thomson Scattering	In person
6	12:00 – 12:20	Shurik Yatom	Characterization of Plasma in RF Jet Interacting with Water: Thomson Scattering versus Spectral Line Broadening	Remote
12:20 – 1:50 pm		**Lunch**		
1:50 – 2:40 pm		**Poster Session I: PICI** (Brookside room)		**In person**
2:40 – 3:30 pm		**Poster Session II: PICI/PACC/SPRF** (Brookside)		**In person**
3:30 – 3:50 pm		**Break**		

	Thursday, September 23, 2021 (continued)			
	Time (Eastern)	Speaker	Title	Mode
	3:50 – 5:30 pm	*Oral Session III: SPRF (White Oak room)*		*Remote*
1	3:50 – 4:10	Shane Sickafoose	Sandia National Laboratories Plasma Research Facility	Remote
2	4:10 – 4:30	Jonathan Frank	Imaging of Methyl Radical in Plasmas by Photofragmentation Laser-Induced Fluorescence	Remote
3	4:30 – 4:50	Matthew Hopkins	Advanced Modeling Capabilities for Low-Temperature Plasma Simulation	Remote
4	4:50 – 5:10	Christopher Kliewer	Development of Hybrid Coherent Raman Imaging and E-FISH Approaches for Low Temperature Plasma Assisted Chemistry	Remote
5	5:10 – 5:30	Amanda Lietz	Simulations of Nonequilibrium Thermionic Cs Plasmas	Remote
	5:30 – 7:00 pm	*Dinner*		
	7:00 – 8:00 pm	*Poster Session III: PCRF/ SPRF/PACC*		*Remote*

	Friday, September 24, 2021			
	Time (Eastern)	Speaker	Title	Mode
	9:00 – 10:00 am	*Oral Session IV: PACC (White Oak room)*		*Hybrid*
1	9:00 – 9:20	Igor Adamovich	Ns Pulse and Hybrid Plasmas for Plasma Assisted Ignition and Catalysis	In person
2	9:20 – 9:40	Yiguang Ju	Studies of Non-equilibrium Plasma Chemistry and Thermal-Chemical Instability	In person
3	9:40 – 10:00	Bruce Koel	Ammonia Synthesis and Decomposition in Plasma-assisted Catalysis	Remote
	10:00 – 10:20 am	*Break*		
	10:20 – 11:40 am	*Oral Session V: PICI (White Oak room)*		*In Person*
1	10:20 – 10:40	Ali Mesbah	Machine Learning and Artificial Intelligence for Low-temperature Plasmas: A Tutorial Overview	In person
2	10:40 – 11:00	Steven Shannon	Accurate Reproducible Power delivery across Multiple Plasma Sources	In person
3	11:00 – 11:20	Peter Bruggeman	Plasma-Surface Interactions: Boundary Layer Effects and Self-organization	In person
4	11:20 – 11:40	Mark Kushner	Plasma Interactions with non-Planar, Wet and Reactive Surfaces	In person
	11:40 am – 12:40 pm	*Discussion: All (White Oak room)*		*Hybrid*

	Poster Session I. Thursday, September 23, 1:50 – 2:40 pm		
	Presenter	**Title**	**Mode**
1	Joshua Morsell	Open Channel Microfluidic Substrate for Investigation of Multi-phase Surface Interactions with Atmospheric Pressure Plasmas	In person
2	Brian Bayer	Design and Operation of an Experimental Setup Used to Study Plasma Catalysis	In person
3	Francis Doherty	The Influence of Plasma-Induced Surface Charging on Single-Atom Catalysis for CO_2 Reduction	In person
4	Michael Hinshelwood	DRIFTS and Gas Phase FTIR Characterization of Plasma-enhanced Catalysis for NOx Production	In person
5	Osakpolo Faith Isowamwen	Efficient Defluorination of Perfluorobutane Sulfonate (PFBS) by Plasma with the Aid of a Surfactant	In person
6	Jingkai Jiang	Control of Reactive Species Fluxes to Substrate and Absolute Density Measurement of Ions and Vibrationally Excited N_2 by Molecular Beam Mass Spectrometry	In person
7	Kseniia Konina	Surface Ionization Wave Interactions with Dielectric Porous Surfaces	In person
8	Yudong Li	Study of Plasma-catalytic Oxidation of Methane: Role of Atomic Oxygen and Surface Species	In person
9	Mackenzie Meyer	Sheath Dynamics around a Water Droplet in an Atmospheric Pressure Glow Discharge	In person
10	Victor Miller	Green Fertilizer: Can Cold Plasmas Enrich Biowaste and Reduce Nitrogen Loss?	In person
11	Keegan Orr	Laser Induced Fluorescence Measurements of Vibrationally Excited Oxygen Produced by Recombination of O Atoms	In person
12	Xin Yang	Measurements of Atoms and Metastable Species in N_2 and H_2-N_2 Ns Pulse Plasmas	In person
13	Caleb Richards	Time-resolved CO_2, CO, and N_2 Vibrational Populations in Ns Pulse Discharge Plasmas	In person

	Poster Session II. Thursday, September 23, 2:40 – 3:30 pm		
	Presenter	**Title**	**Mode**
1	Caleb Richards	N_2 Vibrational Excitation in Atmospheric Pressure Ns Pulse and RF Plasma Jets	In person
2	Ketong Shao	Active Learning-guided Experiment Design for Maximizing Energy Efficiency of NOx Production Using a DC Pin-to-pin Glow Discharge	In person
3	Tanubhav Srivastava	Formation of Self-Organized Patterns at the Plasma-Liquid Interface for a Helium Glow Discharge with Solution Anode	In person
4	Mikhail Vasilev	The Effect of Liquid Residence Time on the Removal of Aqueous Contaminants	In person
5	Jianan Wang	Spatially Resolved Absolute OH-LIF Measurements in a Surface Discharge Generated by an Atmospheric Pressure Plasma Jet	In person
6	Sai Raskar	Spatially Enhanced Electric Field Induced Second Harmonic (SEEFISH) Generation	In person
7	Ning Liu	fs-UV-LAS for Measuring Temperature and OH Concentration in Low Temperature Plasmas	In person
8	David Mignogna	$N_2(A_3\Sigma u+,v)$ Energy Transfer Kinetics in Reacting N_2-CO_2-CH_4 Plasmas	In person
9	Xin Yang	Plasma-Enhanced Ammonia Synthesis over a Catalytic Surface	In person
10	Hongtao Zhong	Kinetic Studies of Excited Singlet Oxygen Atom $O(^1D)$ Reactions with Ethanol	In person
11	Justin Smith	VUV Spectroscopic Investigation of a Low Current Corona Source in Nitrogen	In person
12	Foluke (Jennifer) Ganzallo	Characterization and Treatment Performance of a Plasma Spinning Disc Reactor	In person

	Poster Session III. Thursday, September 23, 7:00 – 8:00 pm		
	Presenter	**Title**	**Mode**
1	Jian Chen	Validated Two-dimensional Modeling of Short Carbon Arcs: Anode and Cathode Spots	Remote
2	Nirbhav Chopra	Characterization of an Atmospheric Pressure Carbon Arc Plasma	Remote
3	Harry Fetsch	Surface Charging in Disinfection by Dielectric Barrier Discharge	Remote
4	Sophia Gershman	Plasma Disinfection by Dielectric Barrier Discharge Devices Suitable for Consumer Use	Remote
5	Haomin Sun	Analytical Model for Estimating Plasma Parameters in a Planar Diode	Remote
6	Lucas Beving	Simulations of Ion Heating in the Presheath Due to Ion-acoustic Instabilities	Remote
7	Timothy Chen	Time-resolved Electric Fields and Electron Properties Measured by Burst Laser pUlse EFISH (BLUEFISH) and Thomson Scattering in CH_4/Ar Nanosecond Pulsed Discharges	Remote
8	Surabhi Jaiswal	Observation of $O(^1S)$ Metastable Transition in Atmospheric Pressure Plasma	Remote

Abstracts - Oral Presentations

Introduction to the LTP Centers and Facilities Annual Meeting 2021

<u>Mark J. Kushner</u> [a], Shane Sickafoose [b], Yevgeny Raitses [c] and Igor Adamovich [d]

    (a) University of Michigan (mjkush@umich.edu)
    (b) Sandia National Laboratory (smsicka@sandia.gov)
    (c) Princeton Plasma Physics Laboratory (yraitses@pppl.gov)
    (d) Ohio State University (adamovich.1@osu.edu)

The Department of Energy Office of Fusion Energy Sciences established low temperature plasma (LTP) research centers and user facilities with the goal of advancing research in LTPs, both fundamentals and applications, and providing research resources to the broader LTP community, domestically and internationally. These centers and facilities, established in September2019, are:

- Center for Low Temperature Plasma Interactions with Complex Surfaces (PICI – University of Michigan, Director Mark J. Kushner)
- Sandia Plasma Research Facility (SPRF – Sandia National Laboratory, Director Shane Sickafoose)
- Princeton Collaborative Low Temperature Research Facility (PCRF – Princeton Plasma Physics Laboratory, Director Yevgeny Raitses)
- Center for Studies of Plasma-Assisted Combustion and Plasma Catalysis (PACC – Ohio State University, Director Igor Adamovich)

With the goal of promoting collaborations and synergies between the Centers and Facilities (C&F), their Annual Meetings are being jointly held. Due to Covid-19 concerns, the first Annual Meeting was canceled and replaced with a pair of virtual meetings. The Annual Meeting 2021 is the first joint meeting of the C&F, held in a hybrid in-person-virtual format.

The Annual Meeting will consist of oral presentations by co-principle investigators and collaborators of the C&F; posters presented by graduate students, post-doctoral researchers and collaborators; and an all-hands discussion. The presentations will highlight the research being performed at the C&F, with an eye towards how collaborations can best be leveraged between the sites for bettering the discipline. The all-hands discussion will focus on:

- How has the field evolved since the C&F were established and what new research challenges have arisen?
- Are the C&F focused on the most critical problems of the day?
- Are resources being best utilized?
- How might the C&F more closely collaborate while retaining their unique qualities?
- How do the C&F configure and prepare themselves for the research challenges of tomorrow?
- What additional talent (collaborators, agencies, facilities) are needed to meet these challenges?

Atomistic Modeling of Plasma-Assisted Catalysis: Opportunities and Challenges

Bryan R. Goldsmith

Department of Chemical Engineering, University of Michigan, Ann Arbor, MI 48109-2136, USA
(bgoldsm@umich.edu)

Non-thermal plasma catalysis is a growing field of research that has reported a variety of synergistic effects for increased activity, yield, or selectivity compared to conventional catalytic systems (i.e., thermocatalytic and electrocatalytic systems). Plasma's effect on surface-catalyzed reactions is multi-faceted and not well-understood at an atomistic level. Computational catalysis approaches have provided numerous insights into catalyst structure-property relations and mechanisms for thermo- and electro-catalysts, but much progress remains to bring plasma-catalytic modeling to the same level of understanding. Modeling plasma-assisted catalysis by quantum mechanical, molecular simulation, and first-principles microkinetics approaches has potential to shed light on underlying structure-property-mechanism relations as a function of the plasma conditions. In this talk, I will discuss the state-of-the-art in terms of computational catalysis modeling of non-thermal plasma-assisted catalysis, on-going challenges, and opportunities for progress.

Interactions of Atmospheric Plasmas with Catalytic Surfaces

Brian Bayer [a], Jingkai Jiang [b], Peter Bruggeman [b] and Aditya Bhan [a]

(a) University of Minnesota, Department of Chemical Engineering and Materials Science
(bayer116@umn.edu, abhan@umn.edu)
(b) University of Minnesota, Department of Mechanical Engineering (jian0284@umn.edu, pbruggem@umn.edu)

Reactions of plasma-produced radicals, electronically and vibrationally-excited species can synergistically impact catalytic processes. Unraveling the interactions among short-lived plasma-derived species with catalytic surfaces places a premium on enumerating the number nd type of plasma-produced species in the gas environment *above the surface* and enumerating the number and type of species these plasma-produced intermediates engender on the catalytic surface. This work introduces an experimental setup to study the plasma-phase and surface catalyzed molecular events that transpire in plasma-assisted catalysis by on-stream measurement of short-lived and stable species that enter and exit a packed catalyst bed. We illustrate the design and operation of this setup for conversion of N_2/H_2 mixtures to NH_3.

The setup (Figure 1) couples a radiofrequency-driven plasma jet with a catalyst bed containing transition metals supported on a nonporous metal oxide. The radio frequency discharge operates in Ar with admixtures of molecular gases up to 5% and enables the generation of large fluxes of radical species and operates at an electron temperature between 1-2 eV and electron densities in the range of 5×10^{18}- 5×10^{19} m^{-3} in the plasma plume, conditions favoring vibrational excitation.
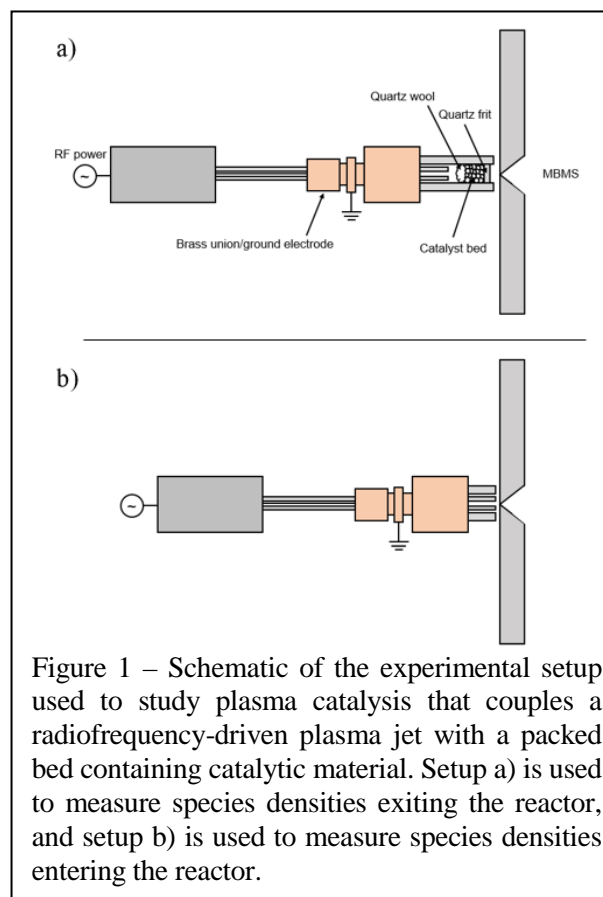

Figure 1 – Schematic of the experimental setup used to study plasma catalysis that couples a radiofrequency-driven plasma jet with a packed bed containing catalytic material. Setup a) is used to measure species densities exiting the reactor, and setup b) is used to measure species densities entering the reactor.

Molecular beam mass spectrometry (MBMS) is used to measure the densities of species entering or exiting the catalyst bed, including stable molecules, radical species, and vibrationally excited species. Species density measurements are made in separate experiments at the effluent of the plasma jet before the packed bed, at the effluent of the reactor tube in the absence of catalytic material, and at the effluent of the reactor tube containing catalytic material to determine the reactivity of different plasma-produced species over catalytic surfaces. Benchmark experiments are performed using this method for the N_2/H_2 system as a proof-of-concept to show how the presence of catalytic material alters NH_3 production. For example, measurements in Ar+1%N_2 yield vibrational temperatures of ground state N_2 up to 2600 K near the nozzle while at distances of 14 mm the vibrational temperature remains above 1800 K while the gas temperature did not exceed 330 K. The N density varies over the same distance from 4×10^{15}cm^{-3} to 2×10^{14}cm^{-3}. The densities of electronically excited $N_2(A)$ were below the detection limit. This result suggests that at for this condition a significant amount of energy being transported to the catalytic bed is stored in vibrational excitation. The impact of these species on the catalytic action on the gas feed will be discussed.

DRIFTS and Gas Phase FTIR Characterization of Plasma-enhanced Catalysis

Y. Li [a], M. Hinshelwood [a], J. Jiang [b], F. Doherty [c], B. Bayer [d], K. Shao [e], P. J. Bruggeman [b], A. Bhan [d], B. R. Goldsmith [c], A. Mesbah [e], and G. S. Oehrlein [a]

(a) Dept. of Materials Science and Engineering and the Institute for Research in Electronics and Applied Physics, University of Maryland, College Park, MD 20742 (oehrlein@umd.edu)
(b) Dept. of Mechanical Engineering, University of Minnesota, Minneapolis, MN 55455
(c) Dept. of Chemical Engineering, University of Michigan, Ann Arbor, MI 48109
(d) Dept. of Chemical Engineering and Materials Science, University of Minnesota, Minneapolis, MN 55455
(e) Dept. of Chemical and Biomolecular Eng., University of California, Berkeley, CA 94720

Cold atmospheric pressure plasma (CAP)-assisted thermal catalysis has shown promise to enhance catalytic efficiency by a process called plasma-catalyst synergy. In an effort to understand its mechanistic basis, we use Fourier-transform infrared spectroscopy (FTIR) to quantitatively measure the downstream gas components in real time and diffuse reflectance infrared Fourier transform spectroscopy (DRIFTS) to analyze the evolution of catalyst surface species in-situ. Our current work focuses on two areas: plasma-assisted decomposition of CH_4 over a Ni catalyst, and plasma-assisted formation of NO_x over a $Pt/SiO_2/Al_2O_3$ catalyst. In both cases, a well-studied atmospheric pressure plasma jet (APPJ) fed with Ar/O_2 is interacted at various plasma power levels with the catalyst located downstream of the APPJ. At the catalyst position, either CH_4 or N_2/O_2 is injected depending on the experiment, and catalyst temperature is varied from 25 ^{o}C to 500 ^{o}C. In addition, Prof. Bruggeman's group and Prof. Bhan's group at UMN are able to quantify plasma-produced reactive species using an identical APPJ operated under the same conditions via molecular beam mass spectrometry. The combination of the quantified reactive species from plasma effluent with the gas phase and surface species measurements can provide valuable information and shed light on the mechanism of plasma catalysis.

By correlating the quantified fluxes of reactive oxygen species from the APPJ effluent with the rates of CH_4 consumption and CO and CO_2 generation, we found that atomic oxygen plays an essential role in the oxidation of CH_4 to CO and CO_2. Operando DRIFTS analysis of surface species showed that trends of surface CO with operating conditions followed that of surface CH_n at 25 ^{o}C, indicating that surface CH_n is an intermediate species that is transformed to surface CO by plasma-produced O atoms. Characteristic changes of the vibrational frequency of surface CO with temperature and plasma power have been seen, and their origin is being examined. In particular, understanding of the bonding interactions of species of interest to a catalyst surface is being enabled through the computational modeling of Prof. Goldsmith's group at University of Michigan.

Similar approaches are being applied to the problem of plasma-catalyst enhanced NO_x production which is of interest as an intermediate of the nitrogen fixation process. As such, power efficient production of NO_x is of interest. In addition, to fully understand the plasma catalytic interaction, it is useful to determine the most efficient parameters for NO_x production within our parameter space. To that end, we are collaborating with Prof. Mesbah's group, whose Bayesian statistical modeling will help elucidate the most power efficient way to produce NO_x in our experimental arrangement. Initially, we have studied this efficiency determination with just an $Ar/O_2/N_2$ fed plasma jet system interacting with an inert $SiO_2-Al_2O_3$ powder in place of the platinum/$SiO_2-Al_2O_3$ catalyst. 150 operating conditions have been characterized, comprising a 5x5x6 parameter space of plasma power, catalyst powder bed temperature, and O_2 flow rate through the APPJ. This work is currently being extended to the interaction of the same APPJ effluents with the Pt catalyst.

Treatment of Aqueous Pollutants in Gas-liquid Plasma Reactors: Identification of the Key Parameters Controlling the Removal

Selma Mededovic Thagard, Xudong Su, Mikhail Vasilev, Jennifer Ganzallo and Faith Isowamwen

Department of Chemical and Biomolecular Engineering, 8 Clarkson Avenue, Clarkson University, Potsdam, 13699, NY, USA, smededov@clarkson.edu

For plasmas contacting liquids, convergent research in which fundamental science is translated into actual technologies is impeded by the lack of understanding of the physicochemical processes occurring at the plasma-liquid interface [1]. Development of plasma reactors for water treatment is largely trial and error based where individual reactors are optimized for the degradation of a single chemical compound usually by varying electrode arrangement, excitation source, discharge power, and solution conductivity, among other parameters, and examining the percentage of the compound degradation following the treatment. This work focuses on bulk liquid mixing, and in particular on examining the roles of physicochemical
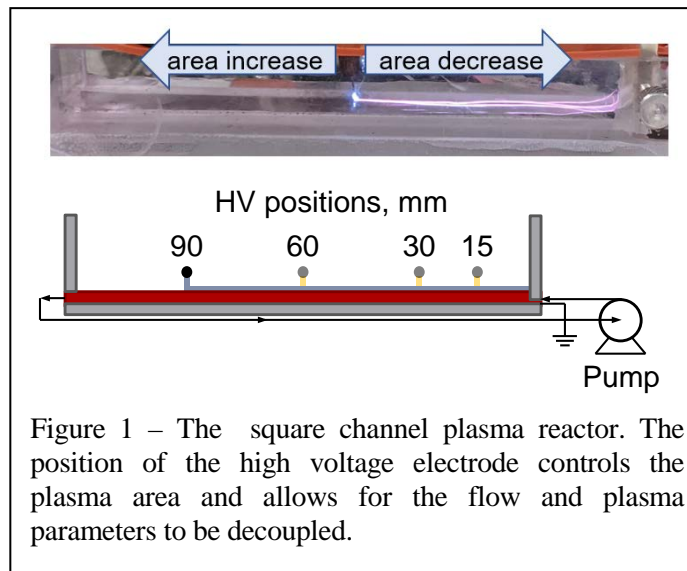

Figure 1 – The square channel plasma reactor. The position of the high voltage electrode controls the plasma area and allows for the flow and plasma parameters to be decoupled.

properties of the compounds treated as well as the convective modes by which they are transported to the plasma-liquid interface. We have measured degradation rates of a range of different compounds in the plasma spinning disc reactor and a square channel reactor with forced liquid recirculation. The latter is shown in Figure 1. Both reactors allow for the control of the fluid flow rate under the plasma of fixed contact area.

Results indicate that a compound's removal is largely determined by its bulk liquid concentration, the area of the plasma contacting the surface of the liquid and the rate of fluid renewal under the plasma. Depending on the relative magnitudes of these parameters, both convection and diffusion can limit the overall process efficiency. The best performing reactors use bubbles and sprays due to the high liquid renewal rates but even under those extreme conditions removal rates for some compounds remain low. In those cases, the reactor and the process design may necessitate unique mixing modes or the presence of a chemical agent that increases the interfacial concentration of the compound(s) in question.

References
[1] P.J. Bruggeman *et al*., Plasma Sources Sci. Technol. **25**, 053002 (2016).

N_2 Vibrational Excitation in Atmospheric Pressure Ns Pulse and RF Plasma Jets

Igor V. Adamovich

Department of Mechanical and Aerospace Engineering, The Ohio State University, Columbus, OH 43210, USA
adamovich.1@osu.edu

The main focus of this work is on (i) characterization of energy nonequilibrium and excited species generation in atmospheric pressure plasma jets (APPJ), and (ii) development of new laser diagnostics for monitoring transient plasma propagation over dielectric substrate surfaces exhibiting complex structure, with high spatio-temporal resolution. In the first thrust, vibrational excitation of nitrogen was measured by CARS in a quasi-two-dimensional N_2-Ar, N_2-He, and N_2-Ne APPJ excited by ns pulse and RF discharges, using CARS (see Fig. 1). The results indicate that N_2 vibrational excitation in RF plasma jets increases considerably as the nitrogen fraction in the mixture is reduced. The N_2/Ar data are compared with the kinetic modeling predictions, showing that vibrational excitation is controlled primarily by electron impact, anharmonic V-V pumping, and V-T relaxation by N atoms. In comparison, energy transfer from the excited electronic state, $N_2(A^3\Sigma_u^+,v)$, populated by energy transfer from the metastable Ar atoms, has a minor effect on the vibrational populations of the ground electronic state, $N_2(X^1\Sigma_g^+,v)$.
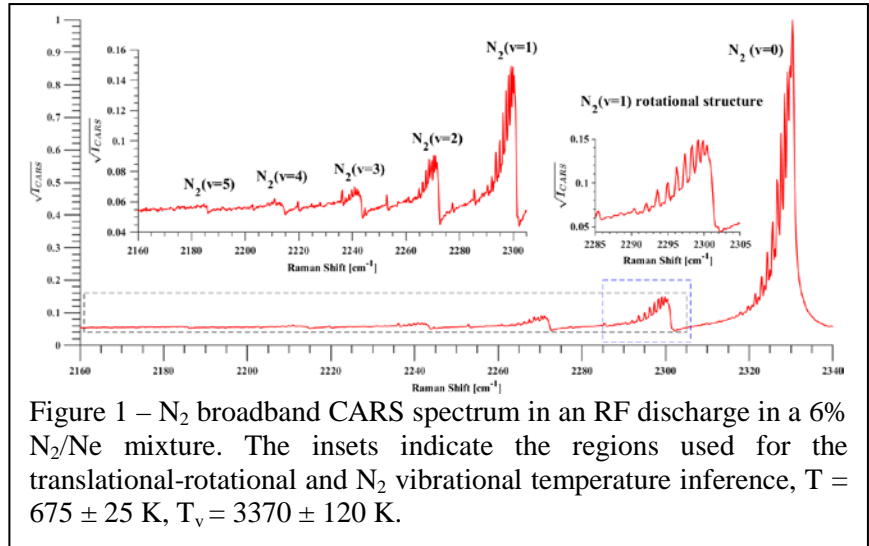

Figure 1 – N_2 broadband CARS spectrum in an RF discharge in a 6% N_2/Ne mixture. The insets indicate the regions used for the translational-rotational and N_2 vibrational temperature inference, $T = 675 \pm 25$ K, $T_v = 3370 \pm 120$ K.

In the second thrust, spatial resolution of ps Electric Field Induced Second Harmonic (EFISH) generation, used for detection of ionization wave formation and propagation in the plasma [1], has been enhanced by using two non-collinear laser beams. The beams overlap only near the focal point, generating the Spatially Enhanced EFISH (SEEFISH) signal over a shorter region compared to that in the collinear phase matching. The resulting SEEFISH signal, spatially isolated from the "conventional" EFISH signal, is detected for the first time. Blocking of either of the two beams results in a complete suppression of the signal. Measurements of a known Laplacian field generated between two parallel cylinder electrodes in ambient air demonstrated that SEEFISH improves the spatial resolution of the measurements by well over a factor of 2. Increasing the beam crossing angle, or reducing the focal distance of the focusing lens, shortens the region from which the signal originates (measured by scanning a glass plate along the crossed beams), thus improving the spatial resolution. However, this also leads to a dramatic reduction of the signal, far more significant than expected from the theoretical predictions. At this time, the reason for the signal reduction is not understood. The new diagnostic has considerable potential for measurements of electric field distributions in high-pressure plasmas near surfaces, with high temporal and spatial resolution. EFISH and SEEFISH measurements of ionization waves in APPJ, propagating over substrate surfaces with a periodic structure (microchannel arrays) by is underway.

References

[1] K. Orr, X. Yang, I. Gulko, and I.V. Adamovich, "Formation and Propagation of Ionization Waves During Ns Pulse Breakdown in Plane-to-Plane Geometry", Plasma Sources Science and Technology **29** (2020) 125022.

ExB Plasmas for Processing of Nanomaterials

Yevgeny Raitses [a], Arthur Dogariu [b], Fang Zhao [c], Shurik Yatom [a], and Kai-Mei Fu [d]

(a) PCRF, PST Department, Princeton Plasma Physics Laboratory (yraitses@pppl.gov)
(b) PCRF, MAE Department, Princeton University (adogariu@princeton.edu)
(c) Physics Department, Princeton University (fangz@princeton.edu)
(d) Physics Department, University of Washington (kaimeifu@uw.edu)

The plasma discharge with applied crossed electric and magnetic fields, operating with argon-hydorgen gas mixture in a mtorr pressure range can generate the flux of hydrogen atoms enabling low damage hydrogenation on an atomically thin 2D material such as graphene [1]. Unlike existing a keV range e-beam plasma sources with applied magnetic field [2], this ExB plasma discharge is sustained by lower energy (< 50 eV) non-thermal electrons esxtracted from a RF plasma cathode [3]. Electrostatic probes, optical emission spectroscopy and fs-Two-Photon Absoprtion Laser-Induced Flurescnence (TALIF) diagnostics are used to characterize the effect of the magnetic field on this discharge. Plasma measurements revealed that the application of the magnetic field allows to confine a larger fraction of energetic electrons in the plasma which generates more hydrogen atoms and ions than that without the magnetic field (Fig. 1). The plasma density and density of hydrogen atoms increases with the magnetic field until they reach their comparable saturation levels ($\sim 4 \times 10^{10}$ cm^{-3}) at about 20-30 Guass. This saturation is associated with plasma instabilities which degrade the magnetic confirment of energetic electrons [3]. The Raman spectra and the XPS spectra investigation demonstrates that at weaker magnetic fields (less than 20 Gauss) this cross-field plasma provides a promising way to achieve higher hydrogen coverage than other reported plasma methods. The plasma measurements explain low damage induced by the ions to the 2D thin films. The main reasons are in 1) a relatively low local electron temperature which determines the sheath voltage drop - the plasma ions accelerated by this voltage drop fail to acquire enough energy to displace the carbon atoms in the graphene; 2) a low plasma density at the periphery of the cylindrical plasma column that limits s a flux of low energy ions, and 3) the direction of the applied electric field that accelerates plasma generated ions away from the

Figure 1 – Density of hydorgen atoms deduced from fs-TALIF measurements in the ExB discharge operating with argon-(20%) hydorgen gas mixture at 9 mtorr.

samples towards the reactor chamber axis. The low damage and high coverage plasma treatment make this low-temperature fine-tunable plasma-based source of low energy ions and radicales attractive for the use in functionalizing thin films, processing of ion energy-sensitive materials etc. This plasma source is now offered to users interested in materials processing science projects at the Princeton Collaborative Research Facility (http://pcrf.pppl.gov).
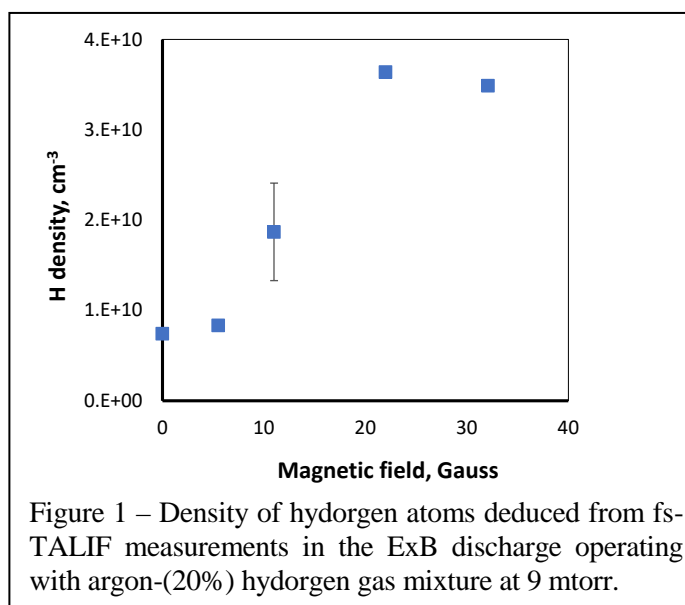
References
[1] F. Zhao, Y. Raitses, X. Yang, A. Tan, and C. G. Tully, Carbon **177**, 244 (2021).
[2] S. G. Walton et al., ECS J. Solid State Sci. Technol. **4**, N5033 (2015)
[3] E. Rodriguez, V. Skoutnev, Y. Raitses, A. Powis, I. Kaganovich, and A. Smolyakov, Phys. Plasmas **26**, 053503 (2019)

Advanced Optical Diagnostics for Low Temperature Plasmas; Neutral Density Mapping and Dynamics in RF-Heated PFRC Plasma

Arthur Dogariu [a], Sangeeta P. Vinoth [b] and Samuel A. Cohen [b]

(a) Princeton University, Princeton, NJ (adogariu@princeton.edu)
(b) Princeton Plasma Physics Laboratory, Princeton. NJ

The talk will first present recent developments and results using advanced optical diagnostics in LTP plasmas at the DOE Princeton Collaborative Research Facility (PCRF). Some of the premiere results include measurements of neutrals densities (such as O, N) using femtosecond Two-Photon Laser Induced Florescence (fs-TALIF) and velocimetry using Femtosecond Laser Electronic Excitation Tagging (FLEET) [1] in an arc jet plasma (with L. Maddalena, Univ. of Texas, Arlington) [2], imaging atomic species induced in a liquid by an impinging plasma jet (with K. Stapelmann, North Carolina State Univ.) via fs-TALIF, and mapping the spatial and temporal profile of the electric field in a corona discharge using E-FISH [3] (with S. Leonov, Notre Dame, and C. Guerra-Garcia, MIT).

The second part of the talk will present the results obtained by using the fs-TALIF diagnostic to measure time and spatially resolved neutral atom densities in RF-heated Princeton Field Reversed Configuration-2 (PFRC-2) [3] plasmas. The density of neutral H^o or Kr atoms is imaged and time resolved using a 100fs amplified laser system with a repetition rate of 1kHz, capable of generating 200 μJ/pulse tunable in the UV region. Figure 1 (Top) depicts the relevant energy levels for the two-photon excitation and the subsequent fluorescent emission for H and Kr. Measurements during the steady-state and termination phases of ~50 kW hydrogen discharges show a spatially uniform H^o density of order 10^{11} cm^{-3}. A ten-fold decrease of the in-plasma Kr^o density was observed in krypton discharges at similar heating power. For the pulsed RF plasma we measure the dynamics of the H^o for pump peak powers between 40-80 kW with microsecond temporal resolution. We compare the dynamics of the H^o with the dynamics of the plasma excited H atoms and measure the neutrals lifetime. In the case of the Kr plasma, the discharge induces a reduction in the ground-state density, as shown in Fig. 1 (Bottom). These measurements are the first measures of H^o and Kr time-dependent profiles in the FRC plasma device, and they help to better understand transport in plasma through the relative importance of ionization, recombination and recycling processes.
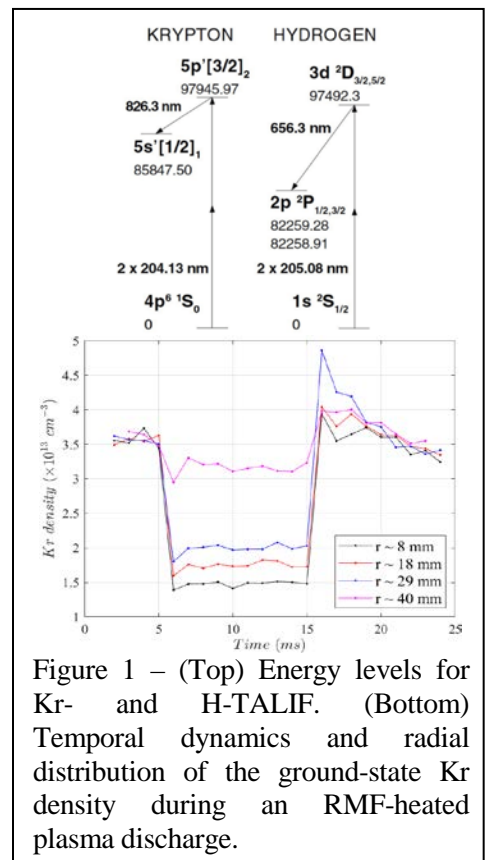

Figure 1 – (Top) Energy levels for Kr- and H-TALIF. (Bottom) Temporal dynamics and radial distribution of the ground-state Kr density during an RMF-heated plasma discharge.

References
[1] J. B. Michael, M. R. Edwards, A. Dogariu and R. B. Miles, Appl. Opt. **50**, 5158 (2011).
[2] https://www.uta.edu/news/news-releases/2020/12/08/arc-wind-tunnel-breakthrough
[3] A. Dogariu, B. M. Goldberg, S. O'Byrne, and R. B. Miles, Phys. Rev. Appl., **7**, 024024 (2017).
[4] S. A. Cohen et al., Phys. Rev. Lett. **98**, 145002 (2013).

Plasma Diagnostics of Mesoporous Silica Packed Bed Reactors for Ammonia Synthesis

S. Gershman [a], H. Fetsch [a], F. Gorky [b], and M. Carreon [c]

(a) Princeton Plasma Physics Laboratory (sgershma@pppl.gov)
(b) South Dakota School of Mines and Technology
(c) University of Massachusetts Lowell (Maria_Carreon@uml.edu)

Plasma catalytic ammonia production at atmospheric pressure holds great promise due to its small scalable design, easy intermittent operation, and use of renewable energy. To meet the ammonia production, plasma-catalytic systems need intelligent design of catalytic materials with specific properties compared to traditional catalysts. Plasma helps to dissociate N_2 through vibrational excitations and produces H* radicals. Based on preliminary experiments and DFT calculations, [1,2] a suitable catalyst in a plasma reactor is one that dissolves H* reducing hydrogen recombination and allowing it instead to react with plasma activated nitrogen to form NH*, while only weakly binding nitrogen. Mesoporous oxides such as silica (SBA-15) have these properties [3,4], but still some report catalytic benefit from metals supported on a porous structure. [5,6] Here we use optical emission spectroscopy (OES), Fourier transform infrared absorption spectroscopy (FTIR-AS), and electrical measurements to characterize plasma-catalytic packed bed dielectric barrier reactors (PB), one type packed with SBA-15 (7 nm pores) and another with SBA-15 enriched with 10% wt.
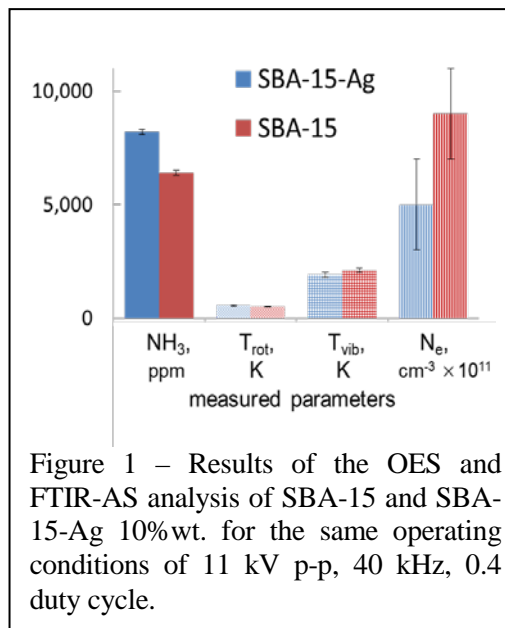

Figure 1 – Results of the OES and FTIR-AS analysis of SBA-15 and SBA-15-Ag 10%wt. for the same operating conditions of 11 kV p-p, 40 kHz, 0.4 duty cycle.

Ag, both operating in a 1:1 N_2 and H_2 gas mixture. OES shows a higher intensity of H lines in SBA-15 as compared to SBA-15-Ag and a measurable NH* band in SBA-15 suggesting a higher concentration of H and NH*. However, at the same applied voltage, FTIR-AS of the effluent show a ~20% higher concentration of NH_3 for SBA-15-Ag. Further OES analysis shows a 10% lower rotational temperature, a higher vibrational excitation temperature and a higher electron density in SBA-15 PB reactor as compared to SBA-15-Ag at the same conditions (Figure 1). This suggests that the presence of Ag affects the plasma conditions which in turn can have an effect on the catalytic pathways. Hence, a study of the plasma conditions can aid in the intelligent design of the catalysts used in plasma catalysis, specifically in PB reactors for ammonia synthesis.

References
[1] J. Shah, et al. ChemCatChem 2020, **12** (4), 1200-1211.
[2] J. Shah, et al. ACS Applied Energy Materials 2018, **1** (9), 4824-4839.
[3] T. Norby, Dalton transactions 2004, (19), 3012-3018.
[4] F. Gorky, et al. J. Phys. D Appl. Phys. 2021, **54** (26), 264003.
[5] F. Gorky, et al., J. Catal. 2021, **393**, 369-380.
[6] P. Barboun, et al., ACS Sustain. Chem. Eng. 2019, **7** (9), 8621-8630.

PPPL Modeling Tools for Low Temperature Plasmas Available through the Princeton Collaborative Research Facility

Igor D. Kaganovich [a], Stephane Ethier [a], Alexander Khrabrov [a], A. Khodak [a], Andrew (Tasman) Powis [a], Dmytro Sydorenko [b] and Yuri Barsukov [c]

(a) Princeton Plasma Physics Laboratory, Princeton University, Princeton, NJ (ikaganov@pppl.gov)
(b) University of Alberta, Edmonton, AB T6G2E9, Canada (sydorenk@ualberta.ca)
(b) Peter the Great Saint Petersburg Polytechnic University, Saint Petersburg, Sankt-Peterburg, 195251, Russia (barsukov.yuri@gmail.com)

The Princeton Plasma Physics Laboratory (PPPL) relies on several simulation tools for the modeling of low-temperature plasma devices. For the fluid plasma simulations, we utilize a modified version of the commercial ANSYS code. For kinetic simulations, we rely on several kinetic particle-in-cell codes: the 2D EDIPIC code and the 3D LTP-PIC on GPUs (see Fig.2). For molecular dynamics simulations, we have experience with several open-source codes as shown in Fig.1. For quantum chemistry, we utilize the Density Functional Theory (DFT) approximation via Gaussian and VASP, as well as codes based on the DFT- Tight Binding approximation.

Figure 1 – Schematics of simulations of boron-nitride nanotubes from the first principles using a variety of quantum chemistry tools from Ref.[1].

Figure 2 – (a) Visualization of the rotating spoke instability within a three-dimensional simulation of a Penning discharge. The two-dimensional slice and iso-volume show ion density. Streamlines indicate electron current. For full animation see online from Ref.[2].

References

[1] Yuri Barsukov, Omesh Dwivedi, Igor D Kaganovich, Sierra Jubin, Alexander Khrabry, and S Ethier, "Boron nitride nanotube precursor formation during high-temperature synthesis: Kinetic and thermodynamic modelling" accepted to nanotechnology (2021) https://doi.org/10.1088/1361-6528/ac1c20
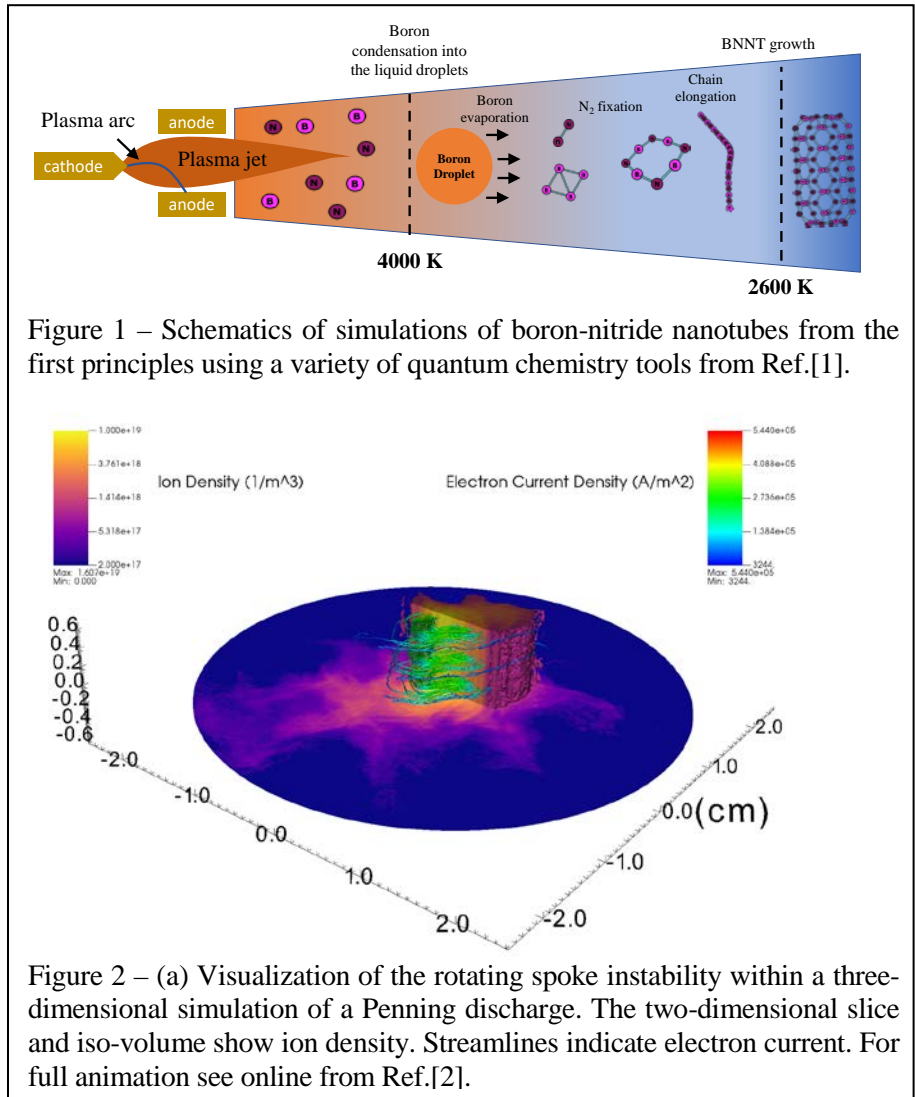[2] A. T. Powis, "Visualization of the rotating spoke instability within a 3Dsimulation of a Penning discharge. https://www.youtube.com/watch?v=Qlz3-by63yw .

Coherent Thomson Scattering

Mikhail Shneider [a], Aleandros Gerakis [b] and Mikhail Mokrov [c]

(a) Princeton University, Princeton, NJ (shneyder@princeton.edu)
(b) Texas A&M University, College Station, TX (agerakis@TAMU.edu)
(c) Institute for Problems in Mechanics, RUS (mmokrov@gmail.com)

The results of a theoretical study of coherent Thomson scattering (CTS) are presented. At the core of the proposed four-wave mixing Thomson scattering scheme is the utilization of optical lattices for the creation of the periodic perturbation of electron density in plasmas and observation of Bragg scattered light from these perturbations. The spectrum of CTS in plasma in the limiting case when the period of the optical lattice is less than the Debye length is analyzed by solving an electron Boltzmann equation. The electric field is calculated self-consistently from the Poisson equation. Qualitatively, in the considered limiting case, the results obtained for the CTS are similar to those obtained earlier for coherent Rayleigh scattering in an unionized gas [1,2]. With low intensities of pump lasers creating the optical lattice $I = 10^9$ W/cm^2, the calculated spectra are nearly Gaussian with widths slightly wider than the incoherent Thomson widths. At higher intensities $I = 10^{12} - 10^{13}$ W/cm^2 the line shape narrows and saturates to a width approximately half of that found at low pump intensities. The four-wave mixing nature of the CTS renders it ideal for application in optically noisy environments, such as those encountered in plasmas - while the necessary angled crossing of the laser beams provides with a high degree of localization and spatial resolution. Furthermore, if one

Figure 1 – (a) The creation of an optical lattice within a plasma, by two almost counter-propagating optical beams. A third probe beam at the Bragg angle on the induced electron periodic density modulation, giving rise to CTS signal beam. (b) - Examples of calculated CTS spectral profiles from non-equilibrium plasma at different pump intensities. The background gas is argon at T = 293 K and p = 45 Torr. Plasma electrons with T_e = 1 eV and n_e = 10^{11}

utilizes a chirped lattice approach [3], it is envisioned that four-wave mixing Thomson scattering scheme will have single shot spectral acquisition, making it an ideal diagnostic for highly dynamic plasma. Possible applications of CTS - remote nonintrusive measuring the electron temperature in plasma. The predicted signal of CTS is tens of times higher than at conventional Thomson scattering under the same conditions.

References
[1] M. N. Shneider, P. F. Barker, X. Pan, and R. B. Miles, Optics Communications **239**, 205 (2004).
[2] H. T. Bookey, M. N. Shneider and P. F. Barker, Phys. Rev. Lett. **99**, 133001 (2007).
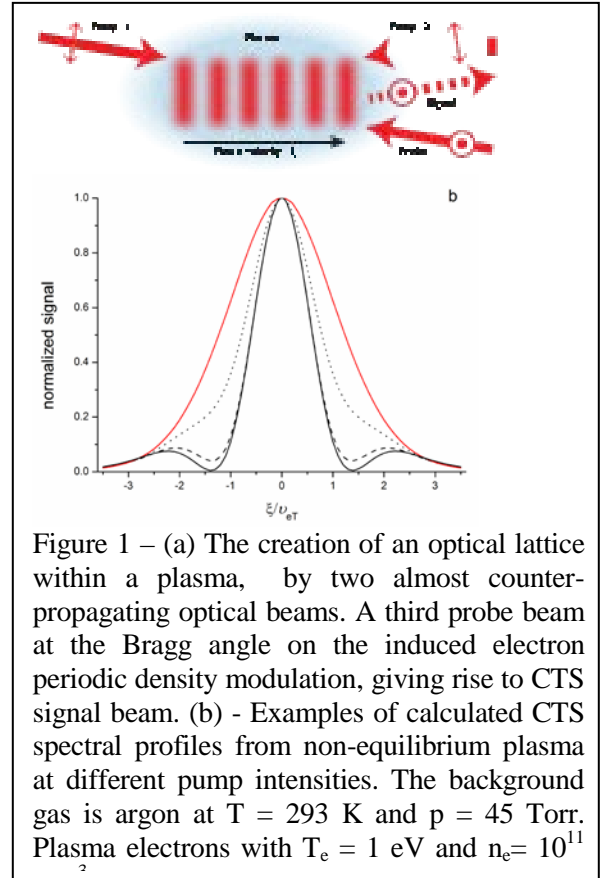[3] A. Gerakis, M. N. Shneider, and P. F. Barker, Optics letters **38**, 4449 (2013).

Characterization of Plasma in RF Jet Interacting with Water: Thomson Scattering Versus Spectral Line Broadening
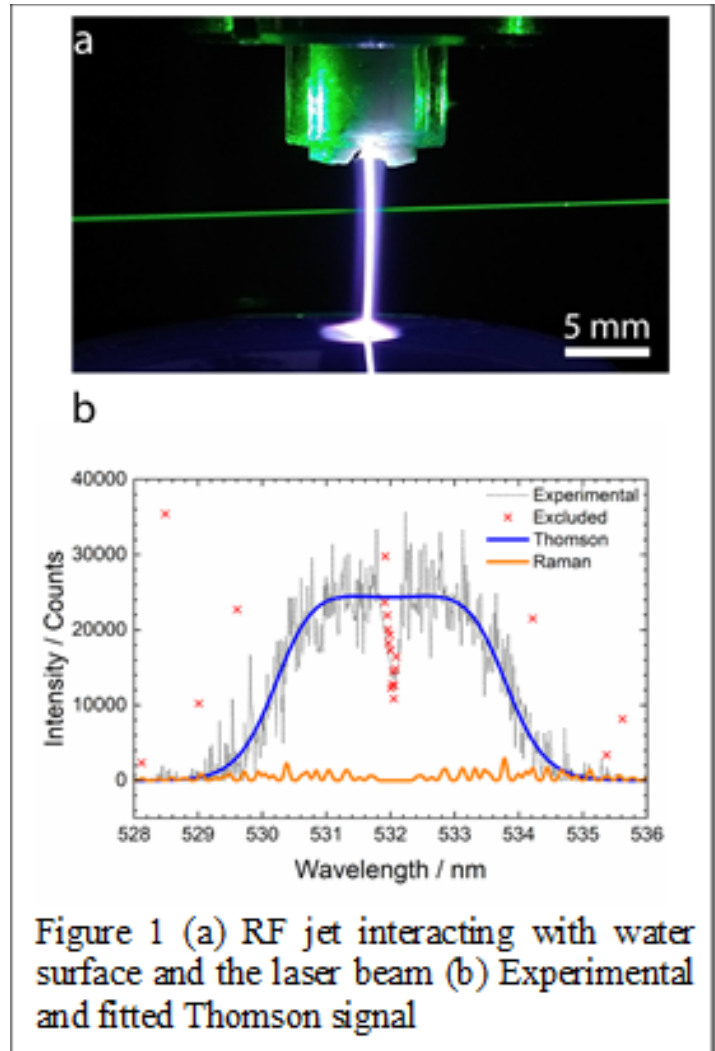
Shurik Yatom [a], Trey Oldham [b], Elijah Thimsen [b], Yevgeny Raitses [a]

(a) Princeton Plasma Physics Laboratory, Princeton University, Princeton, NJ, USA (syatom@pppl.gov)
(b) Energy, Environmental and Chemical Engineering, Washington University in Saint Louis, St. Louis, MO, USA

This work reports on comparison of plasma characteristics measured by means of Thomson scattering and spectral line analysis. Both measurements were performed on RF powered plasma jet, running at 20% duty cycle, with Ar as a carrier gas. The plasma was impinging on a water surface located 1 cm away from the powered needle electrode. To support the plasma analysis, we also have performed gas temperature measurement by means of laser Rayleigh scattering and detailed time-resolved imaging of the plasma filament. The difference between the plasma parameters measured by the two methods is discussed and analyzed. The main observed difference is in the re-ignition of the jet following the voltage switch-off.

In this presentation I will also briefly review other PCRF projects that were carried out during year 2021 and have to do with low-temperature plasma sources and the characterization of thereof.

Figure 1 (a) RF jet interacting with water surface and the laser beam (b) Experimental and fitted Thomson signal

Sandia National Laboratories Plasma Research Facility

Shane M. Sickafoose [a], Brian Bentz [a], Jonathan Frank [b], Nils Hansen [c], Matthew Hopkins [a], Chris Kliewer [c], Amanda Lietz [a], Dirk van den Bekerom [b]

(a) Applied Optical and Plasma Science, Sandia National Laboratories, Albuquerque, NM, USA,
(b) Plasma and Reacting Flow Science, Sandia National Laboratories, Livermore, CA, USA
(c) Gas Phase Chemical Physics, Sandia National Laboratories, Livermore, CA, USA

In this talk we will provide an update on the progress in the hosting of collaborators at Sandia's PRF. Despite the widespread impact of COVID upon the ability for interactions with collaborators, Sandia hosted multiple collaborations this past year. The staff is bringing on new capabilities online in support of fundamental plasma research as well as reaching out to potential collaborators. Our Proposal Call for new submissions is opening in early October.

Imaging of Methyl Radical in Plasmas by Photofragmentation Laser-Induced Fluorescence

Dirk van den Bekerom [a], Caleb J. Richards [b], Igor V. Adamovich [b], and <u>Jonathan H. Frank</u> [a]

(a) Combustion Research Facility, Sandia National Laboratories, Livermore, CA (jhfrank@sandia.gov)
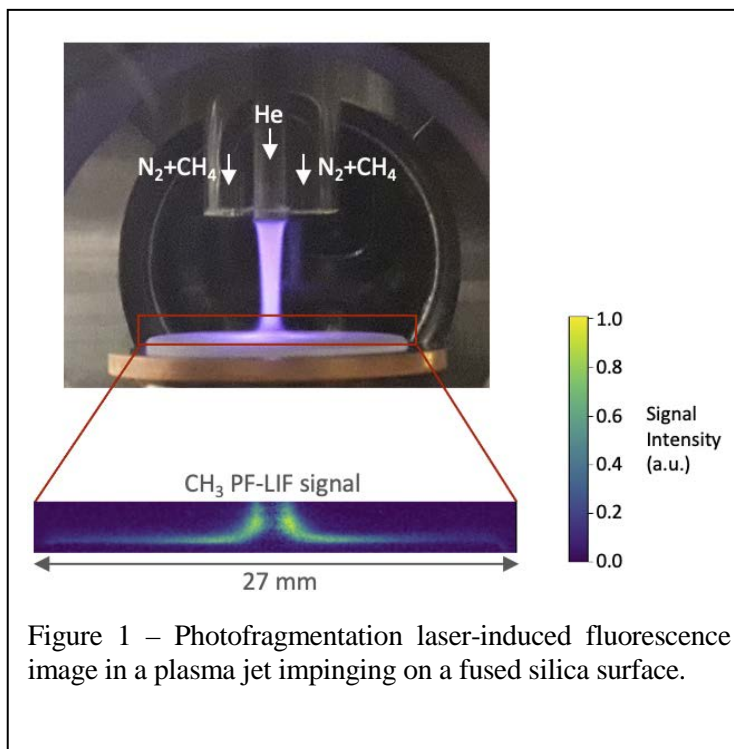(b) Department of Mechanical and Aerospace Engineering, Ohio State University, Columbus, OH
(adamovich.1@osu.edu)

The methyl radical (CH_3) is a key intermediate species in plasma assisted processes such as catalysis and combustion. For example, a key step in the oxidative coupling of methane (OCM) is the initial extraction of a hydrogen atom from methane, which results in the formation of methyl. Subsequent reactions in OCM produce high value products such as C2 species. Despite the importance of methyl in plasma assisted hydrocarbon chemistry, there remains a significant gap in understanding its formation and consumption within a plasma and at plasma-surface interfaces. There is thus a need for spatially and temporally resolved in-situ imaging measurements of methyl distributions in plasma environments. However, imaging of methyl is particularly challenging because it cannot be detected directly by laser-induced fluorescence. One approach for detecting non-fluorescing species is to photodissociate the molecule of interest and detect the resulting photofragments. We demonstrate a technique for imaging the two-dimensional distribution of methyl using photofragmentation laser-induced fluorescence (PF-LIF). In this technique, methyl is photodissociated by a 213 nm laser beam (5th harmonic of a Nd:YAG laser) to produce CH fragments. These photofragments are then detected with LIF imaging by exciting a transition in the B-X band of CH with a probe laser at 390 nm. Collisional B-A electronic energy transfer then populates the A-state of CH, after which fluorescence is detected in the A-X band near 430 nm with a gated ICCD camera and suitable band pass filter. This non-resonant detection scheme enables interrogation of plasmas near surfaces.

Photofragmentation LIF of methyl has previously been demonstrated for qualitative imaging in combustion research [1]. Here, we demonstrate 2D PF-LIF imaging of methyl in nanosecond pulsed plasmas containing hydrocarbon fuels. We investigate the feasibility of calibrating the PF-LIF technique for quantitative measurements by producing a known amount of methyl through photodissociation of a precursor molecule. We evaluate the effects of collisional quenching on the LIF measurements of the CH photofragments by measuring decay times of CH-LIF signals in different collisional environments with and without a plasma.

Figure 1 – Photofragmentation laser-induced fluorescence image in a plasma jet impinging on a fused silica surface.

References
[1] B. Li, D. Zhang, M. Yao, Z. Li, Proc. Combust. Inst. **36**, 4487 (2017).

Advanced Modeling Capabilities for Low-Temperature Plasma Simulation

Matthew M. Hopkins and Amanda M. Lietz

Applied Optical and Plasma Science, Sandia National Laboratories, Albuquerque, NM, USA,
mmhopki@sandia.gov, amlietz@sandia.gov

In this talk we provide an update on the modeling capabilities available at the Sandia National Laboratories' Low-Temperature Plasma (LTP) Research Facility. These capabilities may not be well-known in the broad LTP community. While direct access to the capabilities discussed below requires US citizenship, we have operated in a mode where simulations are undertaken by Facility staff and the results and progress are discussed in close consultation with collaborators.

Our most mature capabilities are found in our particle-in-cell (PIC) direct simulation Monte Carlo code, Aleph. Aleph is a massively parallel, electrostatic, unstructured mesh, code capable of running on 10k's of cores. It is additionally distinguished from other collisional PIC approaches by the inclusion of photonic processes simulated through the Lagrangian particle framework. A variety of applications will be described, including current projects for high aspect ratio etching, ion-acoustic instabilities, and thermionic power generation.

We have recently developed new capabilities in fluid and hybrid modeling of plasmas. In addition to Aleph, we have access to a suite of continuum modeling codes in our Sierra framework, including multiphase fluid models that can incorporate free and moving boundaries, adaptive mesh refinement, etc. An example of this work, simulation of high energy arc faults, will be provided demonstrating coupling of a reduced plasma fluid model, electrostatics, thermal evolution, and radiation transport. Use of these codes is a recent development, and we welcome discussions on possible future collaborations.

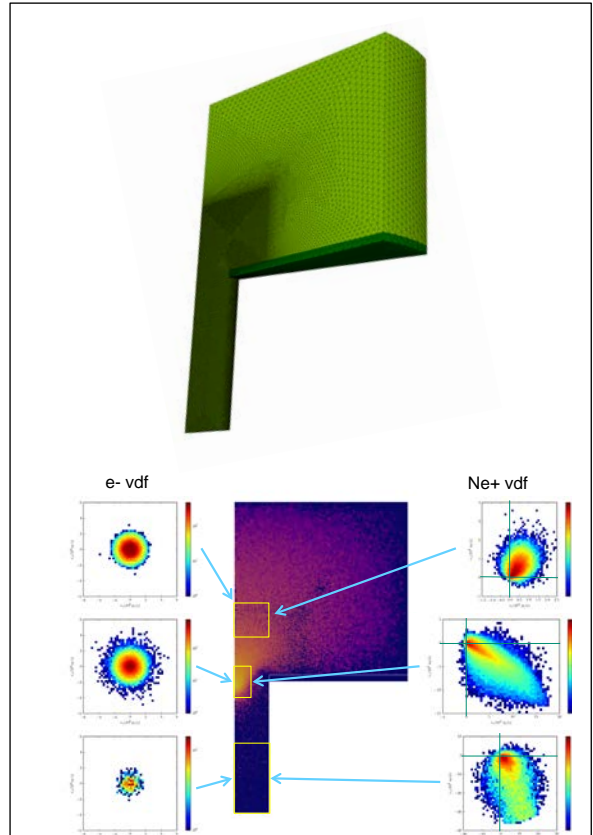Figure 1 - (left) 3D unstructured mesh for hollow cathode Ne discharge at 1 atm. (right) 2D slice through domain with e- and Ne+ velocity distributions at various locations.
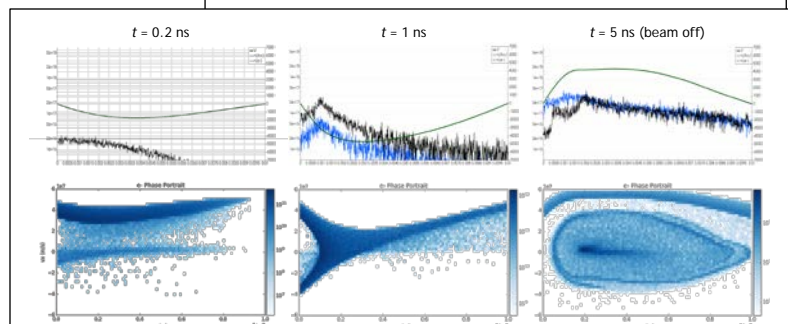

Figure 2 - (top) e- and Ar+ densities, and plasma potential for ~5 keV e-beam propagating left-to-right through 300 mTorr Ar background. (bottom) vx vs. x phase space plots. Columns are different times: 0.2, 1, and 5 ns.

Development of Hybrid Coherent Raman Imaging and E-FISH Approaches for Low Temperature Plasma Assisted Chemistry

Christopher J. Kliewer [a], Madeline S. Vorenkamp [b], Andrey Y. Starikovskiy [c], Yiguang Ju [d]

(a) Sandia National Laboratories, Livermore, CA (cjkliew@sandia.gov)
(b) Princeton University, Princeton, NJ (msv@princeton.edu)
(c) Princeton University, Princeton, NJ (astariko@princeton.edu)
(d) Princeton University, Princeton, NJ (yju@princeton.edu)

Low temperature plasmas provide opportunities for enhancing high-value energy conversion processes in both energy efficiency and chemical selectivity. Nonequilibrium distributions of electronic and molecular rovibronic excitations as well as active speciation in non-thermal equilibrium plasmas offer unique control over the outcome of chemical reactions and process optimization. While the understanding of low temperature plasma assisted chemistry is still emerging, clear benefits have already been demonstrated in such fields as plasma assisted catalysis and plasma assisted combustion. However, improved understanding of the underlying chemical kinetic mechanisms requires new capabilities in in-situ probing of plasma-chemistry interactions.

Recent developments in our lab have allowed for coherent Raman spectroscopy measurements to be extended to multispecies [1] as well as linear [2] and planar imaging [3] within a single laser pulse in complex environments. In this talk, we will discuss the development of nonlinear coherent Raman imaging, and its application to study the nonequilibrium chemical processes of low temperature plasmas. The coupling of additional spectroscopic probes, such as electric field induced second harmonic generation (E-FISH) and laser induced-fluorescence (LIF) for tracking of important chemical pathways of low concentration species will also be discussed.

These approaches are adapted to study the development of a combustion wave as it undergoes a transition from subsonic deflagration propagation to supersonic detonation in a microchannel, the so-called deflagration-to-detonation transition (DDT), in a micro-channel. Low temperature plasma in the pre-reactive mixture is used with the goal of accelerating the DDT transition or

Figure 1 - Microchannel dielectric barrier discharge in the pre-reactive mixture prior to DDT combustion initiation.

stabilizing detonation propagation upon combustion with possible implications for next-generation power generation and engine design.
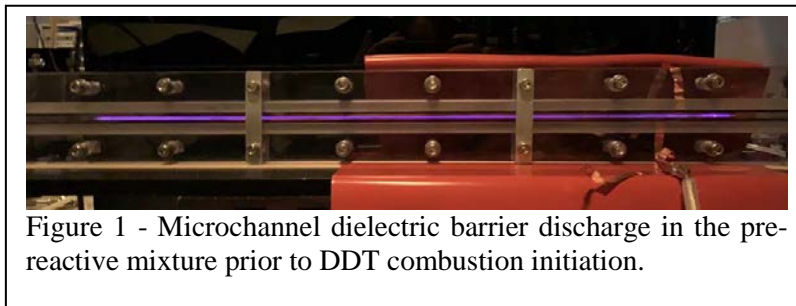
Because of the difficulties associated tight focusing of a femtosecond beam inside a microchannel, novel phase matching and chirping schemes have been developed for successful 1D-CARS and E-FISH measurements of relative molecular species concentration, temperature, and electric field for these measurements.

References
[1] A. Bohlin and C. J. Kliewer, J. Phys. Chem. Lett. **6**, 643-649 (2015).
[2] A. Bohlin, M. Mann, B. D. Patterson, A. Dreizler, C. J. Kliewer, Proc. Comb. Inst. **35**, 3723-3730 (2015).
[3] A. Bohlin and C. J. Kliewer, J. Chem. Phys. **138**, 221101 (2013).

Simulations of Nonequilibrium Thermionic Cs Plasmas

<u>Amanda M. Lietz</u> [a], Roelof Groenewald [b], Peter Scherpelz [b], and Matthew M. Hopkins [a]

(a) Sandia National Laboratories (amlietz@sandia.gov, mmhopki@sandia.gov)
(b) Modern Electron, LLC (roelof.groenewald@modernelectron.com, peter.scherpelz@modernelectron.com)

Thermionic generators are a promising technology for distributed power generation due to their compact size, high power densities, and lack of moving parts. They can convert essentially any heat source directly into electrical power [1]. In these devices, a hot electrode emits electrons by thermionic emission. With a vacuum between electrodes, the emitted electrons produce significant space charge, inducing an electric field that greatly limits the total current and the power density [2]. For this reason, the gap is often filled with a plasma, which provides ions to neutralize this space charge and allow larger currents to flow. Cs is particularly useful because of its low ionization energy (3.89 eV), which means that a plasma can be sustained at low applied voltages [3].

In this paper, we will discuss the results of kinetic simulations of a thermionic generator containing a Cs plasma. Aleph, a particle-in-cell direct simulation Monte Carlo code (PIC-DSMC), was used to model a 1-dimensional plasma in a 250 μm gap. 52 excited states and 862 reactions are included in the model. A 200 nm mesh and 89 fs timestep is used to resolve the collision timescales and length scales.

The results of a simulation at 113 mTorr with 1.82 V applied voltage and a thermionic current of 10 A/cm^2 are shown in Fig. 1. The ion density generated by electron impact processes in the plasma results in a potential that is positive throughout the gap (negative potentials would be seen in a space-charge-limited case). The electron energy distribution (EED) for each region of the discharge is highly non-Maxwellian, and depletion of the EED at 0.1-1.8 eV illustrates the importance of including reactions with excited states in the model. The effect of Cs pressure and comparisons with conventional simplified models used in the field will be discussed.
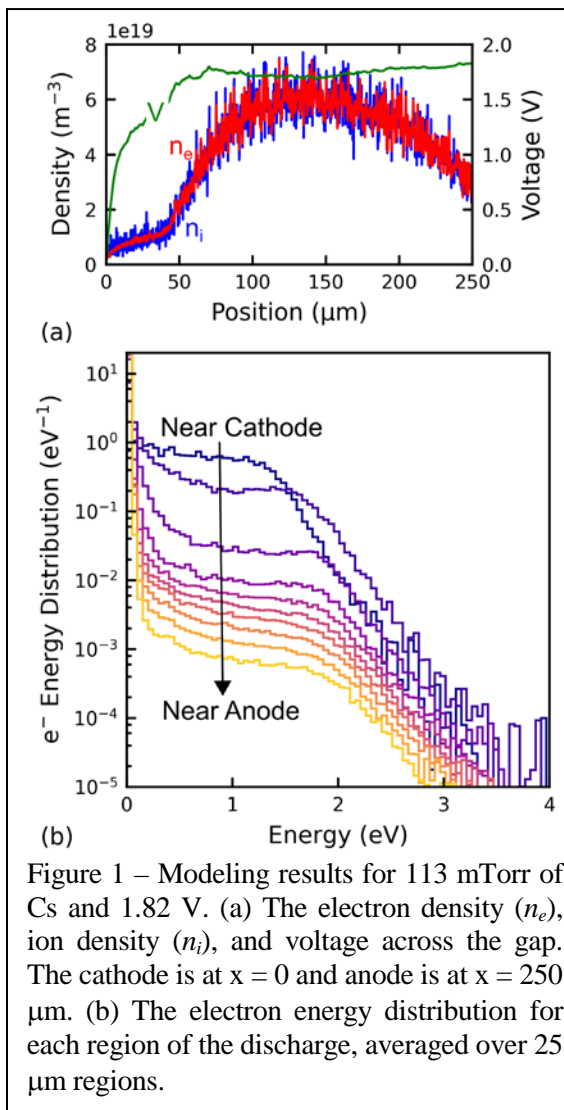
Figure 1 – Modeling results for 113 mTorr of Cs and 1.82 V. (a) The electron density (n_e), ion density (n_i), and voltage across the gap. The cathode is at x = 0 and anode is at x = 250 μm. (b) The electron energy distribution for each region of the discharge, averaged over 25 μm regions.

References
[1] D. B. Go, J. R. Haase, J. George, J. Mannhart, R. Wanke, A. Nohej and R. Nemanich, Front. in Mech. Eng. **3**, 13 (2017).
[2] C. D. Child, Phys. Rev. (Series I) **32**, 492 (1911).
[3] D. R. Wilkins and E. P. Gyftopoulos, J. Appl. Phys. **37**, 2892 (1966).

Ns Pulse and Hybrid Plasmas for Plasma Assisted Ignition and Catalysis

I. V. Adamovich

Dept. of Mechanical and Aerospace Engineering, The Ohio State University, Columbus, OH 43210, USA
(adamovich.1@osu.edu)

The focus of this work is on understanding the underlying kinetic mechanisms controlling plasma assisted combustion and plasma assisted catalysis, using laser diagnostics and kinetic modeling. The experiments have been made in high-pressure, repetitive ns pulse, double dielectric barrier discharge plasmas generated in canonical plane-to-plane geometry. These plasmas exhibit excellent stability and reproducibility, and lend themselves to kinetic modeling analysis. The results are obtained in the following thrusts, (i) measurements and analysis of generation and decay of HO_2, a major radical controlling chain branching and chain termination in preheated H_2-O_2, CH_4-O_2, and C_2H_4-O_2 mixtures diluted in Ar; (ii) time-resolved measurements of vibrational excitation and relaxation of carbon dioxide in CO_2-N_2 plasmas, and its effect on CO_2 dissociation; and (iii) plasma-catalytic generation of ammonia in N_2-H_2 mixtures.

In the first thrust, time-resolved, absolute HO_2 number density in a repetitive ns pulse discharge inan H_2-O_2-Ar mixture flowing through a heated plasma flow reactor is measured by Cavity Ringdown Spectroscopy (CRDS). In an H_2-O_2 -Ar mixture at P=130 Torr and T=400-600 K, HO_2 persists in the discharge afterglow up to 10 ms after the discharge burst, limited by the flow residence time in the reactor. Comparison with kinetic modeling shows that the sustained reactivity after the source of radicals is turned off is due to the chain propagation / hydrogen oxidation process, which dominates the radical recombination reactions at elevated temperature. These results determine the boundary between the chain propagation and rapid chain termination / radical recombination process, which was observed at room temperature.

In the second thrust, time-resolved CO_2 and CO vibrational populations and rotational temperature are measured in a ns pulse discharge burst, by mid-IR tunable Quantum Cascade Laser (QCL) Absorption Spectroscopy, and N_2 vibrational populations are measured by CARS. The results indicate that the ns pulse discharge results in a modest vibrational excitation of N_2 and CO_2. The number density of CO, a product of CO_2 dissociation, is also inferred from the QCL measurements. These results make possible isolating and quantifying two major mechanisms of CO_2 dissociation, (i) decay via excited electronic states populated by electron impact, and (ii) stepwise anharmonic vibration-vibration (V-V) pumping of the asymmetric stretch vibrational mode, sustained by the strong vibrational excitation of N_2 and rapid V-V energy transfer to CO_2.

In the thirst thrust, plasma catalytic ammonia synthesis is studied in a diffuse ns pulse discharge plasma sustained over a catalytic surface in a preheated plasma flow reactor, at P=190 Torr and T= 300^0 C. The catalyst (nickel on alumina powder) is packed into a receptacle and placed into the plasma. Ammonia generated in the reactor is monitored by an FTIR spectrometer in an absorption cell in the reactor exhaust. With the discharge sustained without the catalyst (plasma <u>on</u>, catalyst <u>off</u>), ammonia is detected in the reactor exhaust. No ammonia is detected in the mixture flowing through the reactor with the catalyst in place, but with the discharge turned off (plasma <u>off</u>, catalyst <u>on</u>). Finally, sustaining the discharge in pure N_2 over the catalyst, and then turning it off, results in a significant catalyst reactivity enhancement ("catalyst activation"), such that the yield doubles compared to that in the plasma without the catalyst. The catalyst reactivity is not enhanced by H_2 plasma, and this effect is not observed in alumina powder without the catalyst is. These results suggest that the catalyst is activated by accumulation of N atoms generated in the plasma on the catalyst. When the plasma is operated in N_2-H_2 in the presence of the catalyst (plasma <u>on</u>, catalyst <u>on</u>), the ammonia yield keeps increasing slowly, due to the combined effect of (a) catalyst activation / surface catalytic reactions and (b) reactions in the plasma volume. Adding a sub-breakdown RF voltage waveform between the ns discharge pulses results in an additional moderate increase of the ammonia yield, suggesting that vibrational excitation of N_2 may contribute to the ammonia generation in the plasma. This effect has been observed both with and without the catalyst in the reactor.

Studies of Non-equilibrium Plasma Chemistry and Thermal-Chemical Instability

Yiguang Ju

Department of Mechanical and Aerospace Engineering, Princeton University
Princeton, NJ 08544 (yju@princeton.edu)

Non-equilibrium plasma chemistry and energy transfer play a critical role plasma assisted combustion, chemical synthesis, and plasma dynamics. In this study, at first, the multi-channel reactions of $O(^1D)$ with ethanol, $O(^1D) + C_2H_5OH$, was studied in a photolysis flow reactor coupled with mid-infrared Faraday rotation spectroscopy (FRS) and UV-IR direct absorption spectroscopy (DAS) [1]. The total reaction rate and the multi-channel reaction branching ratios were determined for the first time. A chemical kinetic model for plasma assisted combustion of n-dodecane was developed and experimentally validated by using a plasma reactor with multi-species diagnostics. In addition, the effect of plasma chemistry in CH_4 reforming was studied by using laser Thomson scattering. The results show that contrary to the conventional assumption that the effect of a small amount of fuel addition into plasma has a negligible impact on plasma properties, the present result clearly shows that methane addition in helium resulted in a strong non-linear change in electron number density and temperature [2]. To probe non-equilibrium energy transfer in plasma, spacially resolved one-dimensional imaging of both rotational and vibrational temperatures simultaneously was performed using pure rotational hybrid femtosecond/picosecond coherent anti-Stokes Raman scattering (fs/ps CARS). This enables measurement of rotation-vibration non-equilibrium with high temporal and spatial resolution near surfaces such as in plasma assisted ignition and plasma catalysis [3]. To understand the impact of plasma chemistry on plasma instability, an analytical theory and criterion for the onset of plasma thermal-chemical instability are developed, suggesting the impact of plasma aided chemical reactions on the formation of instability. The controlling plasma reactions are identified by using thermal-chemical mode analysis [4]. To model non-equilibrium plasma assisted combustion, a multiscale adaptive reduced chemistry solver for plasma assisted combustion (MARCS-PAC) was developed by using the PASSKEy discharge modeling package and the compressible multi-component reactive flow solver ASURF+ [5]. This model is applied to simulate the impact of non-equilibrium plasma excitation and electrode geometry and heat loss on the dynamics of plasma assisted ignition kernel development in a H_2/air mixture. The results show that the plasma non-equilibrium excitation and radical production as well as the electrode geometry and separation distance have a significant impact in ignition timing.

References
[1] Zhong, H., et al., Kinetic studies of excited singlet oxygen atom O (1D) reactions with ethanol. International Journal of Chemical Kinetics, 2021. **53**(6): p. 688-701.
[2] Chen, T.Y., et al., Time-resolved in situ measurements and predictions of plasma-assisted methane reforming in a nanosecond-pulsed discharge. Proceedings of the Combustion Institute, 2020.
[3] CHEN, T.Y., et al., One-dimensional imaging of rotation-vibration non-equilibrium from pure rotational fs/ps coherent anti-Stokes Raman scattering. Optics letters, 2020. **45**(15): p. 4252-4255.
[4] Zhong, H., et al., Dynamics and chemical mode analysis of plasma thermal-chemical instability. Plasma Sources Science and Technology, 2021. **30**: p. 035002.
[5] Mao, X., H. Zhong, and Y. Ju. 2D modeling of plasma-assisted H2/air ignition in a nanosecond discharge with detailed chemistry. in AIAA Scitech 2021 Forum. 2021.

Ammonia Synthesis and Decomposition in Plasma-assisted Catalysis

Zhe Chen, Hao Zhao, Surabhi Jaiswal, Sankaran Sundaresan, and Bruce E. Koel

Department of Chemical and Biological Engineering, Princeton University, Princeton, NJ, USA
(bkoel@princeton.edu)

Plasma-assisted catalysis is one possibility for synthesis of fuels and chemicals that takes advantage of the expanding increase of renewable electricity from solar and wind power. This approach utilizes excited gaseous molecules or new reactive species formed in a (non-equilibrium, low temperature) gas discharge plasma, along with a catalyst to enable increases in the activity and selectivity for carrying out desirable chemical reactions at lower temperature and pressure conditions than commonly utilized in commercial thermal heterogeneous catalysis.

Our recent research has focused on fundamental aspects of one of the simplest, and also most important, industrial catalytic reactions, i.e. ammonia synthesis. We report on results from dielectric barrier discharge (DBD) reactors using AC discharges and packed with γ-Al_2O_3 support particles or Ru/γ-Al_2O_3 supported metal catalysts in the discharge zone.

Several aspects of our work will be discussed. First, we have compared the effects of the support and a Ru/γ-Al_2O_3 catalyst on both the forward and the reverse reactions of plasma-assisted ammonia synthesis. Experiments at different plasma power levels found that N_2 conversion was only slightly increased by Ru/γ-Al_2O_3 compared to γ-Al_2O_3 particles. Second, utilizing zero-dimensional plasma kinetic modeling with ZDPlasKin to elucidate the dominant reactions in the presence of γ-Al_2O_3, we found that the direct adsorption of N and H, and two Eley-Rideal (ER) reactions, i.e., H + NH(s) $\rightarrow$ NH$_2$(s) and H + NH$_2$(s) $\rightarrow$ NH$_3$, make the largest contributions to plasma-assisted NH$_3$ synthesis. Third, measurements were made with an electron-ionization molecular beam mass spectrometer (MBMS) that was connected directly to the plasma reactor to enable in-situ detection of stable molecules and radicals in plasma-assisted ammonia syntheses at the exit of the reactor. The detection of NNH radicals in the gas phase of the DBD reactor during ammonia synthesis at 293 K and 1 atm indicates that this reactive species should be considered further in the kinetics of plasma-assisted catalysis for ammonia synthesis. Fourth, experiments with various support particles have been performed. In particular, measurements of N_2 conversion and plasma parameters were compared for highly porous silica particles and nonporous soda lime glass particles to probe the effect of catalyst support porosity on ammonia synthesis and plasma properties. Modeling indicates that gas-phase radicals can diffuse into the pores of the support to some extent.

Overall, these results increase our understanding of plasma-catalysis hybrid systems and aid efforts to achieve the strongest synergistic interactions between the plasma and catalyst to increase performance and overall energy efficiency.

Machine Learning and Artificial Intelligence for Low-temperature Plasmas: A Tutorial Overview

K. Shao [a], A. D. Bonzanini [a], and <u>A. Mesbah</u> [a]

(a) Dept. of Chemical and Biomolecular Eng., University of California, Berkeley, CA 94720, USA
(mesbah@berkeley.edu)

Machine learning and artificial intelligence (AI) have proven to be an invaluable tool in tackling a vast array of scientific, engineering, and societal problems. The main drivers behind the recent proliferation of AI in practically all aspects of science and technology can be attributed to: (i) improved data acquisition and ease of data storage; (ii) exponential growth in computing power; and (iii) widely available open-source software and resources that have made the use of state-of-the-art AI algorithms accessible to non-expert users. The impact of AI on low-temperature plasmas (LTPs) can be particularly beneficial in emerging applications such as plasma catalysis, treatment of interfaces and plasma medicine. This is due to the complex and poorly-understood plasma-interface interactions in these applications that pose a great challenge to the modeling, diagnostics, and real-time control of LTPs. As such, it is increasingly important for the LTP community to be able to assess, critique, and incorporate the concepts/techniques behind these methods. In this talk, we will provide a tutorial-like overview of some of the cutting-edge AI algorithms that can be useful in discovering and correlating patterns in the data that may be otherwise hard to decipher by human intuition alone. We will illustrate the power of AI in real-world plasma applications by using commonly-available, information-rich measurements (such as optical emission spectra (OES), scanning electron microscope (SEM) images, infrared temperature measurements, and current-voltage characteristics) - often in combination with physics-based knowledge - to extract difficult-to-obtain information about plasma behavior. Specifically, we will demonstrate the use of unsupervised learning (autoencoders for dimensionality reduction and hierarchical clustering), supervised learning (convolutional neural networks for classification and deep learning and Gaussian processes for nonlinear regression), as well as active learning approaches such as Bayesian optimization whereby the training data is incrementally chosen to be the most informative based on some predefined criterion. All case studies are implemented in Python and the open-source codes will be made available to members of the Center for Plasma Interactions with Complex Interfaces (PICI).

Accurate Reproducible Power Delivery across Multiple Plasma Sources

Steve Shannon, Josh Morsell, Carl Smith

North Carolina State University (scshanno@ncsu.edu, jkmorsel@ncsu.edu)

Accurate delivery and measurement of applied power to sustain a plasma discharge is one of the most important elements of plasma source design. Plasma conditions are particularly sensitive to power delivery accuracy when compared to other process control variables such as gas flow control, pressure control, or gas composition.[1] Global plasma models typically employ power balance techniques that require an accurate estimate of dissipated power to extract bulk plasma parameters; this is particularly important for plasma sources such as microdischarges and plasma jets where diagnostic access is extremely limited. The challenges of accurate power delivery across multiple plasma sources, even when due diligence is served with respect to unit to unit replication, is one of the primary manufacturing challenges that has plagued plasma assisted manufacturing for decades. Even at the research level, unit-to-unit power delivery accuracy has been one of the primary challenges of the two reference plasma reactors used by the community, the GEC reference cell and the COST plasma jet.

A brief review of the challenges of accurate power delivery will be presented. These can be broken down into three groups: 1.) accurate power output of the generator, 2.) impedance matching of the power delivery network using reactive elements, 3.) control and characterization of non-plasma dissipative elements.

Within these three groups, methodologies will be presented that have been implemented in previous reference source and industrial manufacturing efforts and further developed for the plasma jet sources at PICI center locations that show the impact of unit to unit variability of these characteristics and simple mitigation techniques to reduce this power delivery variability. These methodologies have been designed around the need for unit-to-unit reproducibility as well as the ability for center sites to carry out power measurements and power delivery characterization without high cost analytical equipment:

- Accurate power output of the generator: RF power supplies tend to be rated with output power accuracy in the range of 2% to 5%. This can be improved to some extend through secondary power measurement via voltage and current waveform analysis or the use of inline directional couplers for power measurement. Secondary measurement of the standard RF power generator for the PICI center will be presented, with pathways for power delivery accuracy improvement below 2%.

- Impedance matching characterization: One of the biggest variables, as well as one of the biggest system level characterization headaches, is the impedance matching system. Minimizing reflection to the power supply is straight forward for cases where power delivery is constant but is problematic when power levels change rapidly such as in pulsing. Time resolved impedance measurements will be presented to illustrate these points.

- Dissipated power in the network can also be a significant fraction of the total power dissipated and greatly skew the measurement of power dissipated in the plasma itself. Additionally, dissipation between the match circuit and the plasma, such as resistive losses in powered electrode of the PICI plasma jet, can further contribute to plasma power reduction and unit to unit variability. Match dissipation techniques will be presented to illustrate these points.

References

[1] Kleditzsch, S., & Riedel, U. (2000). Sensitivity studies of silicon etching in chlorine/argon plasmas. Journal of Vacuum Science & Technology A: Vacuum, Surfaces, and Films, **18** (5), 2130-2136

Plasma-Surface Interactions: Boundary Layer Effects and Self-organization

Jingkai Jiang, Tanubhav Srivastava, Jianan Wang and Peter Bruggeman

Department of Mechanical Engineering, University of Minnesota, Minneapolis, MN 55455, USA
(pbruggem@umn.edu)

Plasma-surface interactions at atmospheric pressure remain a relatively unexplored scientific frontier. The increased pressure and reduced Debye length in atmospheric pressure plasmas leads to a reduced sheath thickness of the order of 10s of micrometers compared to the typical sheath structures on a centimeter length scale in low pressure plasmas. These micrometer length scales often combined with self-organizing patterns at liquid and solid plasma interfaces remains a major challenge for diagnostics. In this presentation, we provide an overview on our recent research progress in investigating species fluxes to substrates with molecular beam mass spectrometry (MBMS) and interrogating species gradients near the plasma-substrate interface with laser induced fluorescence. In addition, we will summarize our new insights in the origins of self-organization at the plasma-liquid interface.

Molecular beam mass spectrometry (MBMS) enables directly linking plasma-produced species fluxes with plasma-surface interaction studies, owing to its ability to detect a large range of different species and to measure species fluxes or densities at a substrate. However, at atmospheric pressure, the 'suction region' of the molecular beam can have similar dimensions of the surface boundary layer and hence intrinsically measures the species density at a few orifice diameters from the substrate. We performed a detailed analysis of species gradients near substrates (Figure 1) and showed that near surface gradients might require corrections on the measured MBMS data.

Figure 1 – (a) Axial velocity distributions in the stagnation region for a plasma jet with indicated gas flow rate impinging on a substrate. (b) Corresponding O density distributions obtained by simulation of the 200 μm stagnation region for different surface loss probabilities [1].

Laser diagnostics provide the opportunity to measure the radical density in boundary layers and sheaths although high resolution measurements near surfaces remains challenging. We have measured OH radical density distributions with high spatial resolution laser induced fluorescence in a surface streamer discharge generated by a plasma jet impinging on a quartz substrate. The measurement allows to determine the OH diffusion flux to the substrate at 5×10^{15} cm^{-2} s^{-1}. This value is the same within the experimental accuracy as the kinetic OH flux determined from the measured OH density at the interface. The found OH density distribution can be explained by the measured gradients in water vapor in the discharge and diffusion losses to the substrate.

In the case of a liquid interface, we further investigated the cause of the formation of self-organized patterns at the liquid anode. We found three necessary conditions for pattern formation: solution evaporation, presence of a cation with a reduction potential below a critical value and the presence of O_2 in the gas phase. This finding suggests that the mechanism of pattern formation at the liquid interface has distinct differences with previously reported similar patterns on semi-conductors and even metal electrodes occurring in noble gases.

References

[1] Jiang, J. and Bruggeman, P.J. J. Phys. D. Appl. Phys. **54** (2021): 214005.
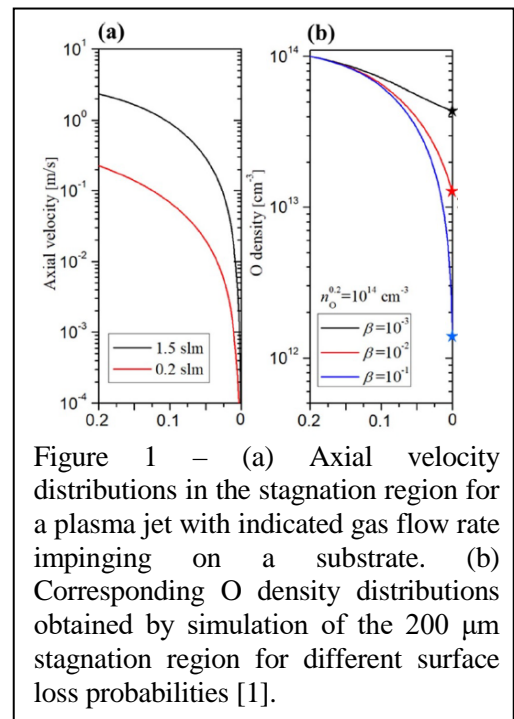
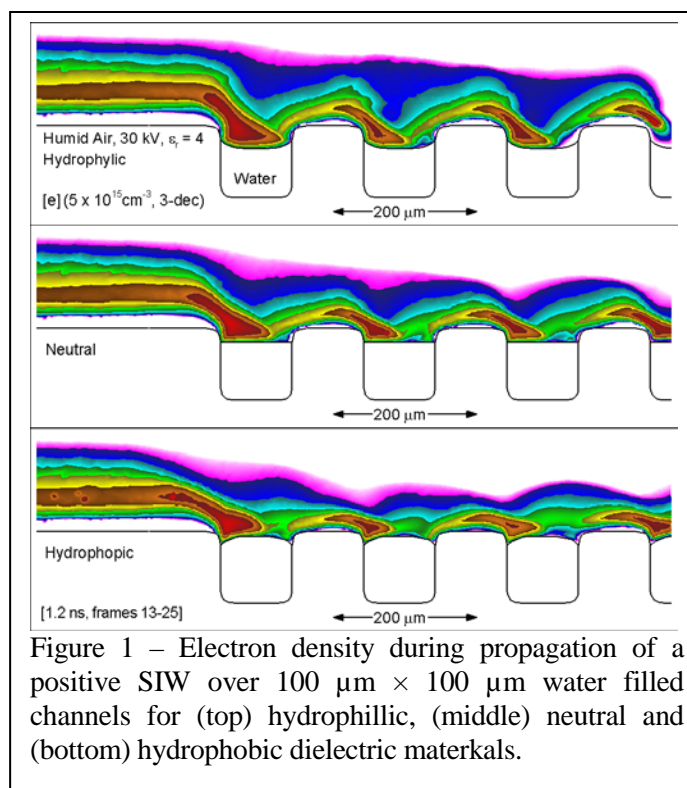# Plasma Interactions with non-Planar, Wet and Reactive Surfaces

Kseniia Konina, Mackenzie Meyer, Sanjana Kerketta, Jordyn Polito, Juliusz Kruszelnicki and Mark J. Kushner

University of Michigan (mjkush@umich.edu)

The use of atmospheric pressure plasmas (APPs) in industrial surface engineering and medical applications is invariably made more difficult by the complexity of the surface. This complexity can take the form of chemical complexity as occurs in functionalization of surfaces, or treating wet or geometric complexity resulting from the surface being non-planar. In each case there may be feedback from the surface to the plasma that affects the propagation of the plasma across the surface or delivery of reactive species to the surface. In this talk, brief updates will be given from computational projects investigating these complexities. These studies were performed using the 2-dimensional *nonPDPSIM* platform and the plug-flow-onto-surfaces option of *GlobalKin*.

The propagation of surface ionization waves (SIWs) over water filled and dry dielectric channels was investigated as part of a Center-wide collaboration on how such microstructure affects and feeds back to plasma properties. The channels are hundreds of microns wide and 100-200 µm deep. Positive and negative SIWs sustained in ambient air propagate across these structures with different characteristics. Negative SIWs are sensitive to electric field enhancement that occurs at edges of the channels. Positive SIWs tend to hug the surface regardless of the topography. Positive and negative SIWs propagate similarly over water filled channels, with some sensitivity to the hydrophobic properties of the dielectric. (See Fig. 1.) Hydrophobic materials produce a water meniscus that is convex, producing electric field enhancement by polarization of the water.

Human skin is a highly complex surface, being moist, and having wrinkles, pores and hair follicles. The plasma treatment of skin has several applications, from cosmetic to sterilization. Cleaning skin of bacteria is a standard practice prior to surgery to reduce contamination of the wound. A significant fraction of skin-resident bacteria is in hair follicles, which are difficult to inactivate using conventional liquid agents. Plasma treatment of in-follicle bacteria is a viable alternative – an example of a complex surface. APP treatment of hair follicles was investigated to determine the ability of plasma to penetrate into the follicle and for reactive oxygen species to either be directly generated in the follicle or diffuse into follicle from the ambient. We found that APP penetration into the follicle is highly sensitive to the orientation of the follicle, with the plasma generally not uniformly filling the hair shaft-epidermis gap. The majority of ROS in the shaft is produced by the penetrating plasma – little diffuses from the ambient. In fact, the opposite occurs. There is more ROS generation in the follicle than in the local ambient, and so ROS diffuses out of the follicle during the inter-pulse period.

Figure 1 – Electron density during propagation of a positive SIW over 100 µm × 100 µm water filled channels for (top) hydrophillic, (middle) neutral and (bottom) hydrophobic dielectric materkals.

Abstracts – Poster Presentations

Open Channel Microfluidic Substrate for Investigation of Multi-phase Surface Interactions with Atmospheric Pressure Plasmas

Joshua Morsell [a], Duncan Trosan [a], Kseniia Konina [d], Jingkai Jiang [c], Greg Allion [b], Mark Kushner [d], Peter Bruggeman [c], and Steven Shannon [a]

(a) North Carolina State University (jkmorsel@ncsu.edu), (b) Nanofabrication Facility, NCSU, Raleigh, NC, (c) University of Minnesota, (d) University of Michigan

The study of atmospheric pressure plasma has been increasing at a steady rate in the past few decades. Fields including medicine, agriculture, surface modification, and additive manufacturing have all benefited from atmospheric plasmas.[1,2] Of particular interest in this study is the interaction of plasma and plasma-generated species with liquids. To date there have been many studies that have focused on such interactions. Previous work has primarily focused on bulk liquid investigation. In many circumstances bulk liquids are prone to convective mixing and surface deformation due to plasma heating and gas flow.[3] These traits are inherent to experiments and can interfere with certain diagnostics and introduce interference to understanding underlying plasma-liquid interactions.

The goal of this work is the design and characterization of a substrate for investigating plasma interactions with complex, multi-phase, surfaces. Fluid control with the substrate must be controllable and mitigate traits that have added interference and limits to previous work. The substrate must also allow access to a wide variety of diagnostics. The result is an open microchannel substrate where flow is driven by capillary flow.[4] The surface allows for a wide range of optical and liquid diagnostics to occur simultaneously. The spatially resolved nature of the surface allows for the substrate to be a diagnostic in and of itself.

The open channel substrate is manufactured using deep reactive ion etching (DRIE) to form the uniform channels of rectangular cross section. The channels are 100um in width and 200um in depth. There are 120 in total and the outlets of the channels are gathered first into pairs and then again into eight reservoirs. Seven of the reservoirs are equally divided on half of the substrate and the other half is a singular reservoir. Substrates are etched into silicon and have a 05nm oxide layer to stabilize the surface against chemical wear. Inlet and outlet flow are controllable via standard medical IV bags and drip tubes, while the outlet is controlled via a peristaltic pump drawing fluid into spatially resolved reservoirs. The plasma source used in this work was developed at the University of Minnesota and is an atmospheric jet capable of operating with RF or pulsed DC. The jet offers coaxial gas flow paths to allow for the use of a working gas and shielding gas.

Characterization of the microfluidic substrate and its diagnostic potential includes several points of analysis. The surface is subject to contact angle tests pre- and post- plasma exposure. FTIR measurements is used to determine whether any surface bonds have been modified by plasma exposure. Surface reflectometry will determine is any of the oxide layer is eroded during plasma exposure. Flow characterization shows that the susbtrate is capable of controlled flow up to 1.2ml/min and illustrate some flow irregularities across the 120 channels. Flow is then characterized during plasma treatment and the resulting liquid samples will be subject to peroxide assay to determine any generated peroxide in a spatially resolved way. Finally, a PicoStar ICCD camera is used to image a propagating ionization wave across the surface of the substrate.

References

[1] P. J. Bruggeman, F. Iza and R. Brandenburg, Plasma Sources Sci. and Technol. **26** (2017).
[2] U. Kogelschatz, Plasma Physics and Controlled Fusion **46** (2004).
[3] V. Santosh et al., Free Radical Biology and Medicine **124** (2018).
[4] J. Berthier et al., Open-Channel Microfluidics (Morgan Claypool Publishers, 2019).

Design and Operation of an Experimental Setup used to Study Plasma Catalysis

Brian Bayer [a], Peter Bruggeman [b] and Aditya Bhan [a]

(a) University of Minnesota, Department of Chemical Engineering and Materials Science
(bayer116@umn.edu, abhan@umn.edu)
(b) University of Minnesota, Department of Mechanical Engineering (pbruggem@umn.edu)

Coupling nonthermal plasma with catalytic surfaces has been shown to enhance the conversion of N_2/H_2 mixtures to NH_3 in reference to plasma-driven or thermal catalytic systems alone at the same conditions. Reactions involving vibrationally-excited or radical species on catalytic surfaces have been proposed to be responsible for this enhancement, although experimental results have been unable to explicitly show the effect that these species have on NH_3 formation rates, since plasma-phase species density measurements are difficult to make in conventional packed-bed dielectric barrier discharge reactor setups. This work introduces an experimental setup to study the plasma-phase and surface catalyzed molecular events that transpire in plasma-assisted catalysis by on-stream measurement of short-lived and stable species that enter and exit a packed catalyst bed.

The setup (Figure 1) couples a radiofrequency-driven plasma jet with a catalyst bed containing transition metals supported on a nonporous metal oxide. Molecular beam mass spectrometry (MBMS) is used to measure the densities of species entering or exiting the catalyst bed, including stable molecules, radical species, and vibrationally excited species. Species density measurements are made in separate experiments at the

Figure 1 – Schematic of the experimental setup used to study plasma catalysis that couples a radiofrequency-driven plasma jet with a packed bed containing catalytic material. Setup a) is used to measure species densities exiting the reactor, and setup b) is used to measure species densities entering the reactor.

effluent of the plasma jet before the packed bed, at the effluent of the reactor tube in the absence of catalytic material, and at the effluent of the reactor tube containing catalytic material to determine the reactivity of different plasma-produced species over catalytic surfaces. Benchmark experiments are performed using this method for the N_2/H_2 system as a proof-of-concept to show how the presence of catalytic material alters NH_3 production.
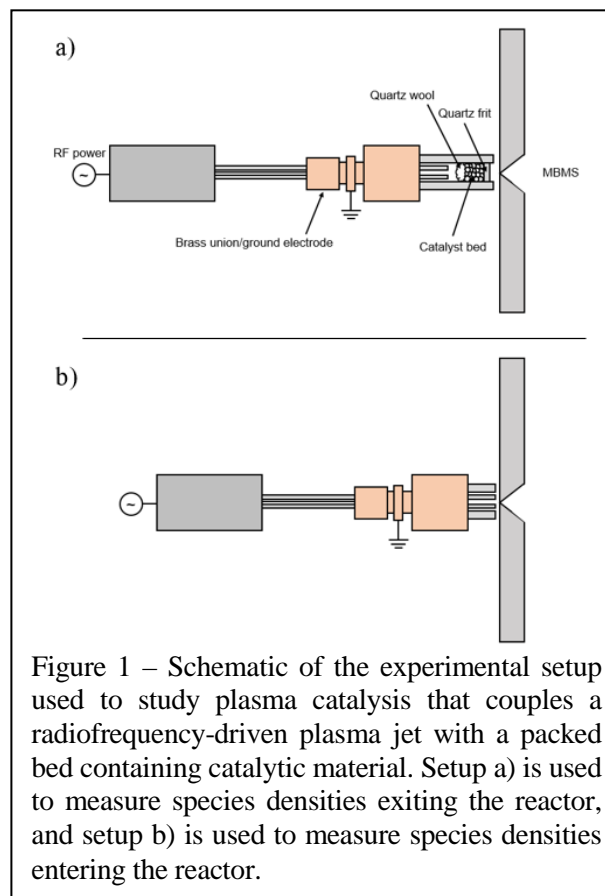
The Influence of Plasma-Induced Surface Charging on Single-Atom Catalysis for CO_2 Reduction

Francis J. Doherty and Bryan R. Goldsmith

Department of Chemical Engineering, University of Michigan, Ann Arbor, MI, USA, bgoldsm@umich.edu

Low-temperature plasma (LTP) catalysis is a growing field of research, reporting various synergistic effects for increased activity, yield, or selectivity compared to conventional thermocatalytic approaches. LTP can activate stable molecules such as CO_2 via interactions with high-energy electrons. Still, the many effects that LTP has on surface-catalyzed reactions are multi-faceted and poorly understood at an atomistic level. It would help to understand the effects of plasma on a catalyst surface by studying each in isolation. For instance, the LTP contains many charged particles and excited electrons, and this causes a negative charge to accumulate on the exposed surface. In this work, we study the effect of surface charging due to LTP in isolation for the CO_2 reduction reaction.

Using density functional theory modeling, we study single-atom catalyst systems across the periodic table to understand the importance of surface charging on CO_2 activation. We analyze six different metals (Co, Ni, Cu, Rh, Pd, and Ag) as dispersed metal ions. These metals are dispersed on three different supports (CeO_2, TiO_2, Al_2O_3), each with varying levels of reducibility.

Our modeling approach is adapted from recent literature[1] and applied to observe the plasma's effect on catalytic activity. We add a negative charge to the single metal atom on the catalyst surface and a counterion (H+) to the vacuum layer to maintain overall neutrality. This simulates an electric field that can be tuned by varying the distance between point charges. We predict CO_2 binding energy and reaction

Figure 1 - The six different metals investigated for CO_2 reduction by plasma catalysis are chosen for their varying number and energy level of d-electrons. Shown here is each metal (Co, Ni, Cu, Rh, Pd, and Ag) on anatase TiO_2. An extra negative charge is imparted to each single metal atom, with a counterion H+ in the vacuum above.

barrier trends to characterize each system's catalytic activity. Our results show that the adsorption and reaction trends for CO_2 reduction differ between plasma and thermal catalysis, implying that insights from one field may not necessarily apply to the other.
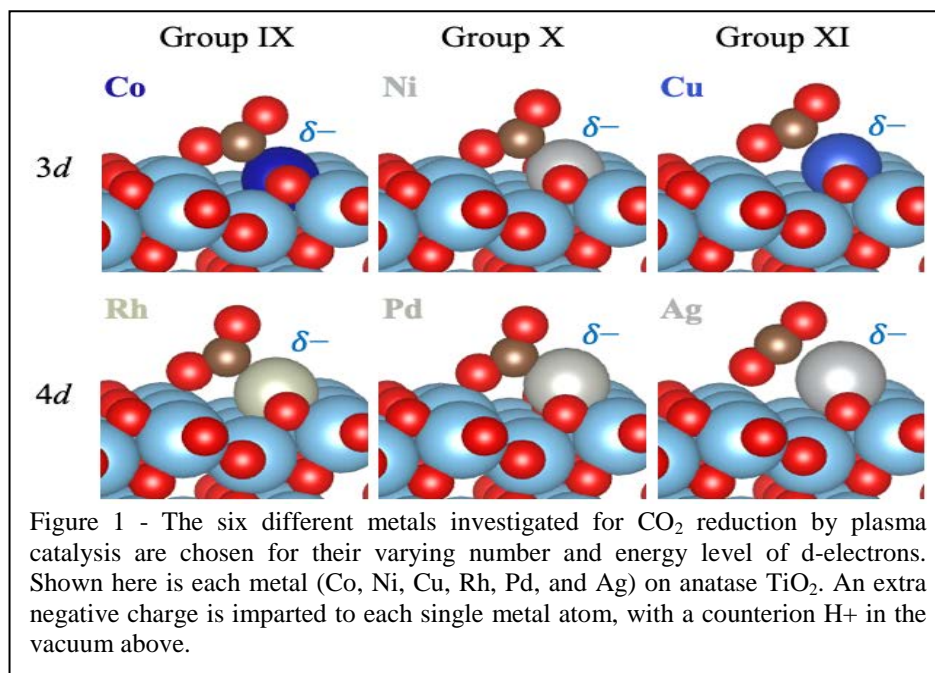
References

1. K. M. Bal, S. Huygh, A. Bogaerts and E. C. Neyts, Plasma Sources Sci. Technol., 2018, **27**, 024001.

DRIFTS and Gas Phase FTIR Characterization of Plasma-enhanced Catalysis for NO_x Production

Michael Hinshelwood [a], Yudong Li [a], Brian Bayer [b], Frank Doherty [c], Ketong Shao [d], Aditya Bhan [b], Peter J. Bruggeman [e], Bryan R. Goldsmith [c], Ali Mesbah [d] and Gottlieb S. Oehrlein [a]

(a) Dept. of Materials Science and Engineering and the Institute for Research in Electronics and Applied Physics, University of Maryland, College Park, MD 20742 (oehrlein@umd.edu)
(b) Dept. of Chemical Engineering and Materials Science, University of Minnesota, Minneapolis, MN 55455
(c) Dept. of Chemical Engineering, University of Michigan, Ann Arbor, MI 48109
(d) Dept. of Chemical and Biomolecular Eng., University of California, Berkeley, CA 94720
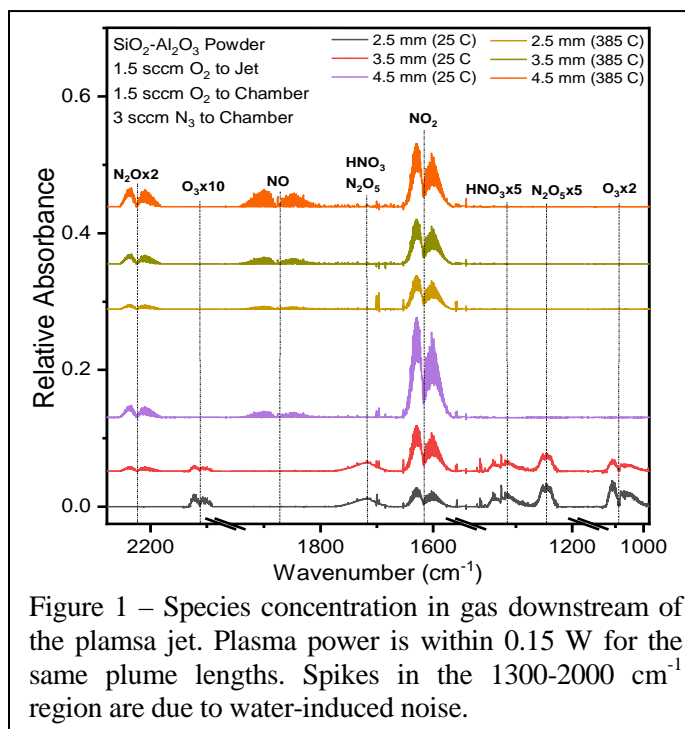(e) Dept. of Mechanical Engineering, University of Minnesota, Minneapolis, MN 55455

Cold atmospheric pressure plasma (CAPP) is a potential tool to enhance thermal catalyst activity for conversion of nitrogen and oxygen to nitrogen oxides relevant to the nitrogen fixation process (NO_x). The enhancement effect results from the interaction of chemically reactive species produced by plasma with the catalyst surface. The nature of these interactions is unclear, and spectroscopic data on surface species is lacking.

In this work, diffuse reflectance infrared Fourier transform spectroscopy (DRIFTS) and gas phase FTIR are being used to characterize the catalyst surface and downstream gas products during treatment by an atmospheric pressure plasma jet (APPJ). The catalyst is a powder of platinum supported by SiO_2-Al_2O_3. The catalyst is concurrently exposed to both the effluent of an RF $Ar/O_2/N_2$ APPJ and unexcited $Ar/O_2/N_2$ flow. Small amounts of O_2 and N_2 are added to the Ar flow in various configurations. By utilizing DRIFTS and downstream gas FTIR, the time dependent evolution of relevant species on the catalyst surface can be observed. Our data will be correlated with that of our collaborators at University of Minnesota, who operate an identical APPJ, and have the capability to observe excited species with their molecular beam mass spectrometer. Further understanding of the bonding interactions of NO_x species to the catalyst surface will be enabled through the Density Functional Theory modeling of our collaborators at University of Michigan.

To fully understand the plasma catalytic interactions, it is useful to determine the most efficient parameters for NO_x production within our parameter space. To that end, we are collaborating with University of California Berkeley, whose statistical modeling will help elucidate the most power efficient way to produce NO_x in our experimental arrangement. Initially, we are attempting to make this efficiency determination with just a plasma system, using an inert SiO_2-Al_2O_3 powder in place of the platinum catalyst. Figure 1 shows initial analysis of O_2-N_2 interactions as inert silica powder is exposed to APP plasma.

Figure 1 – Species concentration in gas downstream of the plamsa jet. Plasma power is within 0.15 W for the same plume lengths. Spikes in the 1300-2000 cm^{-1} region are due to water-induced noise.

Efficient Defluorination of Perfluorobutane Sulfonate (PFBS) by Plasma with the Aid of a Surfactant

Osakpolo Faith Isowamwen [a], Rui Li [a], Thomas Holsen [b] and Selma Mededovic Thagard [a]

(a) Department of Chemical and Biomolecular Engineering, Clarkson University, Potsdam, New York 13699, USA (isowamof@clarkson.edu)
(b) Department of Civil and Environmental Engineering, Clarkson University, Potsdam, New York 13699, USA

This study investigates plasma-assisted degradation of perfluorobutane sulfonate (PFBS), a compound very few advanced oxidative and reductive technologies are able to degrade. PFBS, a member of a group of per- and polyfluoroalkyl substances (PFAS), is used as a replacement of perfluorooctane sulfonate (PFOS) in many consumer products such as nonstick pans, wire coating and firefighting foams. Recent studies have shown that PFBS is as persistent in the environment and bio-accumulative in people as its long-chain counterparts and human exposure to it can lead to serious health effects.

Here, the degradation of PFBS was investigated using a gas-liquid electrical discharge plasma reactor. Experiments were conducted with and without cetyltrimethylammonium bromide (CTAB), a surfactant, whose purpose was to interact with and transport PFBS to the plasma-liquid interface. No removal of PFBS was observed without the surfactant. With CTAB, ~99% of PFBS was concentrated at the interface and subjected to defluorination and desulfonation (Figure 1). We have explored the mechanism of CTAB-PFBS binding, adsorption of such formed complex to the plasma- liquid interface, its interfacial reactivity and orientation, and decomposition byproducts. The addition of a commercially available surfactant that binds with and transports compounds to the plasma-liquid interface is a viable process for the degradation of non-oxidizable and/or recalcitrant contaminants.
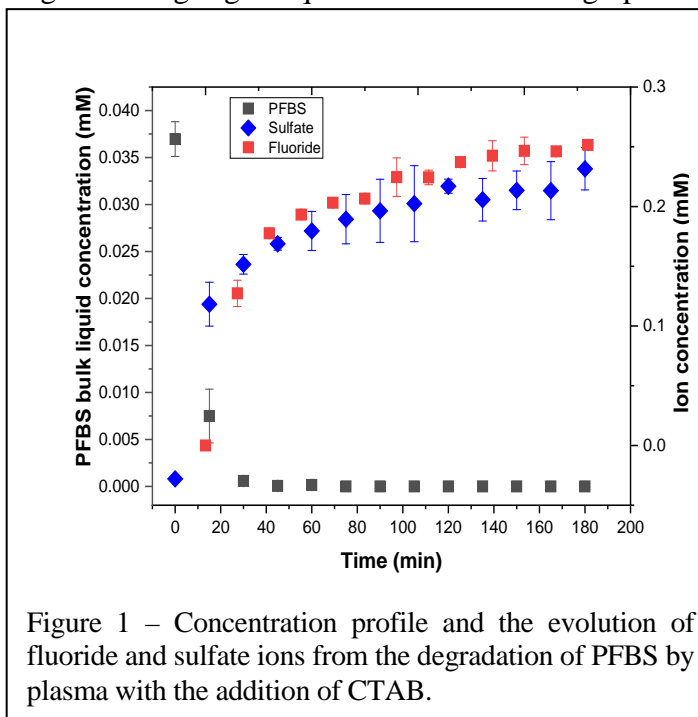

Figure 1 – Concentration profile and the evolution of fluoride and sulfate ions from the degradation of PFBS by plasma with the addition of CTAB.

Control of Reactive Species Fluxes to Substrate and Absolute Density Measurement of Ions and Vibrationally Excited N_2 by Molecular Beam Mass Spectrometry

Jingkai Jiang and Peter J. Bruggeman

University of Minnesota, Minneapolis, MN (pbruggem@umn.edu)

Molecular beam mass spectrometry (MBMS) enables directly linking the obtained fluxes with plasma-surface interaction studies, owing to its ability to detect a large range of different species and to measure species fluxes or densities at a substrate. We have extended the capability of MBMS for plasma diagnostics by developing detection and calibration approaches for the absolute measurement of vibrationally-excited nitrogen $N_2(v)$ as well as the absolute density of positive ions in the effluent of atmospheric pressure plasma jets. In addition, we have explored the possibility to control the dominant reactive species fluxes, relevant for plasma-catalysis, to a substrate in the effluent of an RF driven Ar-O_2 plasma jet.

The spatially resolved measurements of $N_2(v)$ in the effluent of an APPJ were enabled by fitting the MS signals with the electron-impact ionization cross sections of $N_2(v)$ as a function of electron energy, assuming a Treanor-like vibrational distribution function (see Fig. 1). The approach provides a complementary diagnostic technique for detecting $N_2(v)$ near substrates with excellent spatial resolution and detection limits. It also shows that RF-driven plasmas can produce large fluxes of $N_2(v)$ that is believed to be important in plasma catalysis.

Absolute densities of positive ions in the effluents of an APPJ were obtained through calibration with a dc corona discharge with a well-known current density profile [1]. Positive ion densities in the effluent of the APPJ were found to be more than 4 orders of magnitudes lower than the densities of dominant reactive neutral species

Figure 1 – Normalized MS signals of N_2^+ and EII cross-sections of $N_2(v)$ as a function of electron energy. The superscript 'a' and 'b' indicate that these two fittings are truncated at different vibrational levels instead of v=12 as for all other cases.

suggesting that plasma-surface interactions in this case are dominantly due to neutral radical interactions.

Different plasma operating parameters were investigated to alter the dominant species densities in an Ar-O_2 plasma jet [2]. Results show that the short-lived and long-lived species can be effectively separated by changing the treatment distance and the modulation frequency. Furthermore, adjusting the O_2 admixture concentration enables to change the ratio of the $O_2(a^1\Delta_g)$ and O_3 density by more than one order of magnitude. The changes in the trend of ion and O flux were found to be very similar for nearly all investigated parameters. Nonetheless the gas flow rate was able to change the ratio of the O and ion density by more than one order of magnitude. The impact of the surface-dependent loss probability and boundary layer reactions on the species flux to a substrate will also be reported.

References
[1] Jiang, J. and Bruggeman, P.J. J. Phys. D. Appl. Phys. **54**.15 (2021): 15LT01.
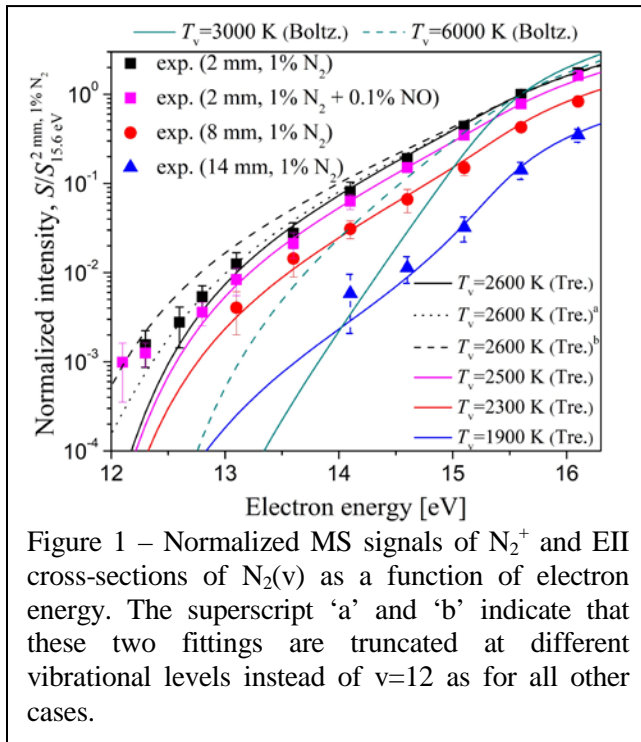[2] Jiang, J. and Bruggeman, P.J. J. Phys. D. Appl. Phys. **54**.21 (2021): 214005.

Surface Ionization Wave Interactions with Dielectric Porous Surfaces

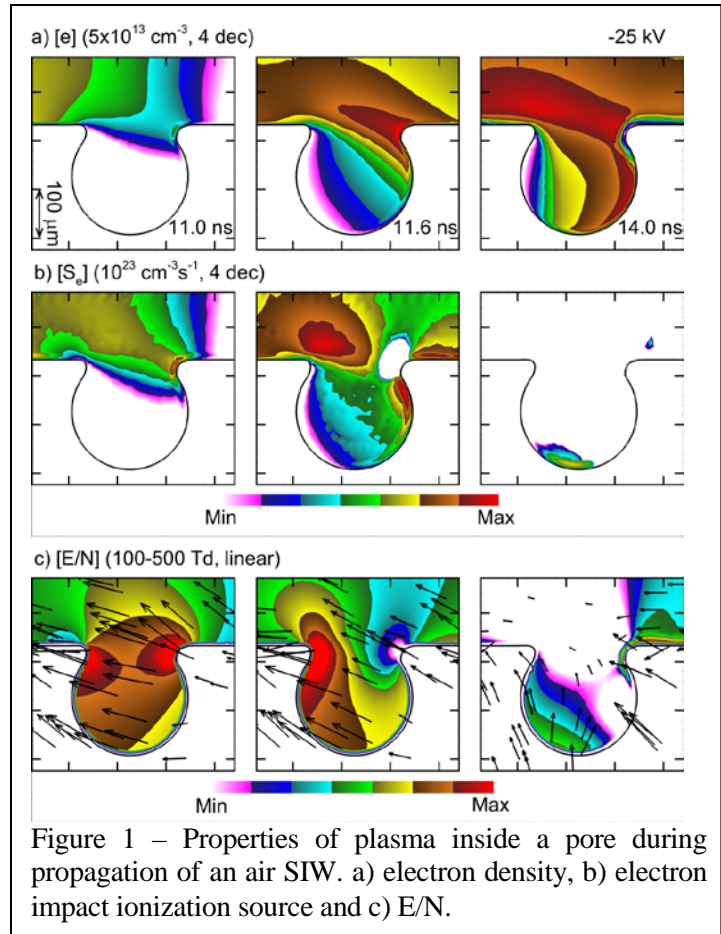Kseniia Konina, Juliusz Kruszelnicki and Mark J. Kushner

University of Michigan, Electrical Engineering and Computer Science Department
Ann Arbor, MI 48109-2122, USA

Porous dielectrics are very common in technologies with applications linked with medicine, environment and catalysis. Alteration of surface properties is a necessary process for compatibility with the application. Atmospheric pressure plasmas are known for beneficial interactions with dielectric surfaces such as modifying hydrophobicity, catalyst activation and change of chemical composition of the surface. To treat porous surfaces, a detailed understanding of a collective interaction of plasma with non-planar surface is needed. This work addresses a computational investigation of atmospheric pressure plasma interactions with porous dielectrics of different kind.

This investigation was performed using a 2-dimensional plasma-hydrodynamics model nonPDPSIM [1]. In this model, continuity equations are solved for charged and neutral species. Poisson equation's is solved for the electrical potential taking into account both charged species and surface charge. Electron energy distributions from solution of Boltzmann's equation are used for transport coefficients based on a mean electron energy. Radiation transport provides rates of photoionization through several processes of photon emission and absorption addressed using a Green's function approach.

Surface ionization wave (SIWs) sustained in atmospheric pressure humid air propagating over a porous surface were investigated. A sample of plasma properties inside pores is in Fig. 1. Several parametric studies were carried out to determine the influence of voltage polarity and magnitude, shape of the pores and width of the pore opening. The main property that governs SIW propagation over dielectric porous surfaces is the curved areas of the pore openings that result in electric field enhancement. Surface charging can cause a restrike inside the pore that treats the surface of the rest of the pore. Plasmas are able to penetrate into the narrow opening of pores that exceed the plasma's Debye length. Plasma can also be seeded in pores having smaller openings by photoionization. Plasmas are able to treat pores with small openings that cannot be treated by other methods such as liquid treatment.

Figure 1 – Properties of plasma inside a pore during propagation of an air SIW. a) electron density, b) electron impact ionization source and c) E/N.

References

[1] S. A Norberg, E. Johnsen, and M. J. Kushner, Plasma Sources Sci. Technol. **24**, 035026 (2015).

Study of Plasma-catalytic Oxidation of Methane: Role of Atomic Oxygen and Surface Species

Yudong Li [a], Jingkai Jiang [b], Michael Hinshelwood [a], Frank Doherty [c], Peter J. Bruggeman [b], Bryan R. Goldsmith [c] and Gottlieb S. Oehrlein [a]

(a) Department of Materials Science and Engineering and the Institute for Research in Electronics and Applied Physics, University of Maryland, College Park, MD 20742, USA (oehrlein@umd.edu)
(b) Department of Mechanical Engineering, University of Minnesota, Minneapolis, MN 55455, USA
(c) Department of Chemical Engineering, University of Michigan, Ann Arbor, MI 48109, USA

Cold atmospheric pressure plasma (CAP) generates reactive species that can enhance catalytic reaction through plasma-catalyst synergy effect. Recently, we have built a plasma-catalyst system to study the plasma-assisted decomposition of CH_4 to CO and CO_2 [1]. A well-studied atmospheric pressure plasma jet fed with 0.5%, 1.0% and 1.5% O_2 in Ar flow was used to treat a Ni-SiO_2/Al_2O_3 catalyst at temperatures from 25 $^{\circ}$C to 500 $^{\circ}$C with various plasma power levels. CH_4 carried by Ar gas was flowed downstream of the plasma to the catalyst bed, where the gases interact with the reactive species from the plasma flux and the catalyst. Real-time Fourier-transform infrared spectroscopy was applied to quantify the composition of downstream gases. Incident reactive oxygen species were quantitatively measured by molecular beam mass spectrometry using an identical plasma jet

Figure 1 – Ni catalyst was activated by 4 W CH_4/O_2/Ar plasma at 500 $^{\circ}$C, but it was deactivated by shutting off the CH_4 flow (no CO was generated).

operating at the same conditions. A correlation of the quantified flux of the atomic O from the plasma effluent with the rates of CH_4 consumption and CO and CO_2 production was observed, and indicates that atomic O plays an essential role in the decomposition of CH_4 to CO and CO_2, in particular at a catalyst temperature of 25°C. We also used diffuse reflectance infrared Fourier transform spectroscopy for operando surface analysis. The abundance of surface CO mirrors that of surface CH_n with plasma at 25 °C, indicating that the CH_n is the precursor species that is oxidized to surface CO by atomic O. Surface CH_n was not detected at 500 $^{\circ}$C, while more surface CO was observed, indicating that the decomposition of CH_4 to adsorbed CH_n might be the rate-determining step in the temperature-dependent plasma-assisted CH_4 oxidation at 500 $^{\circ}$C. We also investigated the interaction between the catalyst and CH_4/O_2/Ar plasma and found that the catalyst remained active after being treated by CH_4/O_2/Ar plasma with large power at 500 $^{\circ}$C, but can be deactivated by shutting off the CH_4 flow. Vibrational frequency of CO was found to change with catalyst temperature and plasma status, and will be discussed.

References
[1] A. J. Knoll, S. Zhang, M. Lai, P. Luan, G. S. Oehrlein, J. Physics D: Applied Physics **52,** 225201 (2019); S. Zhang, Y. Li, A. Knoll and G. Oehrlein, J. Physics D: Applied Physics **53,** 215201 (2020).
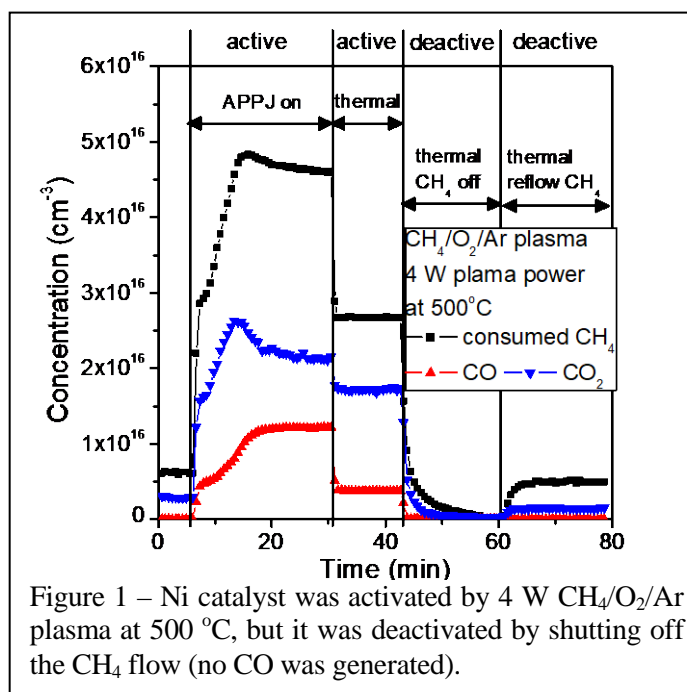
Sheath Dynamics Around a Water Droplet in an Atmospheric Pressure Glow Discharge

Mackenzie Meyer [a], Gaurav Nayak [b], Peter J. Bruggeman [b], and Mark J. Kushner [a]

(a) University of Michigan (maemeyer@umich.edu)
(b) University of Minnesota

Chemical activation of liquids by atmospheric pressure plasmas is limited by transport, as the reactive species produced by the plasma must first reach the interface between the plasma and the liquid and then diffuse into the bulk liquid. Shortening the distance between the plasma and the liquid and a high surface to volume ratio of the liquid mitigates the transport limits.

However, the processes at the interface of the gas and liquid (dense vapor due to evaporation, charging, short-lived species dynamics) are still an active area of research. This work aims to understand the sheath that forms around an 80 µm diameter water droplet immersed in a He atmospheric pressure radio frequency (RF) glow discharge using the 2D model *nonPDPSIM*. 5 W is deposited over the 10 MHz RF cycle, and the droplet is a nonconductive dielectric with $\varepsilon_r = 80$, matching ε_r of water. The liquid phase chemistry is not tracked for computational speed.

The plasma is modeled until a quasi-steady state is reached (>135 RF cycles), and the sheath properties are examined over one quasi-steady state RF cycle. As shown in Figure 1, the electron density around the droplet oscillates out of phase with the applied voltage, as expected with an RC circuit analysis of the system. E/N near the droplet is a superposition of the applied electric field, sheath electric field, and polarization of the dielectric droplet. As the applied electric field flips over the RF cycle, E/N oscillates primarily along the equator of the droplet. The electron temperature reaches its maximum at 45° above and below the equator of the droplet, where the Joule heating per electron is maximized. The droplet charges positively at the poles and negatively at the equator. The electron motion is dominated by the electric field at the equator but by diffusion at the poles, leading to this charge distribution.
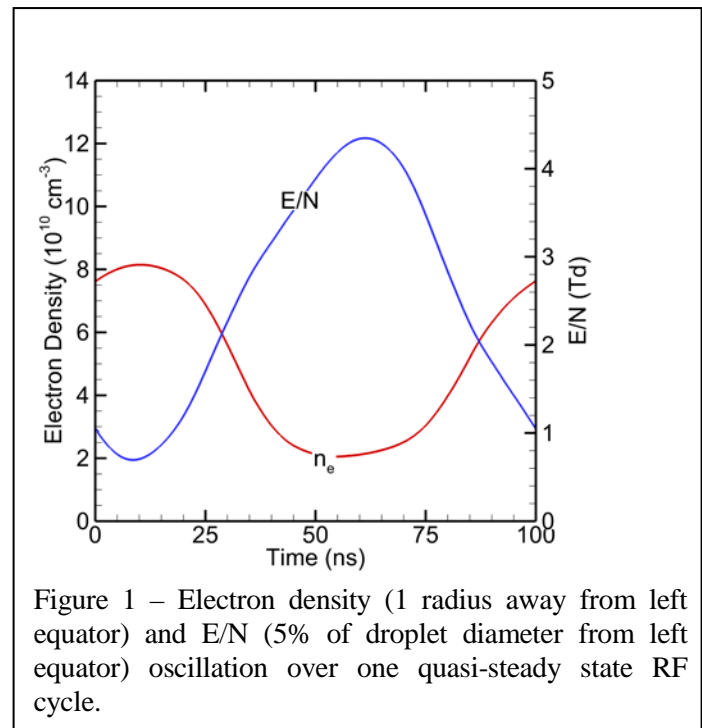

Figure 1 – Electron density (1 radius away from left equator) and E/N (5% of droplet diameter from left equator) oscillation over one quasi-steady state RF cycle.

Changing properties of the plasma (power and RF frequency) changes the bulk plasma, while changing the properties of the droplet (ε_r, conductivity, diameter) does not significantly affect the bulk plasma but does affect the sheath around the droplet. For example, as the conductivity of the droplet increases from 0 to 10^{-1} S/cm, the charge density becomes entirely negative, and the charge oscillates at conductivities at least 10^{-3} S/cm.

Green Fertilizer: Can Cold Plasmas Enrich Biowaste and Reduce Nitrogen Loss?

Victor Miller and Ali Mesbah

Department of Chemical and Biomolecular Engineering, UC Berkeley (vmiller1671@berkeley.edu)

We investigate a non-thermal air plasma process treatment to improve biowaste as fertilizer while reducing emissions of greenhouse gasses and ammonia-related deaths, previously proposed by Ingels et al [1]. This would be a green alternative to the Haber-Bosch ammonia process, which accounts for more than 2% of the world's CO_2 emissions and supplies fertilizer that supports half of the world's population [2 ,3]. Ammonia emissions from agriculture are estimated to be responsible for 3000 deaths per year in the US Corn Belt alone [4].

We hypothesize that plasma treatment of biowaste will reduce ammonia evaporation. We further hypothesize a mechanism by which this occurs: cold plasma generated from air generates nitric oxide radicals that form nitric acid in water. This acidifies the basic biowaste and transforms volatile ammonia to involatile ammonium. This entire process only requires air, biowaste, and electricity.

We propose to investigate the first hypothesis by testing our process on manure samples collected from the California Central Valley. These samples will be acidified to a pH < 6 and then air-dried to allow any volatile ammonia to escape. The manure will be assayed for ammoniacal-N through the modified Berthelot reaction for colorimetric measurement.

The second hypothesis will be tested by tracking the change in pH, nitrate content, and total nitrogen over the course of plasma treatment, and comparing this

Figure 1 – Schematic of treatment process and reactions

over the same time interval to manure drawn from the same sample. Nitrate will be tested by enzymatic transformation to nitrite, then tested by the Griess assay for colorimetric measurement. This would demonstrate exogenous nitrogen addition from the plasma to the manure in the form of nitrate. It would also indicate the acidification of the manure matches ammonia retention. This ammonia retention should be reversed following alkaline treatment of the plasma treated manure. Collected data will guide experiments and fitting in the pursuit of a process model.
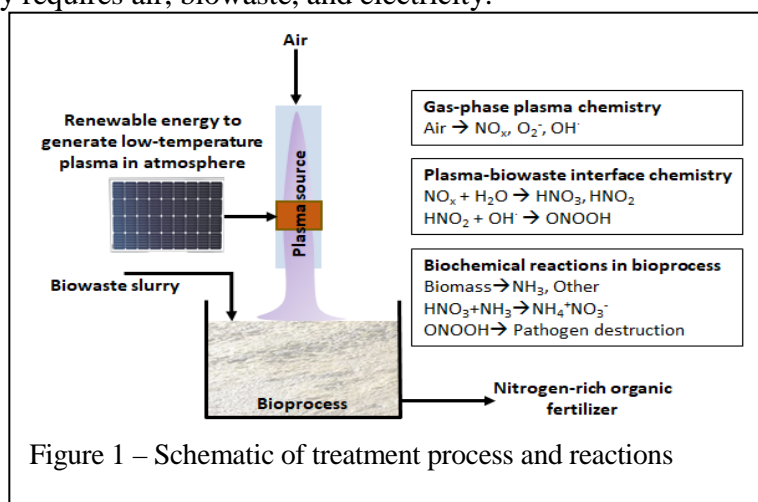
References
[1] R. Ingels and D. Graves, Plasma Medicine **5(2)**, 2016.
[2] J. W. Erisman, M. A. Sutton, J. Galloway, Z. Klimont, and W. Winiwarter, Nat Geosci, **1**, 10 (2008).
[3] International Energy Agency, International Energy Agency Paris, **56**, 2035 (2013).
[4] A. Pozzer, A. P. Tsimpidi, V. A. Karydis, A. de Meij, and J. Lelieveld, Atmos Chem Phys, **17**, 20 (2017).

Laser Induced Fluorescence Measurements of Vibrationally Excited Oxygen Produced by Recombination of O Atoms

Dirk Van Den Bekerom [a], Keegan Orr [a], Elijah R Jans [b], Xin Yang [c], Anam C. Paul [d], and Igor V. Adamovich [e]

(a) Sandia National Laboratories (dvanden@sandia.gov)
(b) The Ohio State University (orr.282@osu.edu)
(c) Sandia National Laboratories (erjans@sandia.gov)
(d) The Ohio State University (yang.5473@osu.edu)
(e) The Ohio State University (paul.1079@osu.edu)
(c) The Ohio State University (adamovich.1@osu.edu)

Vibrationally excited oxygen and nitrogen have been long recognized to be of critical importance in nonequilibrium high-enthalpy flows, primarily encountered behind hypersonic shock waves [1]. To date, no direct experimental verification of vibrational state resolved dissociation rates predicted by different kinetic models has been undertaken, in large part due to the difficulty of measuring these rates directly. We present a framework where state specific recombination rates can be inferred from the time-resolved measurements of O_2 vibrational populations, such that the state specific dissociation rates can be obtained from the detailed balance.

In the present approach, recombination reactions of atomic oxygen are monitored in the afterglow of a diffuse ns pulse discharge burst in an O_2-Ar mixture. The time evolution of $O_2(v)$ populations in the recombining mixture are measured by ps Laser Induced Fluorescence (LIF) in the Schumann-Runge bands, with absolute calibration by NO LIF. By varying the output wavelength of the ps laser / Optical Parametric Oscillator (OPO) system used for the excitation in the 250-450 nm range, levels from v"=7 to 21 have been detected. Two-photon Absorption LIF (TALIF) at 226 nm has been used to measure the atomic oxygen concentration, with absolute calibration by Xe [2].

Within ~1 ms after the discharge burst, a rapid decay of $O_2(v)$ is observed, indicating vibration-vibration (V-V) and vibration-translation (V-T) relaxation of vibrational states populated by electron impact and by quenching of the excited electronic states of Ar. After the rapid initial decay, the vibrational populations level off and remain nearly constant, or exhibit a transient rise, on the timescale of about 10 ms, suggesting the presence of a persistent source of vibrational excitation due to chemical reactions. In addition to O atom recombination to form vibrationally excited O_2 molecules, at low temperatures atomic oxygen may also recombine with O_2 and form ozone. The latter may well generate vibrationally excited O_2 in $O + O_3 \rightarrow O_2 + O_2$ reaction, which would therefore affect the present results. Ozone formation is controlled by heating the excited mixture up to 800 K, as well as increasing the pressure and reducing the O_2 mole fraction, when the production of ozone is reduced significantly.

References
[1] C. Park, Nonequilibrium Hypersonic Aerodynamics, Wiley, New York, 1990, Chap. 3.
[2] K. Niemi, V. Schulz-von der Gathen, and H. F. Döbele, Journal of Physics D: Applied Physics **34** (2001) 2330.

Measurements of Atoms and Metastable Species in N_2 and H_2-N_2 Ns Pulse Plasmas

Xin Yang, Caleb Richards, Elijah Jans, Sai Raskar, Dirk van den Bekerom,

and Igor V. Adamovich

Nonequilibrium Thermodynamics Laboratory, Department of Mechanical and Aerospace Engineering
The Ohio State University, Columbus, OH 43210, USA

Time-resolved, absolute number densities of metastable $N_2(A^3\Sigma_u^+,v=0,1)$ molecules, ground state N and H atoms, and rotational-translational temperature have been measured by Tunable Diode Laser Absorption Spectroscopy (TDLAS) and Two-photon Absorption Laser-Induced Fluorescence (TALIF) in diffuse nitrogen and N_2-H_2 plasmas during and after a ns pulse discharge burst. Comparison of the measurement results with the kinetic modeling predictions, specifically the significant reduction of the $N_2(A^3\Sigma_u^+)$ populations and the rate of N atom generation during the burst, suggests that these two trends are related. The slow N atom decay in the afterglow, on the time scale longer than the discharge burst, demonstrates that the latter trend is not affected by N atom recombination, diffusion to the walls, or convection with the flow. This leads to the conclusion that the energy pooling in collisions of $N_2(A^3\Sigma_u^+)$ molecules is a major channel of nitrogen dissociation in electric discharges where a significant fraction of the input energy goes to electronic excitation of N_2. Additional measurements in a 1% H_2-N_2 mixture demonstrate a further significant reduction of $N_2(A^3\Sigma_u^+,v=0,1)$ populations, due to the rapid quenching by H atoms accumulating in the plasma. Comparison with the modeling predictions suggests that the $N_2(A^3\Sigma_u^+)$ molecules may be initially formed in the highly vibrationally excited states. The reduction of the $N_2(A^3\Sigma_u^+)$ number density also diminishes the contribution of the energy pooling process into N_2 dissociation, thus reducing the N atom number density. The rate of N atom generation during the burst also decreases, due to its strong coupling to $N_2(A^3\Sigma_u^+,v)$ populations. On the other hand, the rate of H atom generation, produced predominantly by the dissociative quenching of the excited electronic states of nitrogen by H_2, remains about the same during the burst, resulting in a nearly linear rise of the H atom number density. Comparison of the kinetic model predictions with the experimental results suggests that the yield of H atoms during the quenching of excited electronic state of N_2 by molecular hydrogen is significantly less than 100%. The present results quantify the yield of N and H atoms in high-pressure H_2-N_2 plasmas, which have a significant potential for ammonia generation using plasma-assisted catalysis.
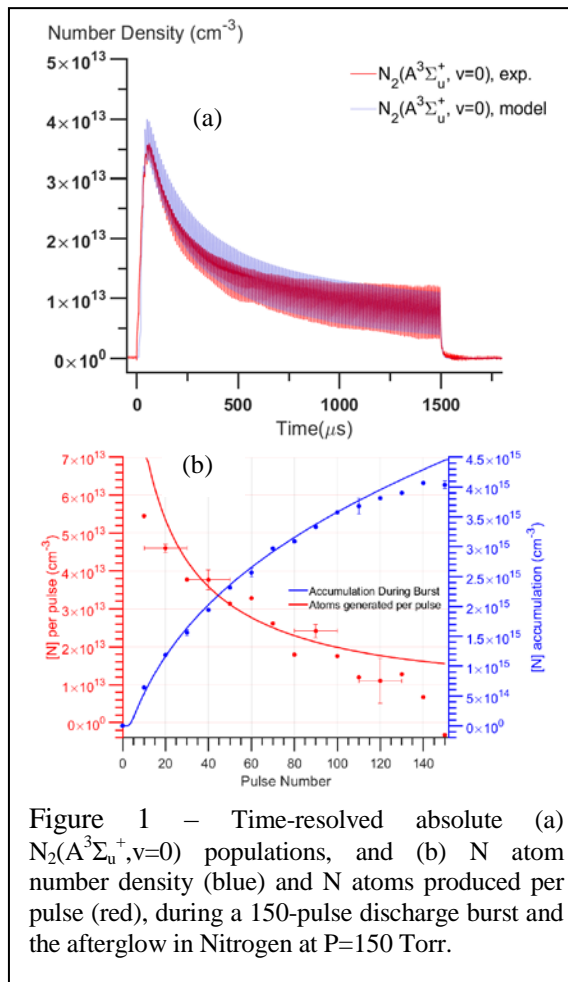

Figure 1 – Time-resolved absolute (a) $N_2(A^3\Sigma_u^+,v=0)$ populations, and (b) N atom number density (blue) and N atoms produced per pulse (red), during a 150-pulse discharge burst and the afterglow in Nitrogen at P=150 Torr.

Time-resolved CO_2, CO, and N_2 Vibrational Populations in Ns Pulse Discharge Plasmas

Caleb Richards, Elijah Jans, and Igor V. Adamovich

Nonequilibrium Thermodynamics Laboratory
Department of Mechanical and Aerospace Engineering
The Ohio State University, Columbus, OH 43210, USA
adamovich.1@osu.edu

Time-resolved CO_2, CO, and N_2 vibrational populations and translational-rotational temperature are measured in a ns pulse burst discharge plasma. The discharge is sustained in a CO_2-N_2 mixture slowly flowing through a rectangular cross section quartz channel, with two parallel plate electrodes external to the channel. CO_2 and CO vibrational populations are measured by mid-IR, tunable Quantum Cascade Laser (QCL) Absorption Spectroscopy, and N_2 vibrational populations are measured by the ns broadband vibrational CARS, in collinear phase matching geometry. The results indicate that a ns pulse discharge operated at a high pulse repetition rate, 100 kHz, results in a modest vibrational excitation of N_2 and CO_2. The number density of CO, a major product of CO_2 dissociation, is also inferred from the QCL measurements. The present diagnostics allow in situ monitoring of the time-resolved, state-specific CO_2 vibrational excitation and relaxation during the discharge and in the afterglow, along with the time-resolved CO vibrational populations. This makes possible isolating and quantifying two major mechanisms of CO_2 dissociation, (i) decay via excited electronic states populated by electron impact, and (ii) stepwise anharmonic vibration-vibration (V-V) pumping of the asymmetric stretch vibrational mode, sustained by the strong vibrational excitation of N_2 and rapid V-V energy transfer to CO_2.
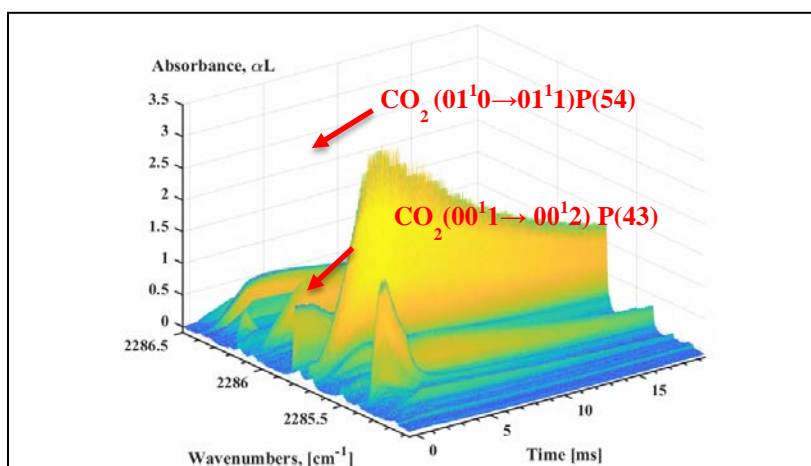

Figure 1 – Time-resolved rotational-vibrational transitions of CO_2 during and after a 100 kHz ns discharge burst 2.5 ms long, in 5% CO_2-N_2 mixture at P=100 Torr.
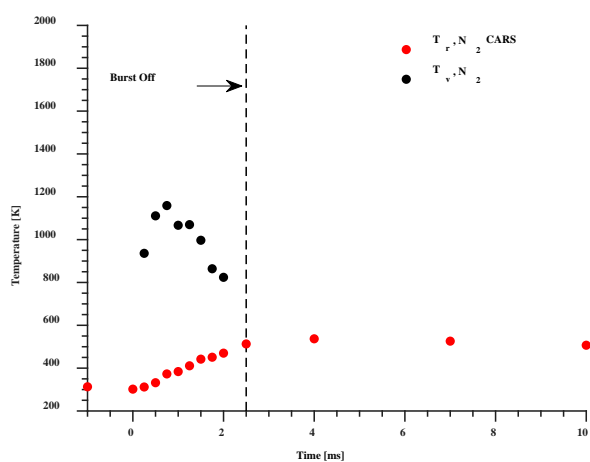

Figure 2 – Time-resolved N_2 rotational and vibrational temperatures measured by ns broadband vibrational CARS.

43

N_2 Vibrational Excitation in Atmospheric Pressure Ns Pulse and RF Plasma Jets

Caleb Richards, Elijah Jans, Ilya Gulko, Keegan Orr, and Igor V. Adamovich

Nonequilibrium Thermodynamics Laboratory, Department of Mechanical and Aerospace Engineering
The Ohio State University, Columbus, OH 43210, USA
(adamovich.1@osu.edu)
.

Time-resolved N_2 vibrational temperature and translational-rotational temperature in quasi-two-dimensional atmospheric pressure plasma jets excited by ns pulse and RF discharges are measured by broadband vibrational CARS, in collinear phase matching geometry. As expected, the results indicate a much stronger vibrational excitation in the RF plasma jet due to both lower reduced electric field and higher coupled power. In a ns pulse discharge in N_2/He, N_2 vibrational temperature is significantly lower compared to that in N_2/Ar, due to the more rapid V-T relaxation of nitrogen by helium atoms. In the RF plasma jets in N_2/Ne and N_2/Ar, the vibrational excitation increases considerably as the nitrogen fraction in the mixture is reduced.

The experimental data in the RF plasma jet in N_2/Ar jet are compared with the kinetic modeling predictions. The

Figure 1 – . Entire N_2 CARS spectrum taken in an RF discharge in a 6% N_2/Ne mixture, illustrating a significant contribution of N_2 in ambient air into $N_2(v=0)$ signal, which was removed for the data processing. The dashed line boundaries (also shown as insets) indicate the regions used for the vibrational and rotational temperature inference. Inferred rotational and vibrational temperatures are T = 675 ± 25 K, T_v = 3370 ± 120 K.

kinetic model solves the electron energy equation (a moment of the Boltzmann equation), the heavy species energy equation, and equations for the species concentrations. The model incorporates the electron impact ionization, dissociation, electronic excitation, and vibrational excitation processes; energy transfer among the excited electronic states of Ar and N_2; and N_2 vibrational relaxation (state-specific vibration-vibration energy transfer for N_2- N_2 and vibration-translation relaxation for N_2-N). Comparison of the modeling predictions with the data shows that nitrogen vibrational excitation in N_2/Ar plasma jets with a small N_2 fraction in the mixture (several percent) is controlled primarily by electron impact, anharmonic V-V pumping, and V-T relaxation by N atoms. In comparison, V-V energy transfer from the vibrationally excited molecules in the lowest excited electronic state, $N_2(A^3\Sigma_u^+,v)$, which are generated by energy transfer from the metastable Ar atoms, has a minor effect on the vibrational populations of the ground electronic state, $N_2(X^1\Sigma_g^+,v)$. Although the discharge input energy fraction going to the generation of N_2 electronic state is significant, the quasi-steady-state $N_2(A^3\Sigma_u^+)$ number density, controlled by the energy pooling and quenching by N atoms, remains relatively low, below ~ 10^{14} cm^{-3}. Because of this, the net rate of $N_2(X^1\Sigma_g^+,v)$ vibrational excitation by the V-V energy transfer from $N_2(A^3\Sigma_u^+,v)$is much lower compared to that by the direct electron impact.
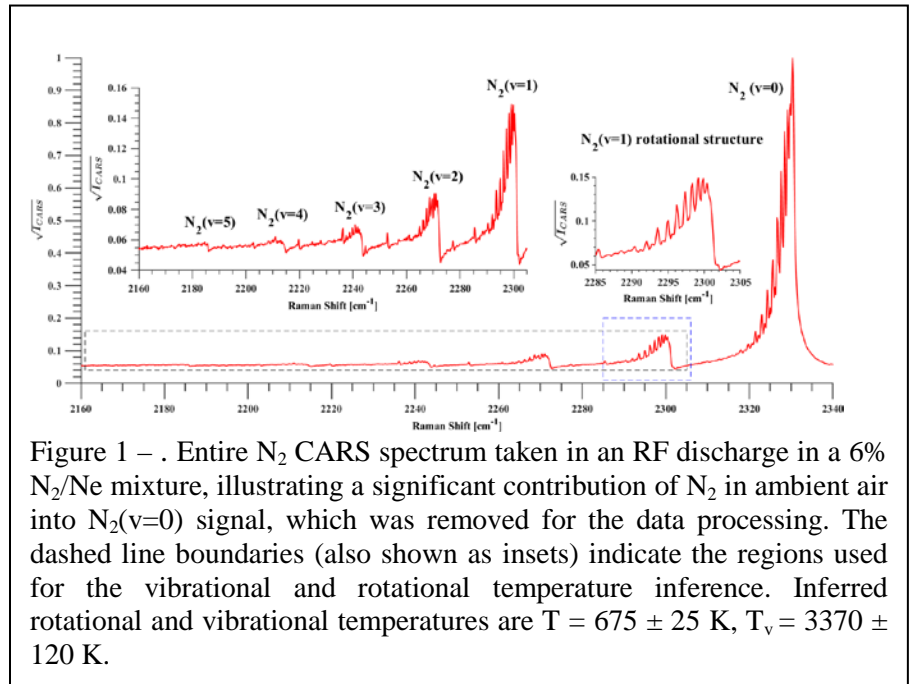
Active Learning-guided Experiment Design for Maximizing Energy Efficiency of NO$_x$ Production Using a DC Pin-to-pin Glow Discharge

Ketong Shao and Ali Mesbah

Department of Chemical and Biomolecular Engineering, University of California, Berkeley

Low temperature plasmas (LTPs) can produce NO$_x$ from air which can be converted into nitric acid for nitrogen-based fertilizer, an inherent green technology. However, current LTP-based nitrogen fixation is far from large-scale industrial practice, as its best efficiency is around 2.0 MJ/mol N in comparison with the Haber-Bosch (H-B) 0.5 MJ/mol N [1]. Optimizing LTP-based N fixation process is challenging due to the complex not fully understood mechanisms and the high design dimension, including operating parameters, reactor structure, and catalyst properties. To address the challenges, we have studied the plasma operating window of a DC pin-to-pin glow discharge without catalysts. The four adjustable parameters of the discharge are inlet flowrate of air, inlet O$_2$ concentration, discharge current, and pin-to-pin gap distance. The output NO$_x$ (NO, NO$_2$ and HONO) concentration is measured using FTIR
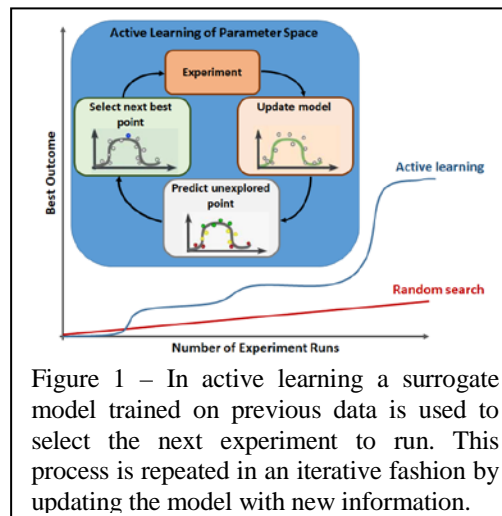

Figure 1 – In active learning a surrogate model trained on previous data is used to select the next experiment to run. This process is repeated in an iterative fashion by updating the model with new information.

spectroscopy. The current and voltage of the glow discharge are recorded to calculate the discharge power. The energy cost is

$$\min_{u} E_{N_r} = \frac{\text{Discharge Power}}{NO_x \text{ Concentration} \times \text{Flowrate}},$$

where, u is the vector of parameters and E_{N_r} has units of GJ/tN. Several active learning strategies (constrained Bayesian optimization) [2,3], as shown in Fig. 1, have been used to explore the operating window of the DC glow discharge.

In this work, the 4-dimensional optimal operating windows of DC glow discharges are investigated for two scenarios: **energy cost minimization of NO$_x$ generation** and **maximum NO$_x$ production rate subject to power constraint**. Systematic exploration of the parameter space is particularly challenging due to their nonlinear and multivariable dependence on the discharge parameters. Exploring this 4-d parameter space would require 5^4=625 experiment runs for 5 values for each parameter. Constrained exploration problems are very common in real practices due to practical limitations and/or system constraints. The active learning strategy enables us to efficiently establish the optimal
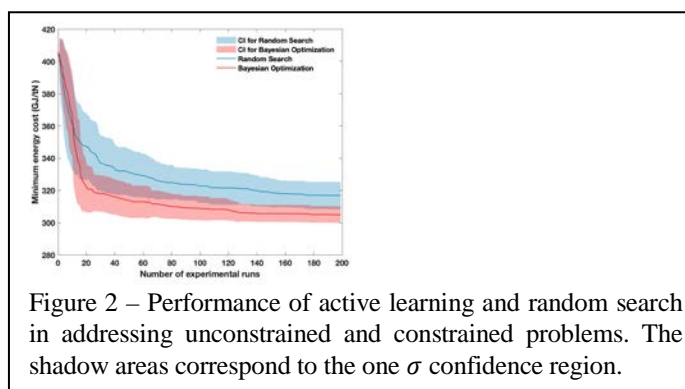

Figure 2 – Performance of active learning and random search in addressing unconstrained and constrained problems. The shadow areas correspond to the one σ confidence region.

operating windows for both scenarios. As shown in Fig. 2, only 100 experiment runs are required to yield the minimum energy cost. Active learning explicitly accounts for the power constraint and determines the optimal operating window with around 130 runs. The minimum energy cost and maximum NO$_x$ production rate were also consistent with literature values [4].

References
[1] F. Jardali et al. Green Chem. **23**, 1748 (2021)
[2] S. Ariafar et al. J. Mach. Learn Res. **20**, 1 (2019).
[3] B. Shahriari et al., Proceedings of the IEEE **104**, 148 (2016).
[4] X. Pei et al., Chem. Eng. J. **362**, 217 (2019)

Formation of Self-Organized Patterns at the Plasma-Liquid Interface for a Helium Glow Discharge with Solution Anode

Tanubhav Kumar Srivastava, Marien Simeni Simeni, Peter J. Bruggeman
Mechanical Engineering Department, University of Minnesota, 111 Church St SE, Minneapolis, Minnesota, 55455, USA (sriva203@umn.edu)

Self-organization at the plasma-liquid interface of a solution anode is a commonly observed phenomenon for atmospheric pressure plasmas, resulting in patterns with distinctive shapes such as circular rings, star shaped and rotating gear-like structures [1], depending on the current and solution conductivity [2]. Recent studies have shown the impact of the electrode gap distance [3], liquid anode solution [4], and gas composition [3] on pattern formation. In the present study, the necessary conditions for pattern formation were investigated. It was also found that patterns develop on a time scale of 10s of microseconds in the initial phase and reach a steady state on millisecond time scales
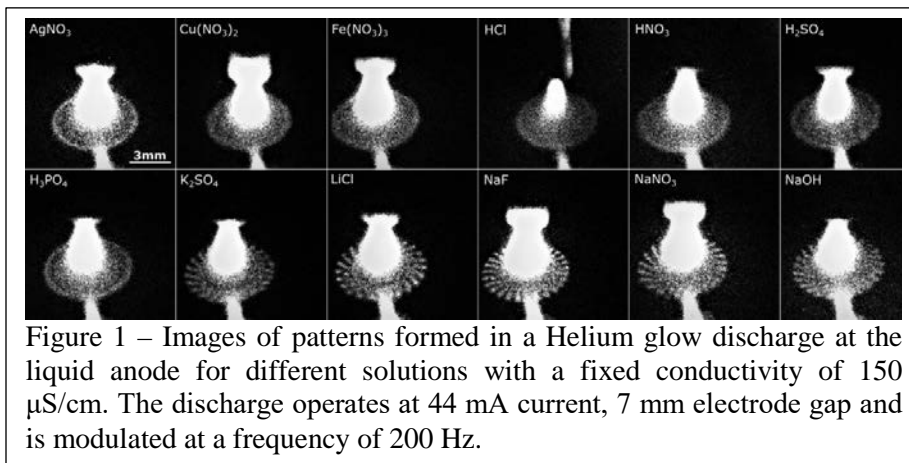

Figure 1 – Images of patterns formed in a Helium glow discharge at the liquid anode for different solutions with a fixed conductivity of 150 μS/cm. The discharge operates at 44 mA current, 7 mm electrode gap and is modulated at a frequency of 200 Hz.

underlining that processes occurring on these time scales enable the pattern formation.

A direct correlation between anode solution evaporation and formation of patterns was observed. The presence of oxygen showed the largest impact on pattern formation amongst all the gas mixtures investigated. Oxygen drastically reduced the current required for a given solution conductivity for pattern formation. As this effect was not observed for other molecular gases, the presence of a strong electronegative gases in addition to water vapor is needed. Patterns were observed to disappear when applying N_2 shielding gas (effectively removing the O_2 entrainment in helium jet) and using an ice bath solution to reduce solution evaporation into the discharge. An investigation of different solutes at the same conductivity (as shown in Figure 1) indicates that pattern formation was only observed for cations with an electronegativity value less than 1.8 on the Pauling scale of electronegativity [5]. The three necessary conditions which all need to be satisfied simultaneously to observe pattern formation for the investigated conditions will be discussed in more detail.

References
[1] J. E. Foster et al., Plasma Sources Sci. Technol. **29**, 034004 (2020).
[2] T. Verreycken et al., J. Appl. Phys. **105**, 088312 (2009).
[3] N. Shirai et al., Plasma Sources Sci. Technol. **23**, 054010 (2014).
[4] S. Zhang and T. Dufour, Physics of Plasmas. **25**, 073502 (2018).
[5] L. Pauling, J. Am. Chem. Soc. **54**, 9 (1932).

The Effect of Liquid Residence Time on the Removal of Aqueous Contaminants

Mikhail Vasilev [a], Xudong Su [a], Patrick Conlon [b], Jaymes Suiter [a], Douglas Bohl [b] and Selma Mededovic Thagard [a]

(a) Department of Chemical and Biomolecular Engineering, 8 Clarkson Avenue, Clarkson University, Potsdam, 13699, NY, USA (smededov@clarkson.edu)
(b) Department of Mechanical and Aeronautical Engineering, 8 Clarkson Avenue, Clarkson University, Potsdam, 13699, NY, USA

Electrical discharge plasma is a promising, cost-effective alternative process to conventional wastewater treatment techniques for removal of a range of contaminants. However, insufficient understanding of physicochemical processes both at the plasma-liquid interface and in the bulk liquid is preventing timely and effective scale up of bench-scale reactors.

The goal of this work was to determine the role of solute transport in the liquid phase of a gas-liquid plasma reactor in degradation of two model pollutants: rhodamine B dye and caffeine. For that purpose, three reactor designs were adopted to achieve a wide range of convective rates: a plasma spinning disc reactor (PSDR), a square channel reactor with forced liquid recirculation (SCR), and a rail-to-plane reactor with plasma-induced mixing (RtPR).[1]

Degradation experiments revealed the existence of three operating regimes; the solute convection limited regime in which degradation rates are proportional to both characteristic flow velocity and solute bulk liquid concentration, the solute diffusion limited regime, in which the degradation rates are proportional to solute bulk liquid concentration, and the reactive species limited regime in which degradation rates are proportional to the rates of hydrogen peroxide production. The transition between regimes is regulated by operational parameters, e.g., bulk solute concentration, discharge energy and liquid flow rate.

Figure 1 – Modeling results of caffeine degradation efficiency as a function of liquid residence time for various hydroxyl radical influx levels.

A mathematical model has been developed for caffeine degradation to establish a relation between the rate of reactive species production (hydroxyl radicals) and different solute transport mechanisms and explore the effects of system parameters on degradation. The acquired results suggest that for all tested systems the main predictor of the overall degradation rate is the liquid residence time under the plasma with lower residence times generally yielding higher degradation efficiency (Figure 1). This result can be used to inform efficient design of plasma reactors by aiding identification of performance-limiting processes.
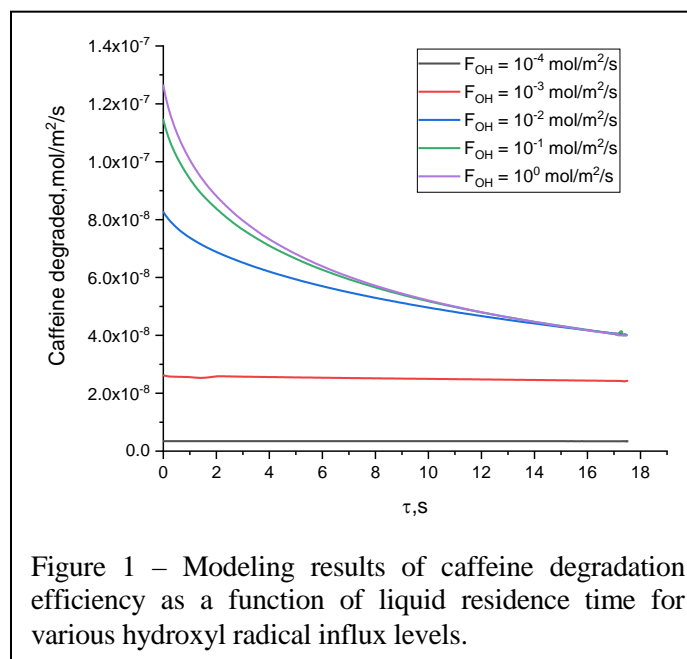
References

[1] S. M. Thagard et al, Plasma Chem. Plasma Process. **38**(4), 719 (2018).

Spatially Resolved Absolute OH-LIF Measurements in a Surface Discharge Generated by an Atmospheric Pressure Plasma Jet

Jianan Wang and Peter Bruggeman

Department of Mechanical Engineering, University of Minnesota, Minneapolis, MN 55455, USA
(wang9597@umn.edu, pbruggem@umn.edu)

While plasma-surface interactions at low pressure are often due to energetic ion etching, at atmospheric pressure, the ion mean free path is much smaller than the sheath thickness resulting in insufficient ion energies. Hence radicals often play an important role in plasma-surface reactions. In addition, sheaths and boundary layers having significant species gradients at the plasma-substrate interface at atmospheric pressure occur on length scales of 100 μm or less. Accessing these length scales remains a huge challenge for diagnostics. Resolving such near surface gradients is particularly important for so-called surface discharges that propagate along the substrate, a common phenomenon at atmospheric pressure.

In this work we report OH radical species density measurements with a spatial resolution of ~10 μm perpendicular to a quartz substrate of a surface streamer discharge generated by an atmospheric pressure plasma jet impinging on the quartz substrate. While OH densities have been measured extensively in atmospheric pressure plasmas, we believe this is the first reported measurement with so high resolution near a substrate allowing to determine near surface gradients of radicals.

The OH-LIF signals were measured 15 ns after the laser pulse to reduce the laser scattering on the surface. A 4-level 0D LIF model is used to interpret the measured signal and obtain an absolute calibration with Rayleigh scattering [1]. The absolute air and water vapor obtained from the lifetime of the laser excited OH(A). The helium jet blows the air away from the substrate leading to an air fraction of 0.03% near the surface which increases to 5% at a distance of 600 μm from the surface. With a relative humidity of 37% in the ambient air, the water vapor increases from 0.08×10^{16} cm^{-3} to 1×10^{16} cm^{-3} (Figure 1).

The OH emission indicates an ionizing plasma region up to 500 μm from the substrate. The OH density, however, has a maximum value of 1×10^{14} cm^{-3} at the edge of the visible plasma and does not exceed 0.5×10^{12} cm^{-3} at the substrate. The OH density reaches the same density at a distance of 800 μm from the substrate. The measurement of the gradient of OH densities near the substrate allows to estimate the OH diffusion flux to the substrate at 5×10^{15} cm^{-2} s^{-1}. This value is the same within the experimental accuracy as the kinetic OH flux determined from the measured OH density at the interface.

The results demonstrate the capability to perform LIF measurements near a substrate with spatial resolution of 10 μm and enable us to determine accurate OH fluxes to the substrate induced by surface discharges which is important to further our understanding of plasma-surface interactions.
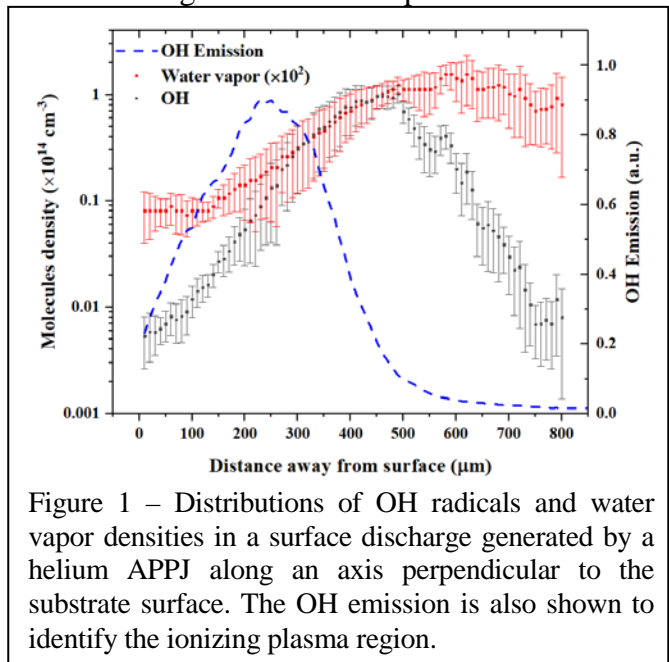

Figure 1 – Distributions of OH radicals and water vapor densities in a surface discharge generated by a helium APPJ along an axis perpendicular to the substrate surface. The OH emission is also shown to identify the ionizing plasma region.

References

[1] T. Verreycken et al 2013 J. Phys. D: Appl. Phys. **46** 464004.

Spatially Enhanced Electric Field Induced Second Harmonic (SEEFISH) Generation

Sai Raskar, Keegan Orr and Igor V. Adamovich

Nonequilibrium Thermodynamics Laboratory, Department of Mechanical and Aerospace Engineering
The Ohio State University, Columbus, OH 43210, USA
(raskar.1@osu.edu)

The spatial resolution of the ps Electric Field Induced Second Harmonic (EFISH) generation has been enhanced by using non-collinear laser beam phase matching geometries, as shown in Fig. 1. The first approach is similar to the one used in Unstable Resonator – Enhanced Detection Coherent Anti-Stokes Raman Scattering (USED CARS). Briefly, the pump laser beam (1064 nm, pulse duration 150 ps, pulse energy 20-40 mJ) is separated into two coaxial beams before the focusing lens. The two beams, with the combined pulse energy of 10-20 mJ, overlap only near the focal point, generating the Spatially Enhanced EFISH (SEEFISH) signal over a significantly shorter region compared to that in the collinear phase matching. The resulting SEEFISH signal is spatially isolated from the "conventional" EFISH signal and measured by a photomultiplier detector.
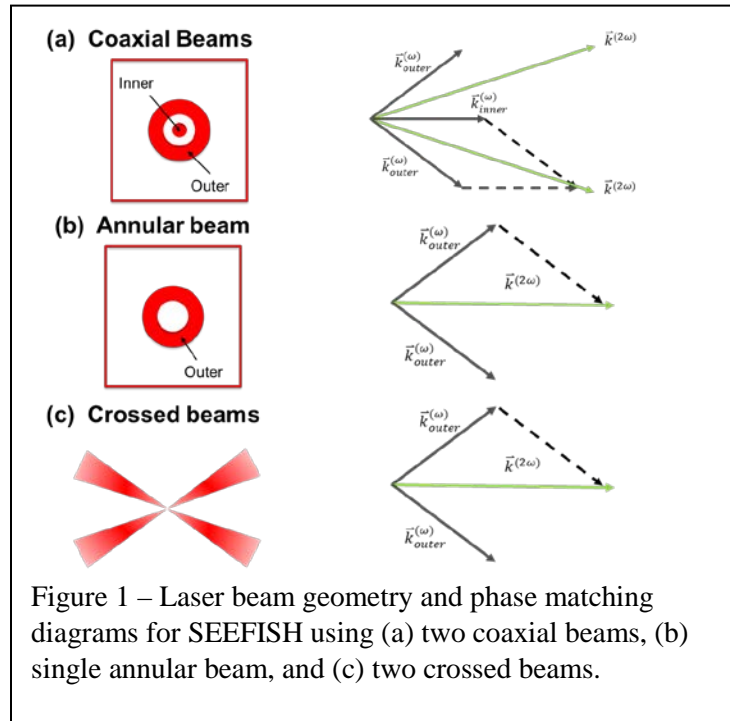

Figure 1 – Laser beam geometry and phase matching diagrams for SEEFISH using (a) two coaxial beams, (b) single annular beam, and (c) two crossed beams.

Blocking of either of the two beams results in a complete suppression of the signal, demonstrating that it is generated by the superposition of the two beams overlapping near the focal point. Measurements of a known Laplacian field generated between two parallel cylinder electrodes in ambient air demonstrated that SEEFISH improves the spatial resolution of the measurements by well over a factor of 2. The spatial resolution is improved further by reducing the focal distance of the lens. As expected, the magnitude of the SEEFISH signal is significantly lower compared to that of the "conventional" EFISH. The second approach is using two crossed laser beams, similar to BOXCARS, as shown in Fig. 1. The results obtained using two crossed beam SEEFISH are similar to those using two coaxial beams. Increasing the crossing angle from 1.4° to 2.0° shortens the region from which the signal originates (measured by scanning a glass plate along the crossed beams) by about a factor of two. However, the signal drops by nearly a factor of 500. At this time, such a significant reduction of the signal is not understood. The new diagnostic has a considerable potential for measurements of electric field distributions in high-pressure plasmas near surfaces, with high temporal and spatial resolution. An additional benefit is blocking the stray EFISH signal originating from the optical access windows.

References

[1] Tat Loon Chng et al, Plasma Sources Sci. Technol. **29**, 125002 (2020).

fs-UV-LAS for Measuring Temperature and OH Concentration in Low Temperature Plasmas

Ning Liu, Hongtao Zhong, Timothy Y. Chen, Ying Lin, Ziyu Wang and Yiguang Ju

Dept. of Mechanical and Aerospace Eng., Princeton University, Princeton, NJ 08544, USA (nl7@princeton.edu)

Recently, femtosecond (fs) laser has attracted tremendous attention across a wide variety of laser diagnostics for plasma and combustion, since it can generate pulses that features femtosecond timescale in the time domain, and broadband spectrum in the frequency domain [1, 2]. This work focuses on the use of broadband spectrum of fs laser for laser absorption spectroscopy (LAS). Currently, the typical commercially-available fs laser has a bandwidth of 10 to 1000 cm^{-1}. Such broadband spectrum can be used to simultaneously probe many transitions (electronic, vibrational, or rotational) of either single or multiple species with fs or ps time resolution. As a result, this benefit can either enable multi-parameter (e.g., temperature and species concentration) measurements (with broadband sensing of single species), or multi-species concentration measurements (with broadband sensing of multiple species). These fs-laser-enabled measurements exhibit two major advantages, compared to the past broadband methods, such as tunable diode laser absorption spectroscopy (TDLAS) [3]. First, the fs laser absorption is more accurate than TDLAS. This is because much more transitions of species can be simultaneously measured by fs laser than the typical TDLAS, given that the typical bandwidth of fs laser is significantly wider than the tuning range of TDLAS. Second, the fs laser absorption has a fs or ps time resolution, considerably shorter than TDLAS. This will further extend the application of fs laser absorption to ultrafast processes.

With the above understanding, this work reports the fs LAS in the ultraviolet (UV) range (code-named fs-UV-LAS) for simultaneously measuring temperature and species concentration with improved accuracy in low temperature plasmas. The fs-UV-LAS was demonstrated based on the OH electronic transitions ($X^2\Pi$-$A^2\Sigma^+$) near 308 nm. Figure 1 shows the experimental setup for implementing fs-UV-LAS for measuring temperature and OH concentration. This setup consisted of three major components: a fs laser system, a plasma reactor, and a spectrometer-camera system. The fs laser system (i.e., a Ti: Sapphire scillator, an amplifier and an optical parameter amplifier, OPA) was first used to generate fs laser pulses with a bandwidth of ~3.2 nm centered at 308

Figure 1 - Experimental setup for fs-UV-LAS for measuring temperature and OH concentration.

nm. Then the fs laser pulses were absorbed by OH radicals in low temperature plasmas produced by a nanosecond voltage pulser and operated at a pressure of 100 Torr. After the absorption, the fs laser pulses were spectrally dispersed and detected by a spectrometer-camera system. By fitting the measured absorption spectrum, both temperature and OH concentration could be obtained with enhanced accuracy and fs/ps time resolution.
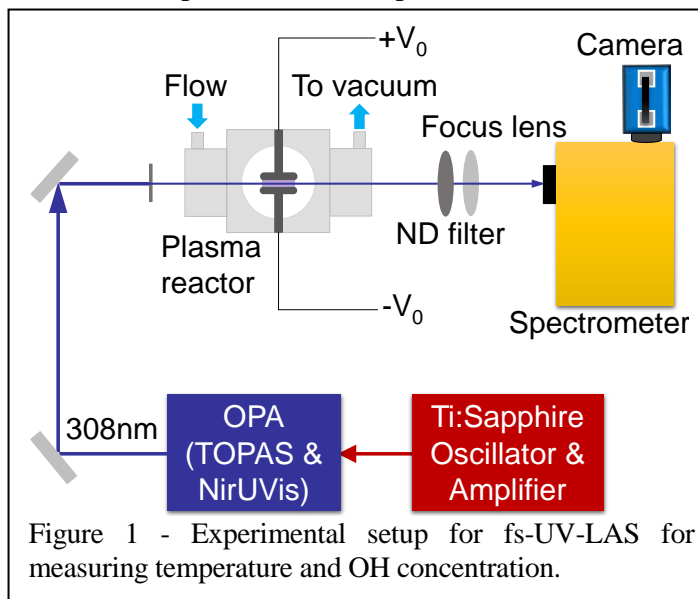
References

[1] S. Roy, W.D. Kulatilaka, D.R. Richardson, R.P. Lucht, J.R. Gord, Optics letters 34 (2009) 3857-385.
[2] J.B. Schmidt, S. Roy, W.D. Kulatilaka, I. Shkurenkov, I.V. Adamovich, W.R. Lempert, J.R. Gord, Journal of Physics D: Applied Physics 50 (2016) 015204.
[3] V. Nagali, S. Chou, D. Baer, R. Hanson, J. Segall, Applied Optics 35 (1996) 4026-4032.

$N_2(A^3\Sigma_u^+,v)$ Energy Transfer Kinetics in Reacting N_2-CO_2-CH_4 Plasmas

D. Mignogna [a], E.R. Jans [b], S. Raskar [c], and I.V. Adamovich [d]

(a) The Ohio State University (mignogna.8@osu.edu)
(b) Sandia National Laboratory (ejans54@gmail.com)
(c) The Ohio State University (raskar.1@osu.edu)
(d) The Ohio State University (adamovich.1@osu.edu)

Energy transfer from metastable $N_2(A^3\Sigma_u^+,v=0,1)$ molecules in ns pulse discharge plasmas sustained in mixtures of nitrogen with CO_2, CH_4, and H_2 is studied using Tunable Diode Laser Absorption Spectroscopy (TDLAS). The plasma is generated in the gas mixtures flowing through a rectangular cross section quartz channel, using a repetitive ns pulse discharge sustained between two parallel plate copper electrodes external to the channel. The discharge gap is 7 mm and the pressure in the cell is 150 Torr. The discharge pulse repetition rate is up to 100 kHz, with up to 50 pulses produced during each discharge burst, and the burst repetition rate of 20-40 Hz. At all operating conditions, the plasma remains diffuse and uniform, and is confined to the space between the electrodes, such that the absorption path is well defined. During the experiment, time-resolved, absolute populations of $N_2(A^3\Sigma_u^+,v=0,1)$ are measured, as the laser is scanned across several fully resolved absorption transitions in the N_2 second positive band system. The temperature in the discharge cell is inferred from the intensity ratio of two rotational-vibrational absorption transitions in the same vibrational band. The experimental data are compared with the kinetic modeling predictions, identifying the dominant $N_2(A^3\Sigma_u^+)$ generation and decay processes.

In pure nitrogen, $N_2(A^3\Sigma_u^+)$ is generated primarily during the cascade quenching of the higher electronic states generated by electron impact. $N_2(A^3\Sigma_u^+)$ decay is controlled by the energy pooling process and quenching by N atoms, generated both by electron impact and energy pooling. Adding CO_2, CH_4, or H_2 to the mixture (up to 10% mole fraction) does not affect the $N_2(A^3\Sigma_u^+)$ quenching in the beginning of the discharge burst, since the quenching rate coefficients by these species are very slow (10^{-4} – 10^{-5} of the gas kinetic rate coefficient). However, dissociation of CO_2, CH_4, and H_2 in the discharge results in a significantly faster $N_2(A^3\Sigma_u^+)$ quenching. Therefore, the acceleration of the $N_2(A^3\Sigma_u^+)$ quenching rate during the discharge burst can be used as an indirect indicator of the enhanced reactivity of the gas mixture (primarily the dissociation fraction). The experimental results also demonstrate clearly that, in spite of
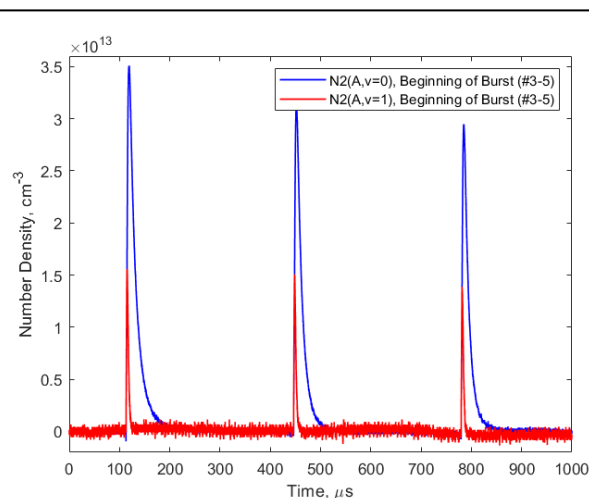

Figure 1 - Comparison of time-resolved absolute $N_2(A^3\Sigma_u^+,v=0)$ and $N_2(A^3\Sigma_u^+,v=1)$ populations at the beginning of a 50-pulse discharge burst in 10% CH_4-N_2 mixture at P=150 Torr.

the slow quenching rate, methane results in a very rapid vibrational relaxation of $N_2(A^3\Sigma_u^+)$ molecules, $N_2(A^3\Sigma_u^+,v=1) + CH_4 \longrightarrow N_2(A^3\Sigma_u^+,v=0) + CH_4$ (see Fig. 1).

Plasma-Enhanced Ammonia Synthesis over a Catalytic Surface

Xin Yang, Caleb Richards, and Igor V. Adamovich

Nonequilibrium Thermodynamics Laboratory, Department of Mechanical and Aerospace Engineering

The Ohio State University, Columbus, OH 43210, USA

Plasma catalytic ammonia synthesis is studied in nanosecond pulse discharge plasma sustained over a catalytic surface in N_2-H_2 mixtures in a plasma flow reactor, at a pressure of 190 Torr and temperature of 300 ^{0}C. A diffuse plasma is generated by a repetitive, double dielectric barrier, ns pulse discharge in plane-to-plane geometry, operated continuously at pulse repetition rates of 1-5 kHz. The catalyst in a powder form (nickel on alumina) is packed into an Macor ceramic receptacle and placed into the plasma. Ammonia generated in the reactor is detected and monitored by an FTIR spectrometer, using an absorption cell placed in the reactor exhaust. With the discharge sustained in the reactor without the catalyst, ammonia was detected in the reactor exhaust (see Fig. 1). The slow increase of the ammonia concentration in the absorption cell, several minutes, is due to the gradual accumulation of the reaction products in the cell, at the flow rate of 100 sccm. No ammonia was detected in the mixture flowing through the reactor with the catalyst in place, with the discharge turned off (see Fig. 1). Sustaining the discharge in pure N_2 over the catalyst for about 30 minutes, and then turning it off, results in a significant catalyst reactivity enhancement, such that the ammonia yield doubles compared to that in the plasma in the same mixture but without the catalyst (see Fig. 1). The catalyst reactivity is not enhanced by sustaining the plasma in H_2. When the plasma is operated in N_2-H_2, the ammonia yield keeps increasing over about an hour (see Fig. 2). These results suggest that the catalyst is activated due to the accumulation of N atoms generated in the plasma on the catalyst [1]. Measurements of plasma-catalytic ammonia synthesis on alumina powder without the catalyst, and on different catalysts is underway. Adding a sub-breakdown RF voltage waveform between the ns discharge pulses [2] resulted in an additional increase of the ammonia yield, suggesting that vibrational excitation of N_2 may contribute to the ammonia generation in the plasma [3]. This effect has been observed both with and without the catalyst in the reactor (see Fig. 2). Further measurements aimed at isolating the effect of vibrationally excited N_2 molecules on ammonia generation are underway.
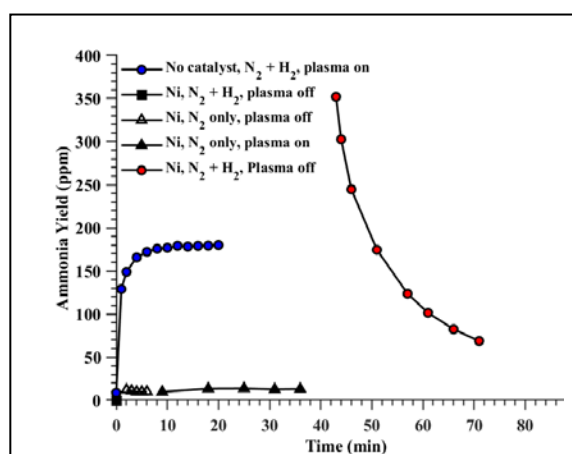

Figure 1 – Ammonia yield with plasma on (without catalyst) and plasma off (after activating the catalyst in N_2 plasma).

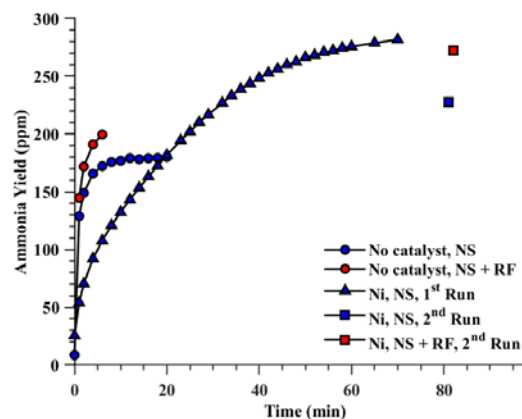Figure 2 – Ammonia yield and in ns pulse and ns / RF plasmas (with and without catalyst).

References

[1] Kunimori, K. et al. Catal. Lett. **16**, 443–446 (1992).

[2] I Gulko et al 2020 Plasma Sources Sci. Technol. **29** 104002.

[3] Mehta, P. et al . Nat. Catal. **1**, 269–275 (2018).

Kinetic Studies of Excited Singlet Oxygen Atom $O(^1D)$ Reactions with Ethanol

Hongtao Zhong [a], Chao Yan [a], Chu C. Teng [b], Timothy Y. Chen [a], Gerard Wysocki [b], and Yiguang Ju [a]

(a) Department of Mechanical and Aerospace Engineering, Princeton University, Princeton, NJ, USA
(hongtaoz@princeton.edu)
(b) Department of Electrical Engineering, Princeton University, Princeton, NJ, USA (gwysocki@princeton.edu)

The electronically excited singlet oxygen atom $O(^1D)$ is one of the most reactive species produced in nonequilibrium plasma [1]. $O(^1D)$ plays an active role in generating important intermediate radicals including the hydroxyl (OH) radical and hydroperoxyl (HO_2) radical and driving the chain-branching of plasma-assisted low-temperature fuel oxidation [2]. In addition, in atmospheric chemistry, the unburnt leaked fuels may react with atmospheric species including $O(^1D)$. The subsequent atmospheric chemical kinetics may greatly influence the O_3 cycle, smog formation, and climate change [3]. As such, kinetics of $O(^1D)$ reactions with fuels and subsequent reactions involving HO_2 and OH would provide insight into plasma-assisted fuel oxidation and fuel leakage effect on the atmospheric chemistry

In this work the reactions of $O(^1D)$ with ethanol were examined in a Herriott cell photolysis flow reactor at 297 K with reactor pressures of 60, 120, and 150 Torr (bath He). $O(^1D)$ was generated by UV photolysis of ozone (266 nm) and quantified by *in situ* actinometry. Time-resolved profiles of products such as the hydroperoxyl radical (HO_2) and the hydroxyl radical (OH) were quantified *in situ* using Faraday rotation spectroscopy (FRS) [4] and direct absorption spectroscopy, respectively. Branching ratios of the target reaction were determined based on fitting the experimental time-dependent concentration retrievals to simulations from an in-house reaction mechanism. Two major reaction channels were identified as $CH_3CHOH + OH$ and $CH_3O + CH_2OH$ and their branching ratios were determined as 0.46 ± 0.12 and 0.42 ± 0.11, respectively [5]. A specific $HO_2 + RO_2$ reaction between HO_2 and $O_2CH_2CH_2OH$ (β-RO_2) at the low-temperature range is estimated in this work as $HO_2 + O_2CH_2CH_2OH \rightarrow$ products with a rate constant of 7×10^{-12} cm^3 $molecule^{-1}$ s^{-1}.

References
[1] Y. Ju and W. Sun, Prog Energy Combust Sci. **48**:21–83 (2015).
[2] C. Yan, C. Teng, T. Chen, et al., Combust Flame. 212:135–141 (2020).
[3] M. Prather, Science. **279**(5355):1339–1341 (1998).
[4] C. Teng, C. Yan, A. Rousso, et al., Opt. Express. **29**(2):2769-79 (2021).
[5] H. Zhong, C. Yan, C. Teng, et al., Int. J. Chem. Kinet. **53**(6):688-701 (2021).

VUV Spectroscopic Investigation of a Low Current Corona Source in Nitrogen

Justin K. Smith [a], Ben Yee [b], Andrew Fierro [a], and Jane Lehr [a]

(a) University of New Mexico (jsmith47@unm.edu)
(b) Sandia National Laboratories (btyee@sandia.gov)

In current photoionization models used in computational studies at atmospheric pressure, there is a lack of experimental spectral data and several assumptions pertaining to the photo-electron production in the gas. In air, electron impact excitations with nitrogen provide the UV photons that result in the ionization of oxygen. It's widely accepted that the wavelength range of 98-102.5 nm are the primary contributors of photoionization of oxygen in an air plasma [1].

This model is derived based on thermodynamic equilibrium whereas streamers are typically not in local thermodynamic equilibrium. For accurate treatment of photoionization, quantification of radiation from a photoionization source from a nonthermal discharge in air has yet to be completed [2]. In developing plasmas, it was found that the dominant transition was the $c_4'\,^1\Sigma_u^+$ state (Carroll-Yoshino) was the dominant source of photoionizing emission, but other transitions may be identified with electron beam induced spectroscopy [3]. Although useful in identifying possible transitions, the electron beam spectroscopy may not reflect the emission spectra from a typical air discharge. Therefore, quantifying the emission spectra from a photoionization source will identify the photoionizing capable emissions that can improve streamer simulations.

A low current corona discharge in nitrogen is connected to a McPherson 1 m vacuum spectrometer coupled to a photomultiplier tube for high-resolution spectral data acquisition. The VUV emission from the plasma is recorded at various pressures from 0.1 – 60 Torr in the wavelength region of 95-105 nm, as shown in Figure 1. Identification of the bands reveal transitions that are photoionizing capable. The radiation characteristics of the plasma source are extracted and the quenching of transitions from 0.1 – 60 Torr are examined.

Figure 1 – VUV emission spectra from a nitrogen discharge.

References

[1] M. B. Zheleznyak, A. K. Mnatsakanyan, and S. V. Sizykh, High Temp. **20**, 357 (1982).

[2] R. Janalizadeh and V. P. Pasko, Plasma Sources Sci Technol. **28**, 105006 (2019).

[3] J Stephens, M. Abide, A. Fierro, and A. Neuber., Plasma Sources Sci Technol. **27**, 075007 (2018).
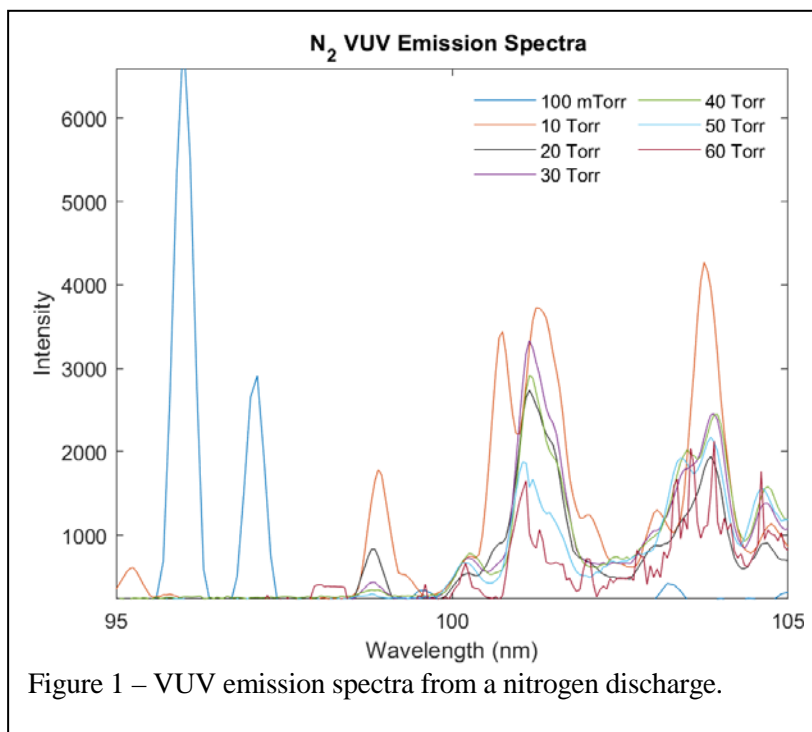
Characterization and Treatment Performance of a Plasma Spinning Disc Reactor

Foluke Jennifer Ganzallo, Xudong Su and Selma Mededovic Thagard

Department of Chemical and Biomolecular Engineering, 8 Clarkson Avenue, Clarkson University, Potsdam, 13699, NY, USA (ganzalfj@clarkson.edu)

Gas-liquid reactors have been identified as one of the most efficient plasma systems for treating aqueous contaminants. Today, there exist hundreds of different gas-liquid plasma reactor designs that feature unique electrode arrangements and are powered by a range of plasma excitation sources. Nevertheless, the physicochemical processes responsible for their performance are largely unknown. Mass transport limitations, however, have been long recognized to be important and the reactors in which those are minimized, exhibit enhanced performance [1]. This work focuses on the characterization of a plasma spinning disc reactor (PSDR) - shown in Figure 1- that allows for a controlled flow of the liquid under the plasma created by an AC-driven plasma jet. To that end, different plasma and flow-related parameters that affect the efficiency of PSDR in removing contaminants, in particular rhodamine B dye, from water were examined.

The parameters investigated include disc rotational speed, liquid flowrate across the disc, discharge power, jet distance from the surface of the liquid, argon gas flowrate and the starting dye concentration. Results revealed a complicated relationship among the plasma area, discharge power and fluid flowrate across the disc. The thickness of the film, which was predominantly controlled by the disc rotational speed, had a minimal effect on the dye removal. The bulk liquid concentration of the dye had a significant impact on its removal, and in fact controlled the processes limiting the overall kinetics. For low dye concentrations, the radial velocity of the fluid across the disc controlled the removal. At high dye concentrations,

Figure 1 – Treatment of Rhodamine B dye in a plasma spinning disc reactor driven by an atmospheric pressure plasma jet.

the removal was controlled by the production rate of OH radicals. PSDR allows for an unprecedented control over the fluid renewal rates under the plasma and as such, shows promise in plasma reactor scale up.
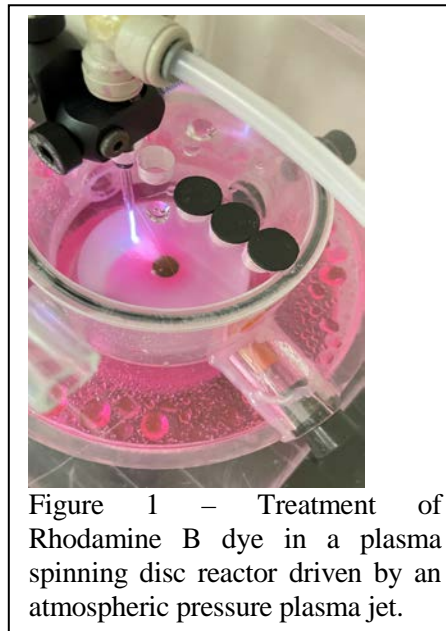
References
[1] Guang-Wen Chu *et al.,* Chem. Eng. J. **377,** 119897 (2019).

Validated Two-dimensional Modeling of Short Carbon Arcs: Anode and Cathode Spots

Jian Chen [a, b], Alexander Khrabry [a], Igor D. Kaganovich [a], Andrei Khodak [a], Vladislav Vekselman [a]
and He-Ping Li [b]

(a) Princeton Plasma Physics Laboratory, Princeton NJ 08542, USA (chenjian0314@outlook.com)
(b) Tsinghua University, Beijing 100084, PRC

In order to study properties of short carbon arcs, a self-consistent model was implemented into a CFD code ANSYS-CFX. The model treats transport of heat and electric current in the plasma and the electrodes in a coupled manner and accounts for gas convection in the chamber [1, 2]. Multiple surface processes at the electrodes are modeled, including formation of space-charge limited sheaths, ablation and deposition of carbon, emission and absorption of radiation and electrons. The simulations show that the arc is constricted near the cathode and the anode front surfaces leading to formation of electrode spots. The cathode spot is a well-known phenomenon and mechanisms of its formation were reported elsewhere. However, the anode spot formation mechanism discovered in this work was not reported before. We conclude that the spot formation is not related to plasma instability, as commonly believed in case of constricted discharge columns, but rather occurs due to the highly nonlinear nature of heat balance in the anode. We additionally demonstrate this property with a reduced anode heat transfer model. We also show that the spot size increases with the arc current. This anode spot behavior was also confirmed in our experiments. Due to the anode spot formation, a large gradient of carbon gas density occurs near the anode, which drives a portion of the ablated carbon back to the anode at its periphery. This can consequently reduce the total ablation rate. Simulation results also show that the arc can reach local chemical equilibrium (LCE) state in the column region while the local thermal equilibrium (LTE) state is not typically achieved for experimental conditions. It shows that it is important to account for different electron and gas temperatures in the modeling of short carbon arcs.

References:
[1] J. Chen, A. Khrabry, I. D. Kaganovich, A. Khodak, V. Vekselman, and H. –P. Li, Phys. Plasmas **27**, 083511 (2020).
[2] A. Khrabry, I. D. Kaganovich, A. Khodak, V. Vekselman, Y. Raitses, arXiv, https://arxiv.org/abs/1902.09991.

Characterization of an Atmospheric Pressure Carbon Arc Plasma

Nirbhav Singh Chopra [a,b], Yevgeny Raitses [a], Shurik Yatom [a], Jorge Muñoz-Burgos [c]

(a) Princeton Plasma Physics Laboratory, Princeton, NJ (nschopra@pppl.gov)
(b) Princeton University, Princeton, NJ (nschopra@pppl.gov)
(c) Astro Fusion Spectre LLC, San Diego, CA (astrofusionspectre@gmail.com)

Atmospheric pressure anodic carbon arc discharges are a promising method for low-cost, high-volume synthesis of nanomaterials. During arc operation, carbon material is introduced into the arc by the ablation of the graphite anode [1]. The anode ablation depends on the power balance at the anode, which is influenced by whether the anode sheath is electron-repelling (negative anode sheath) or electron-attracting (positive anode sheath) [1–4]. Anodic carbon arcs exhibit a transition between low and high ablation modes; at larger arc currents the ablation rate of the anode grows nonlinearly [1,3]. We show the existence of a positive anode sheath in both low and high ablation modes. The electron temperature and density are determined by optical emission spectroscopy and corroborated by a Langmuir probe measurement. The plasma potential is determined with a floating probe. The floating probe potential is related to the plasma

Figure 1 – Fast frame image of the probe in the carbon arc, with H_α filter employed to image arc core position. Here the probe is imaged to be in the arc core, and the interelectrode gap is 4.5 mm.

potential by assuming ions diffuse through neutrals in the probe presheath. Effects of the positive anode sheath on anode ablation rate are discussed. We also discuss a plausible explanation for the discrepancy in experimentally determined discharge voltage and discharge voltage calculated by recent models of the arc [4].
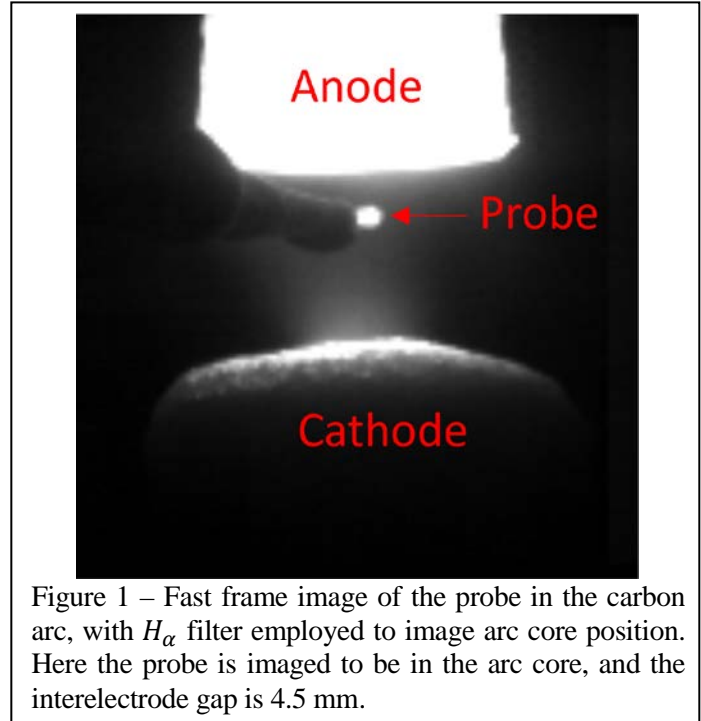
References
[1] V. Vekselman, M. Feurer, T. Huang, B. Stratton and Y. Raitses 2017 Complex structure of the carbon arc for synthesis of nanotubes *Plasma Sources Science and Technology* **26**.
[2] V. A. Nemchinsky and Y. Raitses 2016 Anode sheath transition in an anodic arc for synthesis of nanomaterials *Plasma Sources Science and Technology* **25**.
[3] A. Khrabry, I. D. Kaganovich, A. Khodak, V. Vekselman and T. Huang 2020 Analytical model of low and high ablation regimes in carbon arcs *Journal of Applied Physics* **128** 123303–123303.
[4] J. Chen, A. Khrabry, I. D. Kaganovich, A. Khodak, V. Vekselman and H.P. Li 2020 Validated two-dimensional modeling of short carbon arcs: Anode and cathode spots *Physics of Plasmas* **27**.

Surface Charging in Disinfection by Dielectric Barrier Discharge

Harry Fetsch, Sophia Gershman and Yevgeny Raitses

Princeton Plasma Physics Laboratory (hfetsch@pppl.gov)

Dielectric barrier discharges (DBDs) have shown effectiveness in disinfecting surfaces through a combination of mechanisms including reactive chemical species, charged particles, UV, and electric and electromagnetic fields produced in the plasma. Of these, a relatively little studied factor is the accumulation of charge on the treated surface. The resulting electric fields, when interacting with bacterial cells on the surface, can cause electroporation, the opening of pores in the cell membrane.[1,2] At sufficient strength (about 10kV/cm and greater), these fields can cause irreversible damage to bacteria. At lower field strength (about 5-10kV/cm, and highly species-dependent), where bacteria may recover from electroporation alone, the opening of pores can render
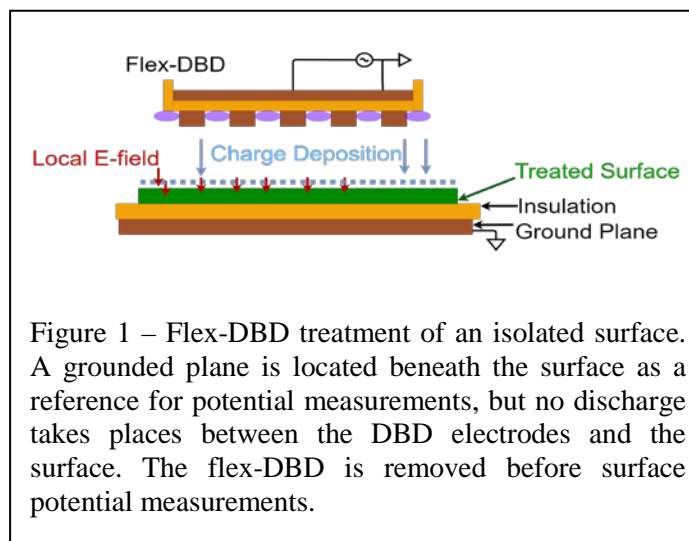

Figure 1 – Flex-DBD treatment of an isolated surface. A grounded plane is located beneath the surface as a reference for potential measurements, but no discharge takes places between the DBD electrodes and the surface. The flex-DBD is removed before surface potential measurements.

bacteria more susceptible to bactericidal chemical species in the environment. Understanding this mechanism is therefore an important step in understanding the synergistic effects that contribute to plasma disinfection.

In this work, we study surface charging post-treatment by a flexible surface dielectric barrier discharge (Flex-DBD), which has been investigated for plasma disinfection.[3] Surface streamers form on the face of the flex-DBD, and so the treated surface does not participate in the discharge directly, but is driven to a positive potential by charged species in the plasma effluent. We measure this potential after treatment using a non-contacting electrostatic voltmeter. The surface potential is used to compute the surface charge and obtain an estimate of the electric field at the surface.

We have measured voltages on titanium, polyimide film, and glass slides, isolated from the grounded reference plane by a thin dielectric (Figure 1). Steady-state voltages following flex-DBD treatment are in the 100-200V range, corresponding to fields around 20kV/cm immediately at the dielectric surface. These preliminary results do not directly probe the transmembrane fields which are crucial in electroporation. However they demonstrate that charge accumulation due to the treatment with a flex-DBD is in the range of potential biological significance. Hence, largely neglected in biological plasma treatment of isolated surfaces not involved in the discharge, surface charging warrants further investigation.

References

[1] J.C. Weaver *et al*, Bioelectrochemistry. **87**, 236-243 (2009).
[2] G. Beretta *et al*, Rev Environ Sci Biotechnol. **18**, 29-75 (2009).
[3] S. Gershman *et al*, Sci Rep.. **11**, 4626 (2021).

Plasma Disinfection by Dielectric Barrier Discharge Devices Suitable for Consumer Use

S. Gershman [a], S. Yatom [a], H. Fetsch [a], Y. Raitses [a], P. Efthimion [a], M. B. Harreguy [b], G. Haspel [b], O. Huang [c], E. Engel [c], H. Dewald [d], P. Bocarsly [d]

(a) Princeton Plasma Physics Laboratory (sgershma@pppl.gov)
(b) New Jersey Institute of Technology (mbh96@scarletmail.rutgers.edu)
(c) Princeton University Neuroscience Institute (haoh@princeton.edu)
(d) New Jersey Medical School, Department of Pathology (hkd17@gsbs.rutgers.edu)

Over the last two decades, the development of cold atmospheric pressure plasmas (CAP) has produced a wide variety of plasma sources including dielectric barrier dishcarges (DBD) that effectively inactivate bacteria, viruses, fungi, and bacterial spores [1]. In spite of these achievements, these devices have not been able to reach the even though a clear need has been brought into focus by the current pandemic. We have developed and tested two flexible DBD plasma sources suitable for consumer use (namely, felx-DBD and weave-DBD) and tested a D'Arsonval device, a floating electrode DBD plasma source currently available for cosmetic purposes. The flex-DBD device is a surface DBD with a printed circuit design [2, 3]. The cloth or weave-DBD is woven from two insulated conductors and can be incorporated into bandages, clothing, and personal protection devices. Optical emission spectroscopy and Fourier Transform Infrared Absorption spectroscopy have shown that these two devices produce reactive oxygen and nitrogen species, both short lived such as OH* and long lived such as ozone
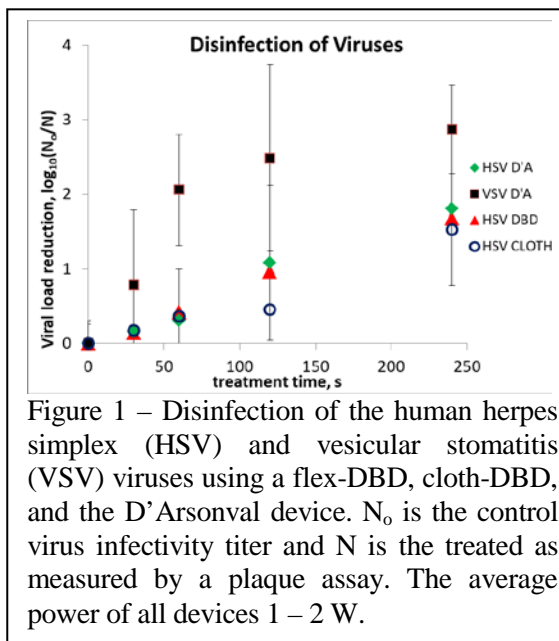

Figure 1 – Disinfection of the human herpes simplex (HSV) and vesicular stomatitis (VSV) viruses using a flex-DBD, cloth-DBD, and the D'Arsonval device. N_o is the control virus infectivity titer and N is the treated as measured by a plaque assay. The average power of all devices $1 - 2$ W.

and nitrogen oxides that along with charged particles and electric and electromagentic fields are responsible for the disinfecting properties of DBD. Flex-DBD applied to contaminated surfaces (glass, metal, or textiles) achieves a 99.99% reduction in bacteria count in under 90 s and 99.9999% reduction or sterilization level when combined with hydrogen peroxide [3]. These devices along with the D'Arsonval have been tested against human herpes simplex virus (HSV-1) and vesicular stomatitis virus (VSV) and show up to 3 $\log_{10}$ reduction for VSV and ~2 $\log_{10}$ for HSV in 250 s.. These projects have demonstrated that flexible atmospheric pressure plasma devices operating at power densities <0.5 W/cm^2 and without a gas flow, can be used for effective surface decontamination from bacteria and viruses.

References
[1] A. Sakudo, Y. Yagyu, , and T. Onodera, Int. J. Mol. Sci., 20, 52165216 (2019)
[2] J. Boekema et al. Phys. D Appl. Phys. 49, 044001 (2016)
[3] S. Gershman et al. Sci Rep 11, 4626 (2021)

Analytical Model for Estimating Plasma Parameters in a Planar Diode

Haomin Sun [a], Jian Chen [b], Alexander V. Khrabrov [b] and Igor D. Kaganovich [b]

(a) Princeton University (haomins@princeton.edu)
(b) Princeton Plasma Physics Laboratory

We report the analytical model for estimating the electron temperature and number density in the plasma of a planar diode by considering the energy and particle balance equations. In a planar diode, two groups of electrons are present: an electron beam emitted from the cathode and cold electrons trapped in the plasma bulk. An electron beam emitted from a cathode excites plasma waves which can heat cold electrons in the bulk via particle-wave interactions. The resulting equation for the cold electron temperature contains six terms, including the energy exchange in the elastic, and inelastic (excitation and ionization) collisions between the cold electrons and neutrals, the energy exchange in the Coulomb collisions between cold and beam electrons, wave heating, and the energy loss due to the wall losses of energetic electrons to the anode. We compare the results of the analytical theory with that of the particle-in-cell simulations using EDIPIC code and find a good agreement. The analytical model also shows that the heating term due to the Coulomb collisions with beam electrons and the energy loss to the anode are dominant, and they mostly balance each other, whereas the energy exchange due to the collisions with neutrals and wave heating are small and can be omitted. By coupling the energy balance equation with the particle balance equation [1], we can solve for both the number density and electron temperature as functions of the current density, electrode distance, pressure, and applied voltage. This model has been validated against past experiments [2] and a good agreement was also found.

References
[1] M. A. Lieberman and Allan J. Lichtenberg (2005), Principles of Plasma Discharges and Materials Processing, John Wiley & Sons.
[2] S. A. Self, Interaction of a cylindrical beam with a plasma. II. experiments and comparison with theory, J. Appl. Phys **40**, 5232 (1969).

Simulations of Ion Heating in the Presheath Due to Ion-acoustic Instabilities

L. P. Beving [a], M. M. Hopkins [b] and S. D. Baalrud [c]

(a) Applied Physics Program, University of Michigan, Ann Arbor, MI (lbeving@umich.edu)
(b) Applied Optical and Plasma Sciences, Sandia National Laboratories, Albuquerque, NM
(mmhopki@sandia.gov)
(c) Applied Physics Program, University of Michigan, Ann Arbor, MI (baalrud@umich.edu)

We find that ion-acoustic instabilities result in significant ion heating near the sheath edge. The heating extends into the presheath since some of the wave power reflects from the sheath. Particle-in-cell simulations were designed to test whether the instability was the source of heating by varying the source electron temperature across the threshold for exciting the ion-acoustic instability. The simulations confirm the instabilities cause heating and demonstrate that the electron-to-ion temperature ratio is locked to the threshold for instability in the unstable region near the sheath edge. The instability heating effect is significant at low pressures, but is eliminated at higher pressures where the instability is damped by ion-neutral collisions. This effect is distinct from the well understood ion heating caused by inelastic collisions with neutrals. Low temperature plasma systems that utilize a presheath for ion acceleration, such as etching and ion beam sources, could experience unwanted and significant ion heating due to this effect.

Time-resolved Electric Fields and Electron Properties Measured by Burst Laser pUlse EFISH (BLUEFISH) and Thomson Scattering in CH_4/Ar Nanosecond Pulsed Discharges

<u>Timothy Y. Chen</u>, Ning Liu, Egemen Kolemen, and Yiguang Ju

Department of Mechanical and Aerospace Engineering, Princeton University
Princeton, NJ 08544 (yju@princeton.edu)

In non-equilibrium plasma discharges, the plasma chemistry is initiated by electron-impact reactions with the neutral gas species. Whether the gas molecules are excited, dissociated, or ionized, depends on the electron energy and the reduced electric field. Furthermore, for applications such CH_4 reforming, the gas composition also influences the available electron-molecule energy transfer pathways. Therefore, it is critical to quantitatively understand how these plasma properties evolve in time and change with mixture composition. With the development of advanced laser diagnostics, such as Electric Field Induced Second Harmonic generation (EFISH) [1] and laser Thomson scattering [2,3], there now exists the capability to measure the electric field and electron properties with nanosecond temporal resolution. The characterization of both the electric field and electron properties well as the development of a new method called Burst Laser pUlse EFISH (BLUEFISH) to make burst electric field measurements of single ionization events in CH_4/Ar nanosecond pulsed dielectric barrier discharges (ns-DBD) will be presented.

A nonlinear decrease in electron density with increasing CH_4 concentration was measured using Thomson scattering. Counterintuitively, the measured electron temperature decay was not accelerated by increasing CH_4 concentration and the overall electron temperature increased. Electric field measurements using EFISH revealed an increase in peak electric field with CH_4 concentration as well as higher sub-breakdown electric fields from pulse reflections. The newly developed BLUEFISH technique splits a single laser pulse into a train of delayed sub-pulses to measure the time-evolving electric field of a single ionization event. The key advantages include enhanced temporal resolution, elimination of relative timing uncertainty between laser pulses, and the ability to characterize non-repetitive and unstable plasmas. BLUEFISH measurements of a single-sided ns-DBD revealed an electric field overshoot when a bare metal cathode was used versus a dielectric barrier cathode, indicating the presence of an ionization wave.

References
[1] A. Dogariu, B. M. Goldberg, S. O'Byrne, and R. B. Miles, "Species-Independent Femtosecond Localized Electric Field Measurement," Physical Review Applied **7**, (2017).
[2] E. Carbone and S. Nijdam, "Thomson scattering on non-equilibrium low density plasmas: principles, practice and challenges," Plasma Physics and Controlled Fusion **57**, 014026 (2015).
[3] T. Y. Chen, A. C. Rousso, S. Wu, B. M. Goldberg, H. van der Meiden, Y. Ju, and E. Kolemen, "Time-resolved characterization of plasma properties in a CH_4/He nanosecond-pulsed dielectric barrier discharge," Journal of Physics D: Applied Physics **52**, 18LT02 (2019).

Observation of O(^{1}S) Metastable Transition in Atmospheric Pressure Plasma

S. Jaiswal [a], Evan Aguirre [b]

(a) Eastern Michigan University (sjaiswa1@emich.edu)
(b) Rouge Space Systems (mopar.aguirre@gmail.com)

We have reported the observation of the "Auroral green line" in a KHz frequency atmospheric pressure pure argon plasma jet. The oxygen metastable transition from O(^{1}S)-O(^{1}D) which is commonly referred to as a source of auroral lines in the upper atmosphere has been observed at a wavelength of 557.7 nm when argon plasma jet interacts with open atmosphere. The intensity of the produced green line is strong enough that the entire plasma plume in the ambient air is visible as a green plasma. The O^{1}S emission was continually present for a variety of parameters including argon flow rate, electrode gap, and applied voltage. However, a threshold is found in all these parameters for the maximum atomic oxygen components in the plasma. The plasma plume length was more than 2.5 cm and was found to produce a variety of reactive species (OH, O, N_2, and N_2^+) that are important for biomedical and technological applications. The chemical formulation for the formation of

Figure 1 – (a) Schematic diagram of the experimental setup. Diagnostics include current and voltage probe, thermocouple, camera and spectrometer. (b) photograph of APPJ system.

reactive oxygen species in pure argon plasma has been established. A comparison of argon plasma jet with excess oxygen formation and helium plasma on the degradation of methylene blue dye was performed to test the experimental setup for industrial applications.
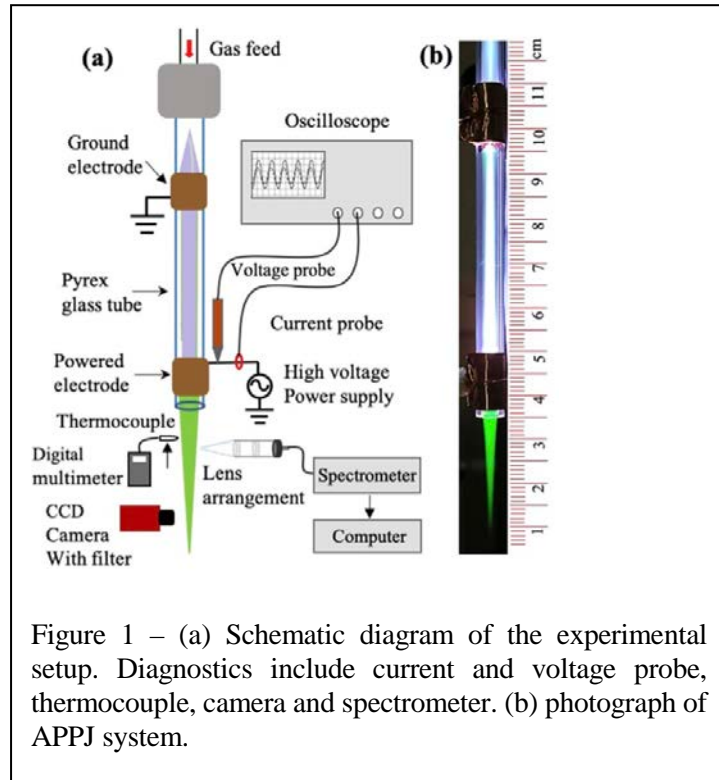
References
[1] S. Jaiswal and E. M. Aguirre, AIP Advances **11**, 045311 (2021).
[2] S. Jaiswal, E. M. Aguirre, and G. Veda Prakash, Sci. Rep. **11**, 1893 (2021).

Meeting Participants

Last Name	First Name	Email	Affiliation	Attendance
Adamovich	Igor	adamovich.1@osu.edu	PICI, PACC	In person
Bayer	Brian	bayer116@umn.edu	PICI	In person
Bekerom, van den	Dirk	dvanden@sandia.gov	SPRF	Remote
Bentz	Brian	bzbentz@sandia.gov	PICI, SPRF	Remote
Beving	Lucas	lbeving@umich.edu	SPRF	Remote
Bhan	Aditya	abhan@umn.edu	PICI	In person
Bruggeman	Peter	pbruggem@umn.edu	PICI	In person
Chen	Timothy	tc8@princeton.edu	PACC	Remote
Chen	Jian	chenjian0314@outlook.com	PCRF	Remote
Chopra	Nirbhav	nschopra@pppl.gov	PCRF	Remote
Chung	Sang-Jin	schung13@terpmail.umd.edu	PICI	In person
Dogariu	Artur	adogariu@princeton.edu	PCRF	In person
Doherty	Francis	fdoherty@umich.edu	PICI	In person
Fetsch	Harry	hfetsch@pppl.gov	PCRF	Remote
Fierro	Andrew	asfierr@sandia.gov	SPRF	In person
Flicker	Dawn	dgflick@sandia.gov	SPRF	In person
Frank	Jonathan	jhfrank@sandia.gov	SPRF	Remote
Ganzallo	Foluke (Jennifer)	ganzalfj@clarkson.edu	PICI	In person
Gershman	Sophia	sgershma@pppl.gov	PCRF	Remote
Goldsmith	Bryan	bgoldsm@umich.edu	PICI	In person
Hadidi	Kamal	kamal.hadidi@gmail.com	Consultant	Remote
Hinshelwood	Michael	mhinshel@umd.edu	PICI	In person
Hopkins	Matthew	mmhopki@sandia.gov	SPRF	Remote
Hsu	Scott	scott.hsu@hq.doe.gov	DOE	Remote
Isowamwen	Osakpolo Faith	isowamof@clarkson.edu	PICI	In person
Jaiswal	Surabhi	sjaiswa1@emich.edu	EMU	Remote
Jiang	Jingkai	jian0284@umn.edu	PICI	In person
Ju	Yiguang	yju@princeton.edu	PACC	In person
Kaganovich	Igor	ikaganov@pppl.gov	PCRF	Remote
Kliewer	Christopher	cjkliew@sandia.gov	SPRF	Remote
Koel	Bruce	bkoel@princeton.edu	PACC	Remote
Konina	Kseniia	kseniiak@umich.edu	PICI	In person
Kushner	Mark J.	mjkush@umich.edu	PICI	In person
Lehr	Jane	jmlehr@unm.edu	SPRF	In person
Li	Yudong	ydli23@terpmail.umd.edu	PICI	In person
Lietz	Amanda	amlietz@sandia.gov	SPRF	Remote
Lin	Kang-Yi	kxl259@umd.edu	PICI	In person
Liu	Ning	nl7@princeton.edu	PACC	In person
Mededovic-Thagard	Selma	smededov@clarkson.edu	PICI	In person
Mesbach	Ali	mesbah@berkeley.edu	PICI	In person
Meyer	Mackenzie	maemeyer@umich.edu	PICI	In person

Last Name	First Name	Email	Affiliation	Attendance
Mignogna	David	mignogna.8@osu.edu	PACC	In person
Miller	Victor	vmiller1671@berkeley.edu	PICI	In person
Morsell	Joshua	jkmorsel@ncsu.edu	PICI	In person
Oehrlein	Gottlieb	oehrlein@umd.edu	PICI	In person
Orr	Keegan	orr.282@osu.edu	PICI	In person
Podder	Nirmol	Nirmol.Podder@science.doe.gov	DOE	In person
Raitses	Yevgeny	yraitses@pppl.gov	PCRF	Remote
Raskar	Sai	raskar.1@osu.edu	PICI	In person
Richards	Caleb	richards.1217@osu.edu	PICI	In person
Shaddix	Christopher	crshadd@sandia.gov	SPRF	In person
Shannon	Steven	scshanno@ncsu.edu	PICI	In person
Shao	Ketong	ketong_shao@berkeley.edu	PICI	In person
Shneider	Mikhail	shneyder@princeton.edu	PCRF	In person
Sickafoose	Shane	smsicka@sandia.gov	PICI, SPRF	Remote
Smith	Justin	jsmith47@unm.edu	SPRF	In person
Srivastava	Tanubhav	sriva203@umn.edu	PICI	In person
Sun	Haomin	haomins@princeton.edu	PCRF	Remote
Vasilev	Mikhail	vasilem@clarkson.edu	PICI	In person
Wang	Jianan	wang9597@umn.edu	PICI	In person
Yang	Xin	yang.5473@osu.edu	PACC	In person
Yatom	Shurik	syatom@pppl.gov	PCRF	Remote
Zhong	Hongtao	hongtaoz@princeton.edu	PACC	Remote